

**HEXACOORDINATE GLOBINS: CHARACTERIZATION AND ENGINEERING FOR
DEVELOPMENT OF NOVEL THERAPEUTIC AGENTS**

by

Matthew Brian Amdahl

B.S. Bioengineering, Rice University, 2011

Submitted to the Graduate Faculty of
The Swanson School of Engineering in partial fulfillment
of the requirements for the degree of
Doctor of Philosophy

University of Pittsburgh

2018

UNIVERSITY OF PITTSBURGH
SWANSON SCHOOL OF ENGINEERING

This dissertation was presented

by

Matthew Brian Amdahl

It was defended on

July 6, 2018

and approved by

Dr. Jesus Tejero, PhD, Assistant Professor, Division of Pulmonary, Allergy, and Critical Care

Medicine

Dr. Prithu Sundd, PhD, Assistant Professor Division of Pulmonary, Allergy, and Critical Care

Medicine

Dr. William Wagner, PhD, Professor, Departments of Surgery and Bioengineering

Dr. Sanjeev Shroff, PhD, Professor and Chair, Department of Bioengineering

Dissertation Director: Dr. Mark T. Gladwin, MD, Professor and Chair, Department of

Medicine

Copyright © by Matthew B. Amdahl

2018

HEXACOORDINATE GLOBINS: CHARACTERIZATION AND ENGINEERING FOR DEVELOPMENT OF NOVEL THERAPEUTIC AGENTS

Matthew B. Amdahl, PhD

University of Pittsburgh, 2018

This work was intended to characterize the hexacoordinate heme globins, most notably cytoglobin (Cygb), in the hopes of learning more about the native function of these proteins, but also exploring the potential of these proteins to be developed into therapeutic molecules.

The first portion of the work examined the reduction of vertebrate globins by the cytochrome b5 (CYB5) reducing system and ascorbate and found that Cygb is reduced by CYB5 much faster than any other globin. This interaction provides some insight into potential physiologic functions of Cygb, which has been theorized to function as an NO dioxygenase *in vivo*, limiting NO diffusion. NO dioxygenation oxidizes Cygb, and so rapid reduction by CYB5 could support rapid Cygb turnover and catalytic NO consumption. The reduction of Cygb by CYB5 was also documented, and found to be very similar, for the zebrafish homologs of these proteins. This level of evolutionary conservation suggests a role of significant physiologic importance, and even suggests that CYB5 and Cygb may have originally evolved together as redox partners.

Subsequent work generated novel recombinant Cygb mutants as potential Cygb-based therapeutic molecules intended to function as either an oxygen carrier or an antidotal therapy

capable of scavenging carbon monoxide (CO) and/or cyanide. Key functional characteristics of these mutants were then quantified, primarily their rates of nitrite reduction (production of nitric oxide from nitrite), autoxidation, and cyanide binding. This work revealed one mutant (V85I) with promise as an oxygen carrier, and a separate mutant (L46F + H81Q) that may function as a CO and cyanide antidote, as it was shown to bind cyanide very rapidly. The V85I mutant produced NO from nitrite more rapidly than the wild-type protein, which may offset the NO scavenging and vasoconstriction that has historically been caused by infusion of cell-free globins. In a small animal model designed to test vasoactivity, this mutant did not show a clear advantage over unmodified Hb. Future work will continue to search for a potential Cygb-based oxygen carrier, as well as further explore L46F + H81Q Cygb's ability to scavenge carbon monoxide and cyanide.

TABLE OF CONTENTS

PREFACE	XIII
1.0 INTRODUCTION	1
1.1 BASIC PRINCIPLES OF VASCULAR PHYSIOLOGY	2
1.1.1 Blood and its components	3
1.1.2 The Vascular Wall: Structure and Function	5
1.1.3 Vascular Nitric Oxide Signaling	6
1.2 HEME GLOBINS	8
1.2.1 Structure of Heme Globins	8
1.2.2 The Globin Superfamily in Vertebrates	14
1.2.3 Prominent Functions of Heme Globins	16
1.2.3.1 The Role of the Heme Iron Redox State	17
1.2.3.2 Ligand-binding behavior: kinetics and affinity	20
1.2.3.3 Reactions of Unbound Ferrous (Fe^{II}) Heme Globins	23
1.2.3.4 Reactions of Oxygen-bound Heme Globins	24
1.2.3.5 Reactions of Ferric (Fe^{III}) Heme Globins	25
1.2.4 Key modulators of heme globin function	26
1.2.4.1 Heme coordination state and distal histidine binding	27
1.2.4.2 Cooperativity	28

1.2.4.3	Thiol residues and disulfide formation	29
1.2.4.4	External Factors	31
1.2.4.5	Specific amino acid residues and mutations	33
1.2.5	UV-Visible spectroscopy of heme globin species	36
1.3	CYTOGLOBIN: STRUCTURE AND FUNCTION	38
1.3.1	Cytoglobin Structure.....	39
1.3.2	Cytoglobin Functional Characteristics	41
1.3.3	Cytoglobin Localization	44
1.3.4	Putative Functions of Cygb <i>in vivo</i>	46
1.4	DEVELOPMENT OF HEME GLOBINS FOR CLINICAL USE	50
1.4.1	Carbon monoxide poisoning, blood loss, anemia, and hemoglobin	50
1.4.2	Hemoglobin-based Oxygen Carriers (HBOCs)	54
1.4.2.1	The First HBOCs: Stroma-free Hemoglobin.....	56
1.4.2.2	Established Methods for HBOC Development.....	57
1.4.3	HBOCs in clinical trials	60
1.4.4	Mechanisms of toxicity observed in HBOC clinical trials	63
1.4.5	Ongoing efforts in HBOC development.....	67
1.4.6	Heme Globins as Antidotal Therapies	68
2.0	MATERIALS AND METHODS	71
2.1	RECOMBINANT PROTEIN EXPRESSION IN <i>E. COLI</i>	71
2.1.1	Expression Vectors	72
2.1.2	Bacterial Culture and Protein Expression: Soluble Method	73
2.1.2.1	Cytoglobins and Cytoglobin Mutants	74

2.1.2.2	Neuroglobin, Neuroglobin Mutants, and Globin X	74
2.1.2.3	Cytochrome b5	75
2.1.2.4	Cytochrome b5 reductase.....	75
2.1.2.5	Final Common Step: Bacterial Harvesting.....	75
2.1.3	Bacterial Culture and Protein Expression: Inclusion Body Method	76
2.2	PROTEIN PURIFICATION	77
2.2.1	Lysis of bacteria	77
2.2.2	Nickel-based affinity purification.....	79
2.2.3	Anion exchange purification.....	80
2.2.4	Size-exclusion purification	81
2.2.5	Inclusion body purification.....	82
2.3	SITE-DIRECTED PROTEIN MUTAGENESIS	87
2.3.1	Selection of Desired Mutants	88
2.3.1.1	Desired functional characteristics	88
2.3.1.2	Identifying promising mutations	89
2.3.2	Generation of mutant plasmids	93
2.3.2.1	Primer Design	94
2.3.2.2	Mutagenesis Reaction	94
2.3.2.3	Transformation into competent bacteria and plasmid isolation	95
2.3.2.4	Sequence confirmation	97
2.3.3	Transformation into expression bacteria	97
2.3.3.1	Glycerol stock production	98
3.0	REDUCTION OF HEME GLOBINS BY CELLULAR REDUCTANTS.....	99

	Rationale and aims	99
3.1	MATERIALS AND METHODS	100
3.1.1	Pseudo-physiologic reduction	100
3.1.2	Kinetic analysis of reduction	101
3.1.2.1	Kinetics of ferric globin reduction by ascorbate	102
3.1.2.2	Kinetics of ferric globin reduction by CYB5	102
3.1.3	Support of NO dioxygenation activity	105
3.2	RESULTS	107
3.2.1	Pseudo-physiologic reduction	107
3.2.2	Kinetic analysis of reduction	113
3.2.3	Support of nitric oxide dioxygenation	125
3.3	DISCUSSION	127
3.4	CONCLUSIONS	131
4.0	CYTOGLOBINS AND THE CYB5 SYSTEM IN ZEBRAFISH	132
	Rationale and aims	132
4.1	MATERIALS AND METHODS	133
4.1.1	Pseudo-physiologic reduction of zebrafish cytoglobins.....	133
4.1.2	Oxygen affinity measurement.....	134
4.1.3	Support of NO dioxygenation activity	135
4.2	RESULTS	136
4.2.1	Pseudo-physiologic reduction	136
4.2.2	Oxygen Affinity Measurement	138
4.2.3	Support of NO Dioxygenation Activity.....	141

4.3	DISCUSSION.....	144
4.4	CONCLUSIONS	145
5.0	CHARACTERIZING NOVEL GLOBIN MUTANTS.....	147
	Rationale and aims.....	147
5.1	MATERIALS AND METHODS	147
5.1.1	Nitrite reduction	147
5.1.2	Autoxidation.....	148
5.1.3	Cyanide Binding	149
5.1.4	Reduction by CYB5 and Ascorbate	150
5.2	RESULTS	151
5.2.1	Nitrite reduction	152
5.2.2	Autoxidation.....	160
5.2.3	Cyanide Binding	163
5.2.4	Reduction of V85I Cygb by CYB5 and ascorbate	166
5.3	DISCUSSION.....	167
5.4	CONCLUSIONS	170
6.0	ASSESSING PROTEIN VASOACTIVITY IN A MOUSE MODEL	171
	Rationale and aims.....	171
6.1	MATERIALS AND METHODS	172
6.1.1	Experimental Groups	172
6.1.2	Protein Preparation.....	173
6.1.3	Experimental Protocol	174
6.1.4	Data Analysis.....	176

6.2	RESULTS	177
6.2.1	Hb + nitrite + ascorbate	177
6.2.2	V85I Cygb + nitrite + ascorbate	179
6.2.3	Coinfusion of the CYB5 reducing system	182
6.2.4	The apparent effect of NADH on hypoxic vasodilation	184
6.2.5	Clearance of V85I Cygb from plasma	187
6.3	DISCUSSION	188
6.4	CONCLUSIONS	191
7.0	OVERALL CONCLUSIONS AND NEXT STEPS	192
7.1	OVERALL CONCLUSIONS	192
	Cytoglobin is reduced very rapidly by CYB5	192
	Mutagenesis can be used to effectively tailor the function of cytoglobin	192
	The therapeutic potential of Cygb mutants remains unclear	193
7.2	ONGOING AND SUGGESTED WORK	193
7.2.1	Cytoglobin-based oxygen carrier	193
7.2.2	CO and cyanide antidotes	194
7.2.3	Vascular physiology during globin/nitrite infusion	194
	APPENDIX A	196
	BIBLIOGRAPHY	206

LIST OF TABLES

Table 1: Redox potentials of selected heme globins, CYB5, and CYB5R.....	20
Table 2: Autoxidation rate constants of vertebrate Cygbs.....	41
Table 3: Nitrite reduction rate constants for select vertebrate globins	43
Table 4: HBOC development strategies and products developed using each strategy.....	56
Table 5: Predicted effect of chosen Cygb mutations on important functional characteristics.....	93
Table 6: Bimolecular rate constants for the reduction of ferric globins by Asc	116
Table 7: Calculated rate constants for the reactions between CYB5 and globins	124
Table 8: Rate constants used for kinetic simulation of CYB5 and Cygb interactions.....	125
Table 9: Oxygen P ₅₀ values and Hill coefficients calculated for <i>DreCygb1</i> and <i>DreCygb2</i>	140
Table 10: Calculated nitrite reduction rate constants for <i>HsaCygb</i> mutants	159
Table 11: Autoxidation rate constants for wild-type <i>HsaCygb</i> and mutants.....	163
Table 12: Rate constants for cyanide binding by wild type and mutant <i>HsaCygb</i>	164
Table 13: Experimental groups for study of globin vasoactivity in mice.....	173

LIST OF FIGURES

Figure 1: Cytoglobin, a Typical Heme Globin	9
Figure 2: Cygb structure, identifying helices A-H.....	11
Figure 3: Active Sites of Cytoglobin	13
Figure 4: Size comparison of Mb and Hb.....	14
Figure 5: Simplified phylogeny of vertebrate globins	15
Figure 6: Summary of important heme globin reactions	17
Figure 7: Sample Ligand-Binding Equilibrium Curves.....	21
Figure 8: Mb distal heme pocket showing residues B10, E7, and E11	34
Figure 9: Distal heme pockets of Cygb and Ngb showing B10, E7, and E11 residues	35
Figure 10: Spectra for four pure species of <i>HsaCygb</i>	37
Figure 11: Crystal structure of <i>HsaCygb</i>	39
Figure 12: Effects of CO poisoning, blood loss, and anemia on blood oxygen capacity	53
Figure 13: Summary of HBOC development strategies	59
Figure 14: Mechanisms of cell-free hemoglobin toxicity.....	63
Figure 15: Distal heme pocket of Cygb, showing primary mutagenesis targets	91
Figure 16: Pseudo-physiologic reduction of globins by the CYB5 system and Ascorbate	108
Figure 17: Globin reduction by NADH and CYB5R without CYB5	110

Figure 18: Michaelis-Menten kinetics of globin reduction by the CYB5 reducing system	112
Figure 19: Reduction of heme globins by varying concentrations of ascorbate.....	114
Figure 20: Initial velocity and kinetic fitting of globin reduction by ascorbate	115
Figure 21: Reference spectra of ferric and ferrous CYB5 showing isosbestic point at 568nm..	118
Figure 22: 568nm absorbance traces during the reaction of ferrous CYB5 with ferric globins.	120
Figure 23: Determination of reaction rate constants between CYB5 and globins.....	122
Figure 24: Simulated and measured reduction of <i>HsaCygb</i> by the CYB5 system and Asc	126
Figure 25: Electrostatic surface potentials of CYB5 and selected heme globins	129
Figure 26: Pseudo-physiologic reduction of zebrafish Cygbs by the zebrafish CYB5 system ..	137
Figure 27: Oxygen-binding equilibrium curves for <i>DreCygb1</i> and <i>DreCygb2</i> at 37°C	139
Figure 28: NO dioxygenation by zebrafish Cygbs supported by the zebrafish CYB5 system...	142
Figure 29: Two-phase kinetics of nitrite reduction by <i>HsaCygb</i> mutants	154
Figure 30: distal heme pocket of L46H <i>HsaCygb</i>	156
Figure 31: Kinetics of nitrite reduction by the H81Q <i>Cygb</i> mutant	158
Figure 32: Autoxidation of <i>HsaCygb</i> mutants.....	161
Figure 33: Reduction of V85I and wild-type <i>HsaCygb</i> by the CYB5 system and Asc.....	166
Figure 34: Timeline of mouse vasoactivity experiments documenting all infusions performed	176
Figure 35: MAP change in mice (n = 3) infused with Hb, nitrite, and ascorbate.....	178
Figure 36: MAP change in mice (n = 3) infused with V85I <i>Cygb</i> , nitrite, and ascorbate	179
Figure 37: MAP change in mice (n = 3) infused with V85I <i>Cygb</i> +CYB5+CYB5R, nitrite, and NADH.....	183
Figure 38: Effect of nitrite and NADH infusions on MAP of mice (n = 2).....	185
Figure 39: Effect on MAP of NADH administration with V85I <i>Cygb</i> , Hb, or no globin	186

LIST OF EQUATIONS

Equation 1-1: Rate of ligand binding to heme	22
Equation 1-2: Rate of ligand release from heme	22
Equation 1-3: Ligand binding reaction for a 6-coordinate globin	27
Equation 3-1: Rate calculation for bimolecular reaction	102
Equation 3-2: Bimolecular reaction of CYB5 and heme globin.....	103
Equation 3-3: Fitting equation for non-pseudo-first order conditions	104
Equation 3-4: Fitting equation to determine k_{fwd} and k_{rev} from η values	105

PREFACE

There are several groups that I would like to acknowledge, as this work would not have occurred without them.

Professionally, I owe a great debt to the entire Gladwin Lab group, especially my mentors Dr. Mark Gladwin and Dr. Jesus Tejero. They are an incredibly accomplished, dedicated group of people, and it's been a pleasure to work with them for four years.

Dr. Tony DeMartino in the Gladwin group, and Dr. Angela Fago and Elin Petersen at the University of Aarhus, were valuable collaborators. They were kind enough to perform experiments that were very important to this work, and the data they gathered is presented (with attribution) in later sections.

Finally, on a personal note, I cannot overstate the help that I received from my wife Ipek, my parents Brian and Darlene, and my cats Pretzel and Pixel. They did not contribute to this work in any material sense, but they provided constant support throughout my years of graduate school, and this dissertation would absolutely not exist without them.

1.0 INTRODUCTION

The work detailed in this dissertation is primarily concerned with the study of the hexacoordinate globins, a recently discovered group of proteins that are related to the more widely known globins hemoglobin and myoglobin. More specifically, this work emphasizes the study of cytoglobin, which is just one of the hexacoordinate globins. The study of cytoglobin and other proteins detailed herein has two overarching goals: to develop new insights into the function of these proteins and their potential roles in physiology and disease, and to explore the potential of various modification strategies to develop potential therapeutic molecules from these proteins.

While this focus on a relatively small group of proteins may not initially seem especially broad, heme globins exist within the context of several much broader biochemical and physiologic pathways. This introductory section attempts to provide an overview of some of the fundamental principles that underlie the work detailed in the remainder of this dissertation, and to provide the reader with enough context to understand the experiments performed and interpret their results. This begins with a cursory review of some key pathways in vascular physiology, mostly those related to heme globins and nitric oxide signaling. This is followed by a somewhat more in-depth summary of heme globins, including their general structural and functional characteristics. After discussing globins more generally, the introduction moves to a discussion of cytoglobin specifically, examining what is already known about this protein, how it functions, and what roles it has been theorized to play in normal physiology.

The introduction concludes with a brief summary of previous efforts to develop therapeutic molecules based on heme globins. These efforts have primarily focused on development of a globin-based oxygen carrier to provide oxygen to tissues in cases of blood loss or severe anemia. In the past several years, new efforts have also begun to explore the potential of heme globins to act as antidotal therapies, scavenging dangerous molecules (most prominently carbon monoxide) and thereby reducing the toxicity associated with exposure to these compounds. Reviewing these efforts, many of which have proven largely unsuccessful, provides an important glimpse into the challenges that must be overcome to develop a globin-based therapeutic that could eventually become part of clinical practice.

1.1 BASIC PRINCIPLES OF VASCULAR PHYSIOLOGY

While the work detailed in this dissertation largely consists of biochemical characterization of purified proteins, it nonetheless exists in the context of vascular physiology. In attempting to understand the native function of heme globins, as well as developing them as therapeutics, there are numerous signaling pathways in and around the vasculature that can be influenced by the activity of heme globins. Before discussing the specific work that was completed, it is important to summarize the normal physiology of the vascular environment, in order to appreciate how heme globins may either participate in or alter that physiology.

1.1.1 Blood and its components

Human blood can be broadly separated into two components: cells and plasma. The cellular component of blood includes erythrocytes (red blood cells), but also numerous cells of the immune system and platelets.

Red blood cells are the most numerous cellular component of blood, often making up 40% or more of the total blood volume. The primary function of the red blood cell is oxygen transport; it picks up oxygen in the lungs and delivers it to the tissues. In order to accomplish this task, the cells are filled with highly concentrated hemoglobin (Hb), with Hb in the cell often reaching concentrations of 30g/dL. The specific function of Hb will be discussed in greater detail in a subsequent section, but it is a protein that binds oxygen in the oxygen-rich environment of the lung, and then releases it in the lower-oxygen environment of the peripheral tissues. Many of the other components in the red blood cells primarily exist to facilitate oxygen delivery by hemoglobin. These include enzymes that support proper oxygen transport, such as cytochrome b5 (CYB5), a protein that prevents the accumulation of methemoglobin – an oxidized and largely nonfunctional form of Hb that cannot bind oxygen – by converting it, in conjunction with cytochrome b5 reductase isoform 3 (CYB5R3), back to the desired form. Most hereditary methemoglobinemias, in fact, arise from mutations of CYB5R3 rather than mutations of CYB5.

The other cells in the blood are leukocytes (white blood cells) and platelets. These make up a relatively small portion of the cells in the blood, and play roles that are less directly related to the work in this dissertation. Leukocytes are primarily cells of the immune system; their roles and functions are diverse and complex, and will not be discussed here. Platelets are technically not full-fledged cells, but rather remnants of larger cells, but play an important role in hemostasis and thrombosis. Following injury, platelets are recruited to the injury site and activated, at which

point they aggregate together and, along with other proteins, form a blood clot and hopefully prevent further blood loss. As with leukocytes, the details of platelet function are beyond the scope of this work. One aspect of platelet function worth noting, however, is that nitric oxide (NO), a molecule that is a key part of the work in this dissertation, has been shown to inhibit platelet function.

The plasma consists of the non-cellular portion of the blood, and if separated from the cells in the blood, is a light yellow or straw-colored liquid. Plasma contains a wide variety of molecules, including salts, proteins, and lipids. These solutes create oncotic pressure, a force that draws water from the extravascular space into the vascular compartment. A dramatic increase in the protein concentration within the plasma, as will occur after infusion of a protein-containing solution, can thus increase blood pressure by drawing additional fluid into the circulation.

Typically, levels of Hb in the plasma should be very low or effectively zero, but when red blood cells hemolyze (rupture), some Hb is released and can be temporarily found in the plasma. There are a number of other molecules that interact with free Hb in the plasma. Ascorbate (vitamin C) is present, and reduces extracellular Hb, in the same way that CYB5 reduces intracellular Hb. This reduction can also be performed by urate in the plasma [1]. Because elevated plasma Hb can have a variety of negative health effects (the reasons why will be discussed in a later section), the plasma also contains systems that are intended to scavenge free Hb. The most prominent such system is the protein haptoglobin, which binds to free Hb; the complex formed is removed from the plasma after binding to CD163 on the surface of macrophages, thus preventing the negative effects of high plasma Hb [2]. In conditions with chronic hemolysis (sickle cell anemia, thalassemia), haptoglobin depletion can occur, leading to complications from elevated plasma Hb. Similar complications have been observed following

infusion of heme globins as therapeutic molecules, and have greatly complicated previous efforts to develop treatments that utilize heme globins.

1.1.2 The Vascular Wall: Structure and Function

The vascular wall has a three-layered structure, with three distinct regions. Each layer has a distinct composition and specialized functions, but there is substantial signaling between the layers, with each layer influencing other layers in a variety of ways.

The tunica intima is the innermost portion of the vascular wall and makes direct contact with the blood. Typically, this layer consists of a single layer of endothelial cells. These cells serve as a barrier between the blood and the remainder of the body, regulating transport of solutes between the surrounding tissue and the blood. These cells also contain endothelial nitric oxide synthase (eNOS), an enzyme that uses L-arginine to make nitric oxide (NO). The resultant NO leaves the endothelium via passive diffusion, resulting in movement in all directions. While some will diffuse into the lumen of the vessel, another portion diffuses deeper in to the vascular wall, where it reaches the tunica media.

The tunica media sits outside the tunica intima (further from the lumen) and is composed almost entirely of contractile smooth muscle cells. As these cells contract, the diameter of the vessel decreases, increasing resistance to blood flow, thus increasing blood pressure and/or decreasing blood flow. As might be expected, this area is much larger in arteries than veins, as arterial walls have developed to maintain blood pressure via the increased stiffness and elastance of the wall, characteristics provided by the abundant smooth muscle. Vascular smooth muscle cells express a protein called soluble guanylate cyclase (sGC); when sGC binds nitric oxide, it

converts guanosine triphosphate (GTP) to cyclic guanosine monophosphate (cGMP), a compound that promotes relaxation of the smooth muscle.

The outermost layer of the vessel wall is the tunica adventitia. This layer is composed mostly of collagen and fibroblasts, and primarily serves to anchor the vessel in the surrounding tissue. Its contribution to vascular signaling is minimal, and it does not play an appreciable role in the vascular biology that is relevant to this dissertation.

1.1.3 Vascular Nitric Oxide Signaling

NO represents arguably the single most important signaling molecule in vascular physiology and is a major regulator of vascular tone and blood pressure. In fact, before the identity of NO was determined, it was referred to as endothelial-derived relaxing factor (EDRF) and was well-known to act as a potent vasodilator.

NO in the vasculature has two major sources: it is produced from L-arginine by eNOS in vascular endothelium, and it is produced from the nitrite anion by Hb via nitrite reduction, a process that requires one electron and one proton. Interestingly, these two processes occur in different conditions: NO production by eNOS requires oxygen, while hypoxia increases the rate of nitrite reduction to NO by Hb, as only deoxyhemoglobin (not oxyhemoglobin) is capable of this reaction.

As mentioned in the previous section, the primary mechanism by which NO causes vasodilation is via stimulation of sGC in the smooth muscle. After stimulation by NO, sGC produces cGMP, which promotes relaxation of the vascular smooth muscle. This specific pathway has become a major pharmacologic target. Perhaps the most well-known drug that

targets this pathway is Sildenafil (commercial names include Viagra and Revatio), which slows the degradation of cGMP and thus prolongs the vasodilatory signaling that originates with NO.

Sildenafil illustrates an important principle in pharmacologic manipulation of NO signaling pathways: as a radical, NO is highly reactive, and in plasma the half-life of NO is typically on the order of several seconds. As a result, exogenous NO administration is unlikely to have any lasting therapeutic effect. This has spurred a search for other molecules that can provide a longer-lasting manipulation of NO signaling. One such molecule is nitrite.

Nitrite, NO_2^- , participates in numerous signaling pathways. The most important fate of nitrite in the context of this work, however, is its conversion to nitric oxide via nitrite reduction. This reaction can be performed by numerous proteins, including virtually all heme globins. This reaction requires deoxygenated heme, however, and thus only occurs at appreciable rates under hypoxic conditions. Nitrite reduction by deoxyhemoglobin has been shown to play a role in hypoxic vasodilation, with infusion of sodium nitrite increasing blood flow in human subjects.

Nitrite is often obtained from the diet, either through direct intake of nitrite or through consumption of nitrate. While humans lack the enzymes to convert nitrate to nitrite, the normal bacterial flora that inhabit the human mouth can make nitrite from nitrate. Recently, oral or injected nitrite (usually as sodium nitrite) has been explored as a potential therapy to manipulate NO signaling. Because nitrite is converted to NO, but has a substantially longer half-life in plasma than NO itself, treatment with nitrite can provide longer-term modulation of NO signaling than direct administration of NO itself. Coadministration of nitrite with globin-based therapeutics has been documented to have some effect on blood pressure [3], and this interaction between heme globins and nitrite is fundamental to much of the work detailed in this dissertation.

1.2 HEME GLOBINS

1.2.1 Structure of Heme Globins

While the exact structure of heme globins varies substantially, there are some broad structural characteristics shared by all heme globins. Figure 1 depicts the structure of Cytochrome b5 (Cygb), and provides an example of these universal structural features. Every heme globin consists of two parts: a heme molecule and a globin protein. The first part, the heme prosthetic group, is composed of a porphyrin, a small, roughly circular organic molecule, and an iron atom in the center of the porphyrin. In figure 1, the porphyrin is shown in tan, while the iron atom is shown in red. The globin itself is a protein that folds around and binds the porphyrin, and is depicted in dark grey in figure 1. In general terms, the protein folds such that some empty space is left on both sides of the heme; these spaces are referred to as the “heme pocket”, with one side referred to as proximal (below the plane of the heme group in figure 1) and the other side referred to as distal (above the heme in figure 1).

There are also typically two histidine residues, depicted in teal in figure 1, that extend into these spaces, with one histidine on each side; they are accordingly referred to as the proximal and distal histidine. In some globins, including Cygb, both histidines are able to directly coordinate with the heme iron, while in other globins the distal histidine sits slightly further from the heme iron and is thus incapable of direct binding. This difference in histidine position is relatively minor in terms of molecular structure, but nonetheless has significant ramifications for the function of heme globins, and will be explored in greater detail in a subsequent section.

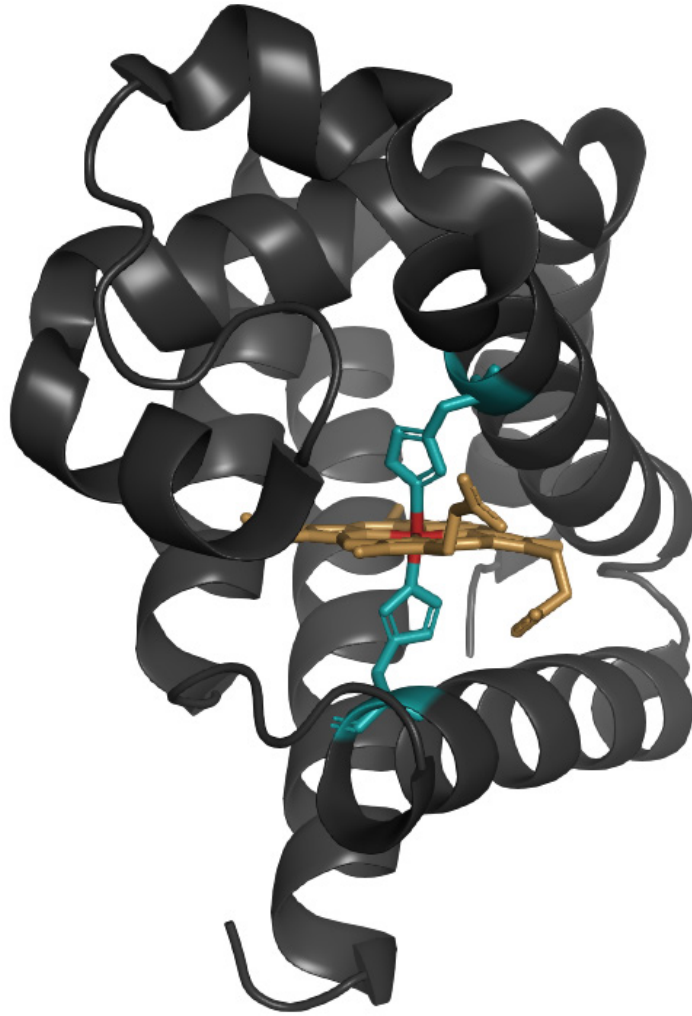


Figure 1: Cytoglobin, a Typical Heme Globin

While no two heme globins possess identical structures, most exhibit a fairly similar configuration. In addition to the heme group and the proximal and distal heme pockets (and corresponding histidines), the proteins themselves are typically made up of eight separate α helices, designated A through H, as well as short “loops” that connect these helices. Figure 2 depicts Cygb again, with helices A through H each having unique colors and labels. Figures 1 and 2, as well as all other figures depicting protein structure, were generated using PyMol software (Schrodinger LLC).

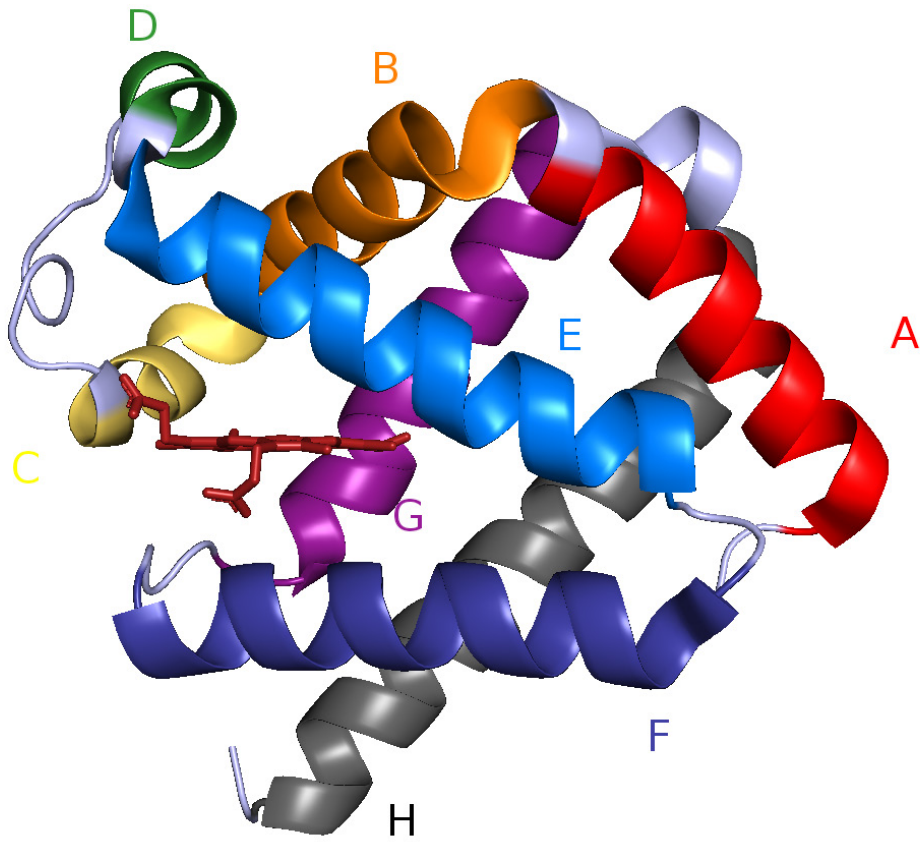


Figure 2: Cygb structure, identifying helices A-H

These helices allow for easy identification of corresponding residues between different globins: for example, the distal histidine sits in position 64 in Ngb, but position 81 in Cygb. However, in these two proteins and virtually all other vertebrate globins, it is the 7th amino acid in the E helix, and thus can be referred to as “E7”. These designations become very important when generalizing the effect of single amino acid mutations in different globins, as the more general helix-based notation stays consistent between proteins.

Each heme globin molecule has multiple active sites, specific chemical groups within the protein structure that are responsible for the various functions performed by these proteins. Figure 3 features yet another depiction of Cygb, this time from a different angle, and highlights the key active sites present on the molecule. The most important of these active sites, which is present in all heme globins and is required for many of their canonical functions, is the iron in the center of the heme group, shown in red in figure 3. This iron is the site of a wide variety of functions including ligand binding and electron transfer reactions. Another important active site on many globins is found at cysteine residues on the protein surface. Cygb has two such residues, which are shown in green in Figure 3. These cysteine residues possess reactive thiol (-SH) side chains (colored yellow in Figure 3), which can form disulfide bridges with other thiols on the same protein or other molecules, as well as participate in other redox-sensitive reactions. In certain cases, the redox state of these thiols has been implicated in regulation of globin function, affecting such characteristics as ligand affinities and reaction kinetics at the heme iron.

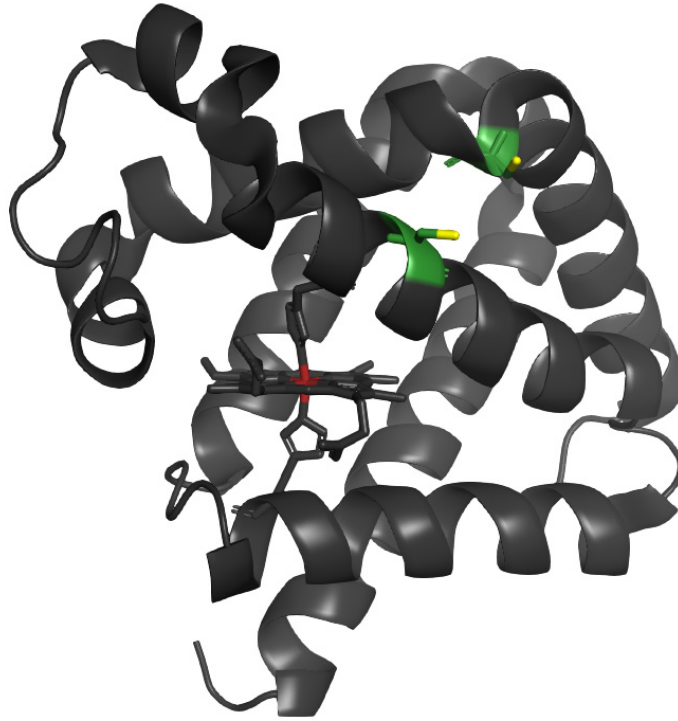


Figure 3: Active Sites of Cytoglobin

One final important structural variation in heme globins relates to the size of the globin molecule. There are two primary determinants of globin size: the length of the globin protein and the number of subunits that combine into a single functional unit. A single subunit is most commonly defined as one heme group and one surrounding globin. The subunits of the human globins vary in size from roughly 15 to over 20 kilodaltons (kDa). Many human globins, including myoglobin (18 kDa), neuroglobin (17 kDa), and cytoglobin (21 kDa), often exist as single-subunit monomers. Hemoglobin, however, the protein responsible for oxygen transport in blood and perhaps the single most-studied protein in human history, primarily exists as a tetramer, with two 16 kDa alpha chains and two 16 kDa beta chains combining to form a single 64 kDa molecule. The size of a globin can have a significant effect on globin function by

influencing the compartmentalization and diffusion of the protein *in vivo*. This size variation is illustrated in figure 4, which depicts the 18 kDa Mb monomer as well as the 64 kDa Hb tetramer.

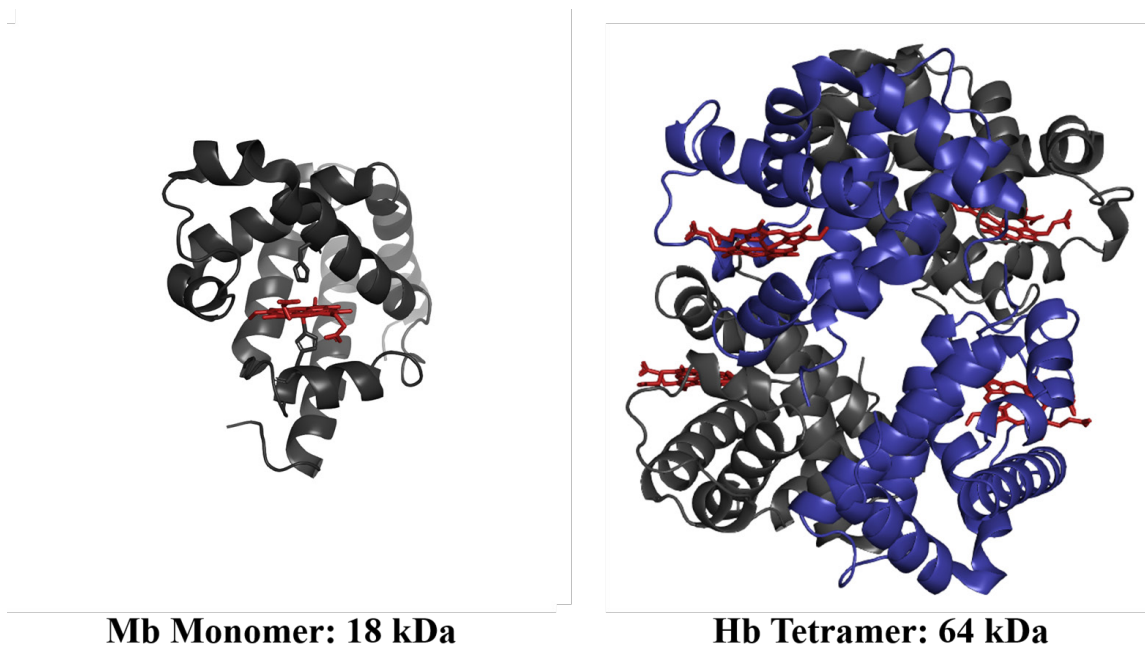


Figure 4: Size comparison of Mb and Hb

1.2.2 The Globin Superfamily in Vertebrates

The heme globin superfamily consists of hundreds, if not thousands, of individual proteins, in organisms from bacteria and archaea all the way up through plants and animals. This work will focus only on those globins found in vertebrate animals. While this sample represents a very small portion of all known globins, it nonetheless includes a significant number of globins with a lengthy evolutionary history.

Even more specifically, this work will directly characterize globins from two animals: humans (*Homo sapiens*, with all proteins designated by *Hsa*) and zebrafish (*Danio rerio*, with all proteins designated by *Dre*). Humans and zebrafish represent nearly opposite ends of the evolutionary spectrum of vertebrates, with fish representing the most ancient vertebrates, and humans one of the more recently evolved. Despite this evolutionary distance, zebrafish have emerged as a valuable model organism, well-suited to studies involving developmental biology and organogenesis. Furthermore, every mammalian globin has at least one ortholog in zebrafish, making zebrafish a useful model for the study of heme globins.

Much like vertebrate animals themselves, the vertebrate globins lie on an evolutionary spectrum, which has been elucidated through phylogenetic analysis and is depicted in figure 5.

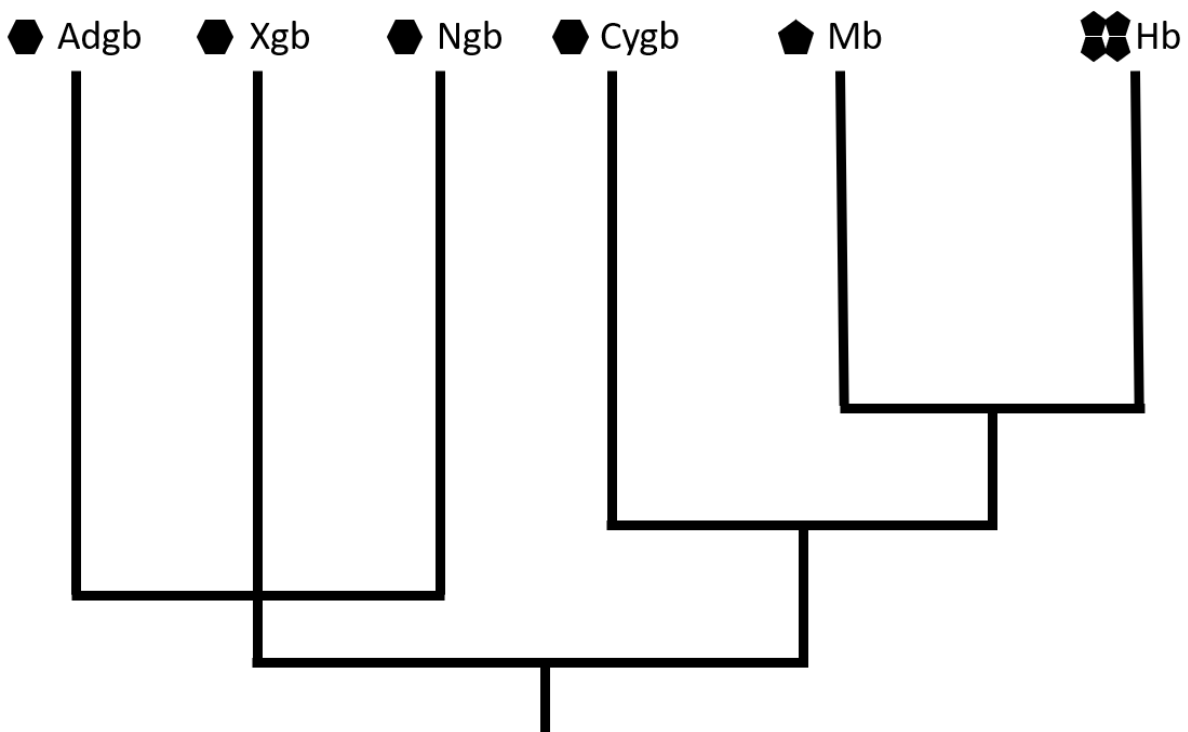


Figure 5: Simplified phylogeny of vertebrate globins

The most ancient vertebrate globins are now thought to be the precursors to androglobin (Adgb), neuroglobin (Ngb) and globin X (GbX), though the exact order in which these three globins developed has not been determined. These three globins all possess hexacoordinate hemes (the difference between hexa- and pentacoordination will be discussed in detail later), suggesting that hexacoordination was the original coordination state of the globin heme. Pentacoordinate hemes, as found in the most recently-evolved respiratory globins hemoglobin (Hb) and myoglobin (Mb), are thought to be the result of a relatively recent divergence event. Cytoglobin (Cygb), which is almost always hexacoordinate, is now believed to represent something of a transitional state between the ancient globins and the newer pentacoordinate globins, and one that may provide valuable insight into the evolution of vertebrate globins.

Different vertebrate animals have varying profiles of globin expression. Zebrafish, for example, express all globins shown in figure 5 and, along with all other teleost fish, even possess two different cytoglobin (Cygb) genes and proteins, arising from an ancient gene duplication event and subsequent divergence. Mammals, including humans, express a more limited set of globins which does not include some of the more evolutionarily ancient proteins like GbX. The most well-studied mammalian globins are Hb and Mb, but humans also express their own forms of Ngb, Cygb, and Adgb.

1.2.3 Prominent Functions of Heme Globins

Heme globins are versatile proteins that have been documented to perform a wide variety of functions and fill a number of important physiologic roles. The full range of these functions is far too extensive to discuss here and continues to expand as globins are further characterized. Most

of these arise from a relatively small number of biochemical reactions performed by heme globins, the most important of which are summarized in figure 6.

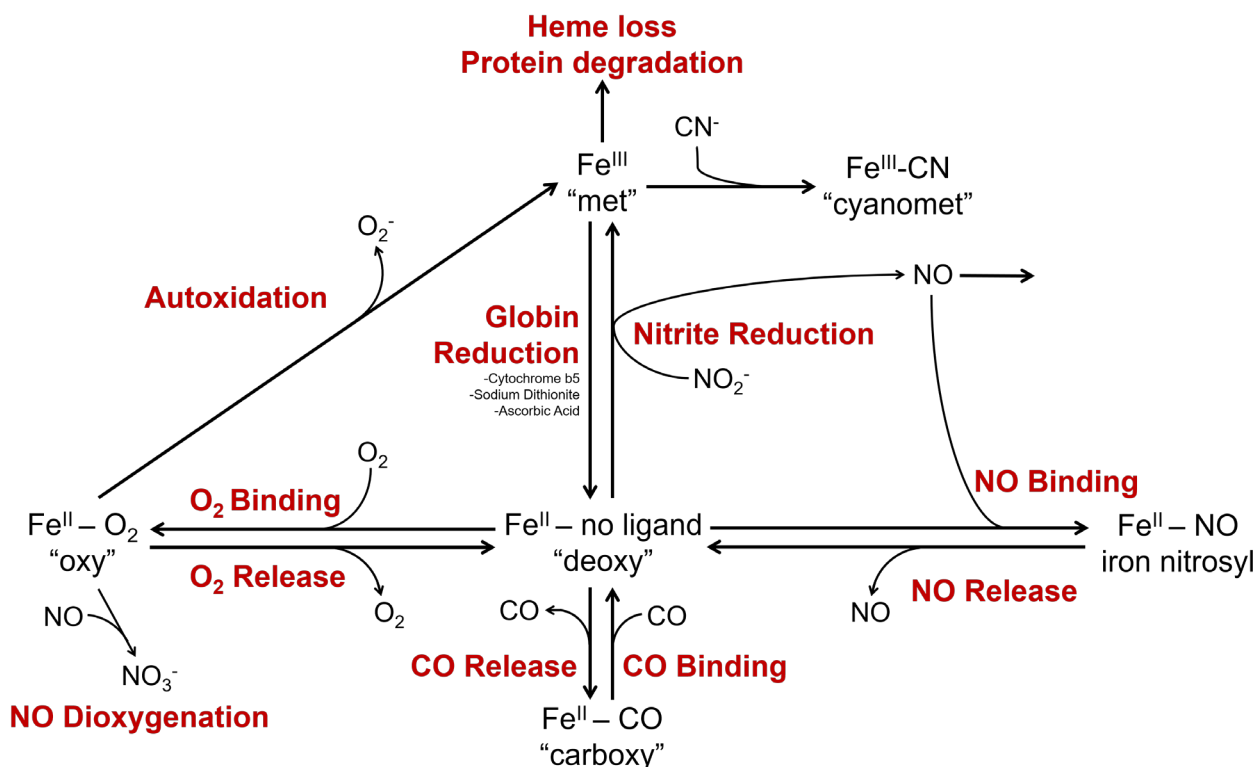


Figure 6: Summary of important heme globin reactions

1.2.3.1 The Role of the Heme Iron Redox State

Iron, like many other metals, can exist in numerous different redox states, and the specific redox state of the iron atom is a major determinant of globin function. The two most common redox states for the heme iron are the reduced, Fe^{II} , ferrous state, and the oxidized, Fe^{III} , ferric or "met" state. There is also a Fe^{IV} ferryl state, but this is formed during reactions with peroxides or other oxidants and is largely beyond the scope of this work. The ferric iron is unable to perform many

prominent heme globin functions, to be discussed below, but is also inherently less stable than the ferrous form; prolonged time in the ferric state can ultimately lead to the loss of the heme group from the protein and subsequent protein degradation. This is prevented via the action of various reducing systems that exist to transfer an electron to the ferric iron, returning it to the ferrous state.

This work focuses on two different reducing systems that are known to reduce heme globins (converting the ferric state back to the ferrous). The first of these is ascorbate or ascorbic acid, a small molecule that can donate two electrons to a variety of different downstream targets. Ascorbate is more commonly known as vitamin C and is perhaps the best-known of the “antioxidant” (or, put another way, pro-reductant) molecules that have become a focus of certain health-related products and schools of thought. Ascorbate is known to reduce hemoglobin in plasma and has been shown to reduce many other heme globins, including Cygb.

The second reducing system covered in this work is Cytochrome b5 (CYB5). CYB5 is itself a hexacoordinate heme protein, but unlike the globins, is incapable of binding oxygen or any other ligand. Instead, the function of CYB5 seems to revolve entirely around electron transfer. One form of CYB5, CYB5a, is found in relatively high concentrations in the red blood cells, where it is the primary reducing agent for Hb. Under normal conditions, 2% of Hb in RBCs oxidizes every day; accumulation of oxidized Hb is prevented by CYB5a, which reverses this process. CYB5a has also been identified in the liver, appearing in human liver microsomes, while CYB5b is found in a variety of somatic tissues. Besides heme globins, numerous other targets of CYB5b have been identified, including Cytochrome P450 enzymes in the liver.

CYB5 provides electrons to its identified targets via direct transfer but is largely nonfunctional in this role without other important components. After CYB5 passes an electron to

a target molecule, CYB5 is in turn reduced by its own specialized reductase, CYB5 reductase (CYB5R). CYB5R is a flavin-based protein and requires its own source of electrons in turn; this role is filled by NADH, which serves as the initial source of electrons and allows reduction by what is referred to as the CYB5/CYB5R/NADH system.

These reducing systems prove extremely important, as numerous different function of heme globins require specific redox states, with many functions only being performed by the ferrous state of the protein. Among the functions performed by heme globins, arguably the most common and most well-documented is the binding of various gaseous ligands at the heme iron. This binding generally requires the ferrous form of the protein, and is most commonly characterized in terms of the affinity of a globin for a specific ligand.

An important principle in understanding the redox functions of heme globins is the idea of redox potential. A protein's redox potential is a standardized measurement of its ability to donate or receive electrons. In general, if two molecules with different redox potentials interact, the one with the lower redox potential will transfer electrons to the one with the higher potential. The rate of this transfer can depend on many factors. The most comprehensive description of electron transfer is the Marcus theory of electron transfer, named for 1992 Nobel Laureate Rudolph Marcus. To dramatically oversimplify the Marcus theory, the rate of electron transfer will typically increase as the difference in the compounds' redox potentials (the "driving force") increases. Table 1 lists the redox potential of several globins, as well as CYB5 and CYB5R.

Table 1: Redox potentials of selected heme globins, CYB5, and CYB5R

<i>Protein</i>	<i>Redox potential (mV)</i>	<i>Reference</i>
<i>HsaCygb</i>	-37	[4]
<i>DreCygb1</i>	-58	[4]
<i>DreCygb2</i>	-26	[4]
<i>Ngb</i>	-118	[5]
<i>GbX</i>	-119	[6]
<i>swMb</i>	59	[7]
<i>Hb</i>	85	[8]
<i>CYB5</i>	-40	[9]
<i>CYB5R</i>	-265	[10]

1.2.3.2 Ligand-binding behavior: kinetics and affinity

All heme globins have characteristic affinities for each ligand they are able to bind. Affinity, in this context, refers to the tendency of the heme iron to bind a specified ligand, and is typically expressed in terms of the fractional saturation (the fraction of all heme iron atoms that have bound a specific ligand) at specific ligand concentrations. This is most thoroughly expressed as a saturation curve, depicting the fractional saturation at a wide range of ligand concentrations or partial pressures, typically whatever range is necessary to go from 0% saturation up to 100%. Sample saturation curves can be seen in figure 7.

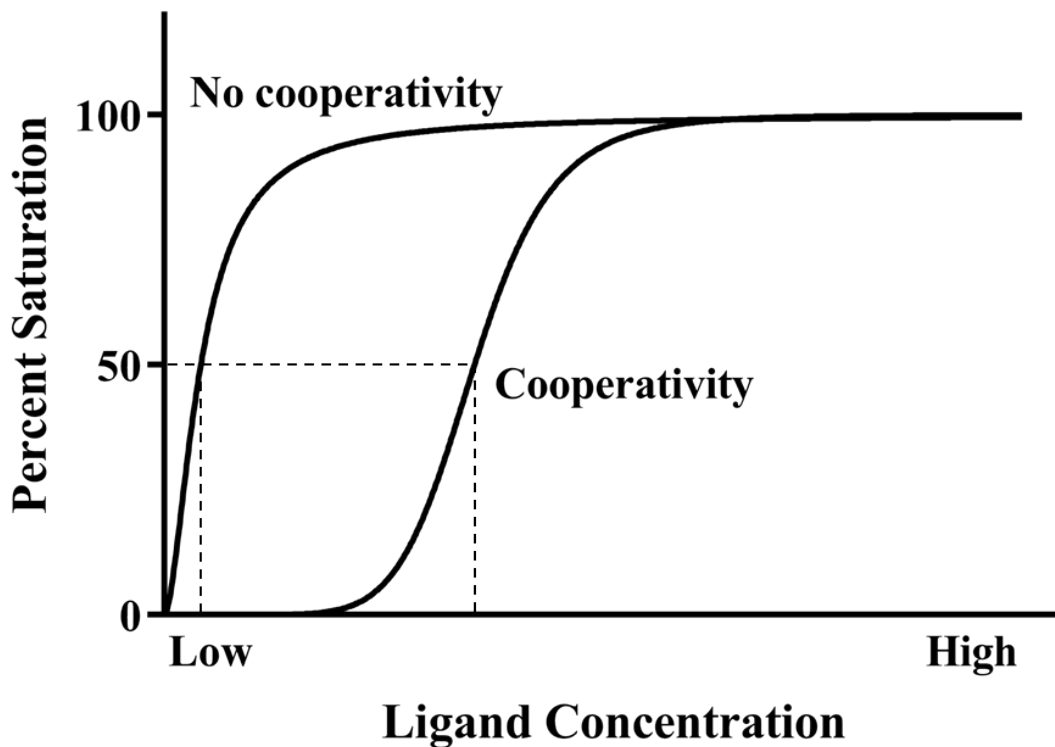


Figure 7: Sample Ligand-Binding Equilibrium Curves

There are two different curves depicted, one hyperbolic (on the left) and one sigmoidal (on the right). The hyperbolic curve represents ligand-binding behavior in a globin with no cooperative binding, such as myoglobin. The sigmoidal curve, on the other hand, resembles the data seen for a globin that exhibits cooperativity, such as hemoglobin. The mechanism underlying cooperativity, as well as its physiologic and functional significance, will be discussed in a subsequent section. The affinity of a globin for a certain ligand can be more concisely expressed as the P_{50} , or half-saturation point, the partial pressure of a specific ligand that results in 50% globin saturation. Because of this convention for defining the P_{50} , a low P_{50} value somewhat non-intuitively indicates very high affinity, and vice versa. For the two hypothetical

globins depicted in figure 7, the P_{50} values are the concentrations where the dotted lines intersect with the x-axis. Of course, while P_{50} provides a quick indication of ligand affinity, certain information, including the presence or absence of cooperativity, cannot be communicated with this single value. Hb in red blood cells, for example, has an oxygen P_{50} of approximately 27 mmHg, and also exhibits significant cooperativity, with an equilibrium curve similar similar to the sigmoidal curve in figure 7.

These affinities are largely a consequence of the kinetics of ligand binding and release. For every combination of globin and ligand, there are specific rates at which the unbound globin will bind free ligand molecules, and once bound, specific rates at which the ligand will be released. Both processes are constantly occurring, and even when the overall fractional saturation of a globin remains steady, individual globins and ligands are constantly in flux, with binding and unbinding events continually occurring. Increasing the concentration of ligand increases the overall binding rate. The release rate increases similarly as the saturation increases. The rates of ligand binding and release for a heme globin solution depend upon the intrinsic k_{on} and k_{off} of the heme globin-ligand pair, but also the concentrations of free ligand, unbound heme, and ligand-bound heme. These rates are given by equations 1-1 and 1-2.

$$\text{Rate of ligand binding} = k_{on} * [\text{ligand}] * [\text{unbound heme}] \quad \text{Equation 1-1}$$

$$\text{Rate of ligand release} = k_{off} * [\text{ligand-bound heme}] \quad \text{Equation 1-2}$$

The overall affinity of a heme globin for a specific ligand is proportional to the ratio of the k_{on} value to the k_{off} value. A very high k_{on} and very low k_{off} , for example, will result in very

high-affinity binding (and consequently a very low P_{50} value), with complete saturation at even low concentrations of ligand, and very slow release even if the ligand concentration further decreases.

1.2.3.3 Reactions of Unbound Ferrous (Fe^{II}) Heme Globins

The most common reaction for ferrous heme globins with no bound ligand is the reversible binding of a gaseous ligand. Oxygen is the canonical ligand for hemoglobin and myoglobin, and has been documented to bind cytoglobin and neuroglobin as well. In general, compared to other gases, the affinity for oxygen tends to be relatively low. This low affinity becomes very important, as it allows for release of bound oxygen in regions of tissue with relatively low levels of oxygen. This principle is what allows hemoglobin to function as an oxygen transporter; in the high-oxygen environment of the lungs, the protein is completely saturated with oxygen, but in less oxygenated peripheral tissues, some oxygen becomes unbound and can diffuse into the surrounding tissue. In less oxygenated tissue, the amount of oxygen released will increase, thus matching oxygen supply from hemoglobin to the oxygen demand of the tissue.

The other gaseous ligands that are most commonly bound by heme globins are carbon monoxide (CO) and nitric oxide (NO). In general, globins exhibit much higher affinity for these gases than for diatomic oxygen, with their affinity for NO typically being the highest. Because the affinity for these gases greatly exceeds that for oxygen, significant concentrations of either gas will effectively outcompete and displace oxygen from heme globins. This mechanism is one of the underlying drivers of carbon monoxide poisoning. Sufficient dissolved CO in the blood will take the place of oxygen on hemoglobin, preventing oxygen transport to tissues and resulting in tissue hypoxia. While this is theoretically also possible for NO, the half-life of NO in living organisms tends to be very short, as NO is consumed by numerous sources including

oxygenated heme globins (to be discussed in more detail later). Practically, this means that NO does not accumulate to a level that can displace a meaningful amount of oxygen from hemoglobin, and thus does not demonstrate similar toxicity to CO.

In addition to binding gaseous ligands, heme globins in the ferrous state have been shown to participate in various electron transfer reactions. The most significant of these reactions for this work is nitrite reduction, in which the nitrite anion (NO_2^-) is converted to NO via a one-electron transfer from the heme iron. The first step in this process is binding of nitrite to the heme iron; because nitrite must compete with oxygen for any available binding sites, this reaction becomes far more prevalent in hypoxic conditions. There is ample evidence to suggest that nitrite reduction and NO generation by deoxyhemoglobin in red blood cells is a major contributor to the process of hypoxic vasodilation, wherein the vasculature in hypoxic areas dilates to increase blood flow and oxygen delivery to the region.

1.2.3.4 Reactions of Oxygen-bound Heme Globins

Following oxygen binding, the oxygenated $\text{Fe}^{\text{II}}\text{-O}_2$ or “oxy” form of a heme globin can perform a number of different reactions. The first, which has been discussed above, is oxygen release. All oxygen-bound globins will release oxygen with some characteristic off rate, regardless of oxygen concentration in the immediate environment. However, with high enough local oxygen levels, this release will likely be followed immediately by rebinding.

The second is a process referred to as autoxidation. This is a chemical reaction in which the heme iron transfers an electron to bound oxygen. The oxygen is released as a superoxide radical, and the iron is oxidized to the ferric form. Every globin that is capable of binding oxygen autoxidizes at a characteristic rate. For hemoglobin, for example, this rate is relatively slow, with roughly 2% of oxy-hemoglobin autoxidizing per day.

A third important reaction performed by oxygen-bound heme globins is nitric oxide dioxygenation. In this reaction, oxygen-bound globin reacts with free nitric oxide. This reaction results in the conversion of nitric oxide to the nitrate anion, and the oxidation of the heme iron to the ferric state. Recent studies have suggested that this specific function may play a key role in controlling the diffusion of NO through various tissues *in vivo*, and likely functions as a prominent regulator of NO signaling.

1.2.3.5 Reactions of Ferric (Fe^{III}) Heme Globins

While the ferric form of globins is often considered somewhat nonfunctional, as it is incapable of binding canonical ligands like oxygen, it is typically able to take part in several different reactions.

Perhaps the most common reaction of ferric globins is a reaction with any of a number of different reductases in which an electron is transferred from the reductase to the heme iron, reducing the heme back to the typically more-desirable ferrous state. As mentioned elsewhere, common reductases that perform this role include ascorbate (vitamin C) and Cytochrome b5.

However, there are certain reactions that require the heme iron to be in the ferric state. The most relevant of these is binding of cyanide (CN⁻), which can only occur with ferric heme. Because cyanide is highly toxic to tissue (via disruption of the mitochondrial electron transport chain), one therapy that has been used for cyanide poisoning consists of administering a large dose of a chemical, often sodium nitrite, that oxidizes Hb to the ferric state. This ferric Hb is then able to bind the cyanide in the blood, preventing it from reaching the tissues and causing harm.

Another reaction that requires the ferric heme is reductive nitrosylation. While the ability of ferrous Hb to bind NO has already been discussed, ferric Hb has also been shown to bind NO. This ferric-NO Hb formed then decays into the ferrous-NO form of Hb, which can subsequently

react with hydroxide ions to generate nitrite. In many ways, this reaction is considered the reverse of nitrite reduction, and further characterization of the reaction's mechanism and potential physiologic significance is ongoing [11]. While this reaction is very interesting from a biochemical standpoint, it is largely unrelated to the work performed in this dissertation and will not be discussed further in subsequent sections.

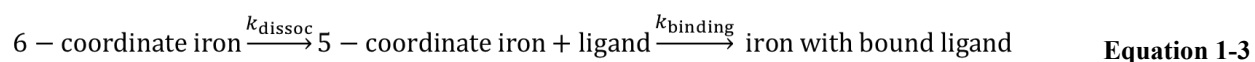
Finally, globins in the ferric form are generally less stable than the ferrous form, as the protein component of the globin has a lower affinity for the ferric heme than the ferrous, and thus is more likely to release the heme [12]. Extended time in the ferric form can lead to the heme group being lost from the protein, and subsequent denaturation and loss of the protein. Similar behavior can be seen in other non-globin proteins that include a heme group, such as soluble guanylate cyclase. This is likely to be a rare occurrence *in vivo* under normal conditions because, as mentioned previously, most globins are accompanied by one or more reductases that function to limit the accumulation of the ferric form.

1.2.4 Key modulators of heme globin function

While heme globins all exhibit a certain degree of similarity in terms of both structure and function, no two globins are exactly alike, with each possessing a unique set of functional characteristics. While the specific differences that result in this functional variation relate to many aspects of protein structure, there are a few specific characteristics that can exert a large influence on the activity of heme globins, typically by modulating the shape and size of the heme pocket or the availability of the heme iron to perform chemical reactions.

1.2.4.1 Heme coordination state and distal histidine binding

In some heme globins, the distal histidine is able to directly coordinate with the heme iron. Because the distal histidine occupies the iron's sixth coordination site, these proteins are referred to as hexacoordinate heme globins. Cygb, Ngb, and GbX are all hexacoordinate globins. In these proteins, the distal histidine proves to be a major determinant of protein activity. Iron is only capable of forming six coordinate bonds, and so while the distal histidine is bound to the iron, the protein is unable to bind ligands or perform any reactions. In order for a ligand to be bound by the heme iron, the distal histidine must first dissociate, which occurs with some characteristic rate constant k_{dissoc} . This reaction is reversible, and the distal histidine can subsequently reassociate with some rate constant k_{assoc} ; this reassociation will compete with binding of an exogenous ligand to the heme iron. As such, any ligand binding is actually a two-step process in hexacoordinate heme globins, with distal histidine dissociation followed by a second ligand-binding step, which proceeds according to some rate constant $k_{binding}$. The overall scheme of this reaction is shown in equation 1-3:



For most such reactions, the rate constant for distal histidine dissociation proves far slower than the rate constant for binding. Consequently, for ligand binding and reactions like nitrite reduction at the heme iron, distal histidine dissociation functions as the rate-limiting step for the overall reaction. This provides a unique opportunity for protein engineering; numerous studies have shown that replacing the distal histidine with a residue with a smaller side chain, one that cannot bind the heme iron, can massively influence protein activity. An H64Q mutant of

Ngb, for example, where the distal histidine is replaced with a smaller glutamine residue, is capable of reducing nitrite roughly 500 times faster than the wild-type protein [13].

Those globins in which the distal histidine cannot directly bind the heme iron, by contrast, are referred to as pentacoordinate globins. Hb and Mb are both pentacoordinate globins. In these globins, the distal histidine can act to stabilize bound ligands, but does not affect the rate of reactions at the heme iron. As expected, mutations of the distal histidine in pentacoordinate globins have been shown to have a relatively minimal effect on overall protein reactivity.

1.2.4.2 Cooperativity

Figure 7 depicts two different equilibrium curves for ligand binding, one hyperbolic and one sigmoidal. The sigmoidal shape arises as a result of cooperativity, a process that exclusively affects multi-subunit globins. In these globins, reactions at one subunit can affect the reactivity of the others, typically by induced shifts in the spatial arrangement of the protein as a whole.

Hb natively exists as a tetramer and is the canonical example of cooperative binding in heme globins. Each hemoglobin subunit can exist in two states, the “tense” T state, and the “relaxed” R state. When all four of the subunits of Hb are unbound, the protein is in the T state, and exhibits relatively low ligand affinities and reaction rates. As binding sites are occupied, however, all four of the subunits shift toward the R state, with higher ligand affinities and reaction rates. This gives rise to the sigmoidal curve shape seen in figure 7; as saturation begins to increase from 0%, the affinity of the remaining unbound sites for the ligand increases. As the affinity increases, a set increase in ligand concentration will result in a greater increase in saturation, resulting in a steeper slope. The affinity continues to increase all the way up to a maximum value at 100% saturation, where the protein is fully in the R state. As this occurs, the number of available binding sites decreases, and eventually very few sites remain available. This

reduced availability of binding sites limits additional binding, causing the equilibrium curve to flatten back out and approach 100% saturation asymptotically, despite the continuing increase in affinity with increased saturation.

1.2.4.3 Thiol residues and disulfide formation

Another powerful modulator of heme globin activity is the redox and binding state of surface thiols on globin proteins. Many (but not all) globins have one or more cysteine residues on the surface of the protein. Cysteine features a thiol group (-SH) in its side chain, and like all thiols, these side chains are both reactive and redox sensitive, and thus represent an important regulator of protein function.

The simplest state for a thiol is the reduced state (R-SH). When surface thiols are in this state, the function of the protein is generally found to be similar to that of mutants that have had the cysteine residues removed; this thiol-reduced state can thus be thought of as “neutral”, with no appreciable influence on protein activity.

The thiols can also become oxidized, which often results in the binding of another thiol to form a disulfide bridge (R-S-S-R). These disulfide bridges can be formed between any two thiols in close enough proximity to bond. As such, these disulfides can be formed between thiols on two different molecules or proteins (intermolecular disulfides), or between two thiols on the same protein (intramolecular disulfide).

Intermolecular disulfides can result in the formation of protein multimers, as multiple proteins are joined via disulfide linkages. These can be homo- or heteromultimers, as the identity of the protein does not matter as long as thiols are present. While this can greatly influence protein size, the overall effect on protein activity seems to generally be minimal, as the conformation of the protein itself is not dramatically altered by the formation of these bonds.

Intramolecular disulfides, on the other hand, have been shown to exert large effects on protein activity. This effect was first observed in Ngb, where disulfide formation was found to have effects on both the oxygen affinity and nitrite reduction rate of the protein [13, 14]. In Cygb, disulfide formation has been shown to increase nitrite reductase rates by well over an order of magnitude [15]. The putative mechanism for this change relies upon the proximity of one of Cygb's cysteine residues (C83, in the 83rd position) to its distal histidine (H81, in the 81st position). When C83 binds C38, the resultant disulfide bond exerts tension on the protein helix that contains both C83 and H81. This tension is believed to displace the distal histidine slightly, in a way that favors dissociation of the distal histidine from the heme iron. As was discussed in previously, this dissociation is the rate-limiting step in nitrite reduction. By increasing its rate substantially, the overall rate of nitrite reduction is also seen to increase greatly. In a related fashion, there is evidence that intramolecular disulfide formation in Ngb greatly increases the oxygen affinity of the protein (P_{50} drops from roughly 10 to 1 mmHg), again by altering the relative binding affinity of the distal histidine for the heme iron [16]. The disulfide-induced structural change in Ngb has been reported to be much larger than the corresponding change in Cygb, potentially explaining the much larger effect on oxygen affinity in Ngb [17].

Cysteine residues can also bind other molecules beyond simply other cysteines. One well-studied cysteine variant is a nitrosothiol (-RSNO). S-nitrosothiols are formed as the product of S-nitrosation, a reaction between a thiol (specifically in the form of a thiolate, $R-S^-$) and some form of nitrosating species, typically HNO_2 or N_2O_3 [18]. These nitrosating species are formed from either nitrite under acidic conditions, or NO in the presence of oxygen. This is thought to be a relatively common method of post-translational modification of proteins and has been implicated as a contributor to numerous signaling pathways in both normal and pathologic

conditions. Hb with nitrosothiols, referred to as SNO Hb, has been suggested by some to play a role in nitric oxide transport in the blood and hypoxic vasodilation, although the exact extent of SNO Hb's role in these processes remains controversial.

1.2.4.4 External Factors

In addition to factors intrinsic to the heme globins, a wide variety of external molecules and conditions have been shown to influence heme globin affinity and reactivity.

Several external modifiers of Hb function have been discovered and well characterized. Among the most important are the compound 2,3-diphosphoglycerate (2,3-DPG), pH, and carbon dioxide. 2,3-DPG stabilizes the T state of Hb, decreasing ligand affinity and causing a rightward shift of the equilibrium curve. High levels of 2,3-DPG are present in red blood cells, and this significantly affects the function of intraerythrocytic Hb. In the red blood cell, Hb has an oxygen P_{50} of about 26.6 mmHg. In contrast, when Hb is removed from the cell and washed to remove 2,3-DPG, forming what's referred to as "stripped hemoglobin", the oxygen P_{50} is much lower, somewhere around 4 or 5 mmHg (much higher affinity).

H^+ and CO_2 also both act as T-state stabilizers. As pH decreases, Hb's affinity for oxygen decreases, promoting oxygen release in acidic tissues. This has been named the Bohr Effect, and is physiologically significant mostly due to the contribution of carbon dioxide to local pH. CO_2 in solution can form carbonic acid, which lowers pH; as CO_2 levels increase, the pH becomes more and more acidic. Because CO_2 is a product of respiration, highly metabolically active tissues (such as contracting muscle) will generate more CO_2 . This will lower the pH, and as both protons and CO_2 accumulate they will promote oxygen release in that area, thus supplying more oxygen to metabolically active tissue and supporting ongoing respiration. The Bohr Effect

appears to be specific to Hb, however, as other globins such as Mb have not been shown to exhibit any change in ligand affinity in the presence of CO₂.

Many globins have also been found to bind lipids, which is thought to perform several different functions. Most simply, lipid binding allows globins to become membrane-associated, a pattern that seems especially common in bacterial globins. This can allow localization of globins to specific regions or organelles where some specific function of the globin, such as NO consumption or peroxidase activity, is required [19]. There is also some evidence that lipid binding can influence heme globin structure and activity, with the binding of certain classes of lipids changing the behavior of the globin. This effect has been well-documented in Cygb, and will be discussed in detail in a subsequent section [20].

Finally, globin activity can be influenced by more general environmental influences. Rather than any specific molecules, general factors like temperature and pH also influence globin activity, as they affect most chemical reactions. Increased temperature will typically increase the rate of reactions involving globins, including redox reactions like nitrite reduction. Increased temperature is also known to decrease the affinity of Hb for oxygen, likely by increasing the rate of oxygen release from the protein. Because the temperature increases in metabolically active areas, this effect allows for increased oxygen release in those tissues that need it most to support a high rate of metabolism. pH also affects the reactivity of heme globins through mechanisms independent of the Bohr Effect discussed earlier. Many reactions performed by globins, such as nitrite reduction, require one or more protons to proceed; as the pH drops and more protons become available, the rate of these reactions will tend to increase.

1.2.4.5 Specific amino acid residues and mutations

As a general rule, most factors that affect heme globin functional characteristics do so by, in one way or another, altering the overall structure of the heme protein. As recombinant protein expression and mutagenesis became widespread techniques, this allowed for single amino acid mutations to be made, determining the effect of specific amino acid residues on protein structure and function.

This work began well before the discovery of the hexacoordinate globins, and focused on the pentacoordinate globins Hb and Mb. A number of residues were targeted, but many of the residues found to be most influential were located in the distal heme pocket, which is typically the site of ligand binding. In the late 1980s and early 1990s, a series of studies performed with Mb mutants found that modifying either the size or the charge of amino acid side chains in the distal heme pocket exerted a significant effect on the ligand-binding behavior of the protein. Three residues were identified as having particularly strong influences on ligand-binding: the distal histidine at position E7, a valine at position E11, and a leucine at position B10. Figure 8 depicts the distal heme pocket of Mb and specifically identifies these three residues, colored in green, and shows their proximity to the heme group in red, as well as the space typically occupied by a bound ligand in blue.

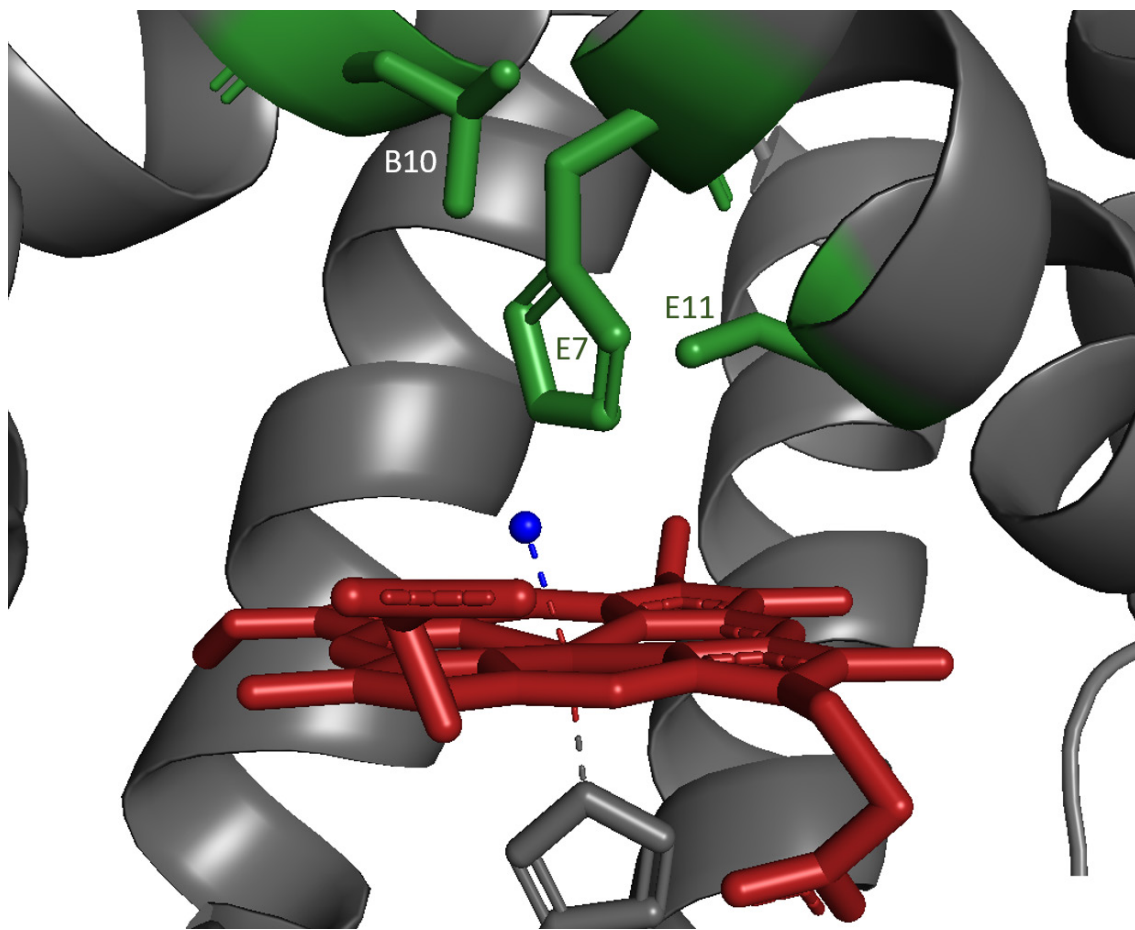


Figure 8: Mb distal heme pocket showing residues B10, E7, and E11

As the structures of Ngb and Cygb were determined, became clear that these three residues occupied very similar locations in the distal heme pockets of those proteins. Figure 9 provides images of the heme pockets of both Ngb and Cygb, again showing the B10, E7, and E11 residues in green.

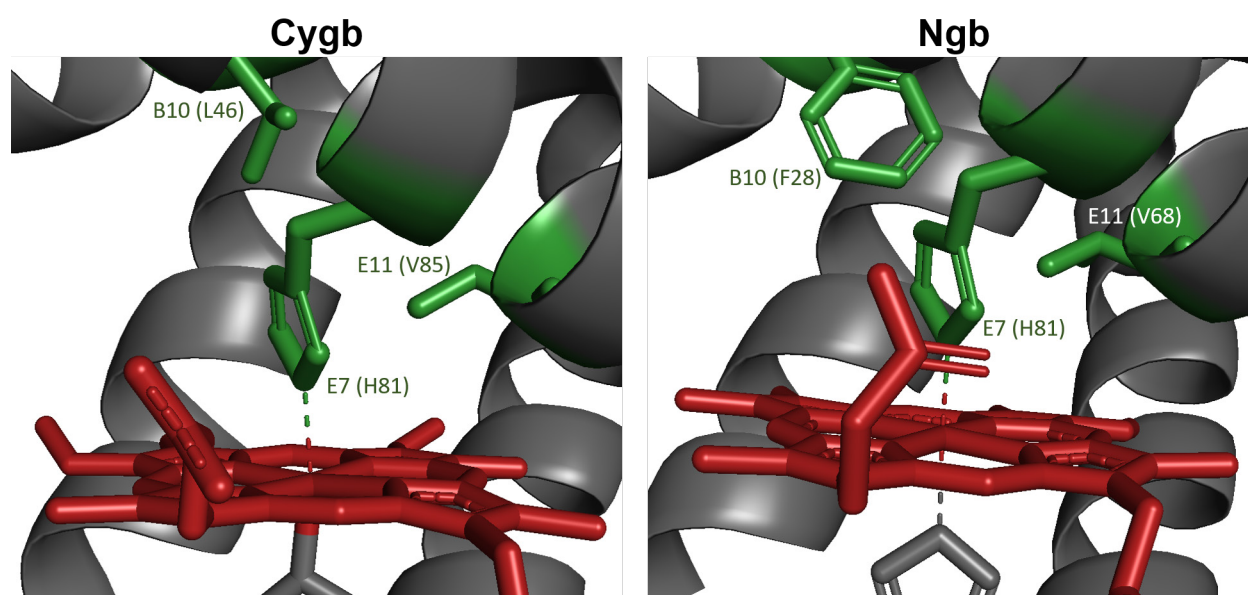


Figure 9: Distal heme pockets of Cygb and Ngb showing B10, E7, and E11 residues

Based on the similar positions of these residues in these three proteins, it was expected that mutations at these sites would influence the function of Ngb and Cygb as they did Mb. Indeed, studies of Ngb conducted within our lab have found that these same three residues exert large effects on autoxidation, nitrite reduction, and the redox potential of Ngb. In fact, mutations at the E7 site have incredibly large effects on the function of Ngb. Because Ngb is hexacoordinate, the histidine at position E7 can directly coordinate with the heme iron, and as

mentioned before, must dissociate before any external molecule can bind to the iron. When this histidine is mutated to an amino acid with a smaller side chain, one that cannot get close enough to the heme iron to form a direct bond (such as glutamine or alanine), the oxygen affinity and nitrite reductase rates for the protein have been documented to increase by up to several orders of magnitude [13]. Mutations at B10 and E11 have also been found to markedly affect Ngb function, but to a lesser extent than mutations at site E7. One prominent example is the phenylalanine present at position B10 in Ngb, which appears to play a role in stabilizing bound oxygen; replacing this residue with any other amino acid results in a notable increase in the rate of autoxidation of the protein.

Cygb mutations have been less extensively characterized, but there is evidence that E7 mutants of Cygb also exhibit very large increases in oxygen affinity and reaction rates. The effect of mutations at B10 and E11 in Cygb has not been explored as extensively, but given the similarity of the distal heme pockets, mutations at these sites are likely to have very similar effects to the corresponding mutations in Ngb.

1.2.5 UV-Visible spectroscopy of heme globin species

In most proteins, differentiating between the numerous different redox and binding states exhibited by heme globins would prove an immensely difficult task. It is fortunate, then, that every change that occurs at the iron of a heme globin, be it electron transfer or ligand binding, produces a measurable change in the UV-visible range absorbance spectrum of the protein. This represents an invaluable tool for observing the behavior of heme globins.

In general, significant information about the heme can be found in two different wavelength regions: the first occurring around 400 nm, which has been designated the “Soret peak”, and the second, often referred to as the “Q bands”, falling between 500 and 600 nm.

In both regions, globins tend to show unique spectra depending on their specific redox and ligand-binding state. An example of this can be seen in figure 10, which depicts the spectra of four pure human Cygb (*HsaCygb*) species between 450 and 700 nm: the Fe^{II} unbound state (“deoxy”), the Fe^{II} oxygen-bound state (“oxy”), the Fe^{II} NO-bound state (“iron-nitrosyl”), and the Fe^{III} oxidized state (“met”).

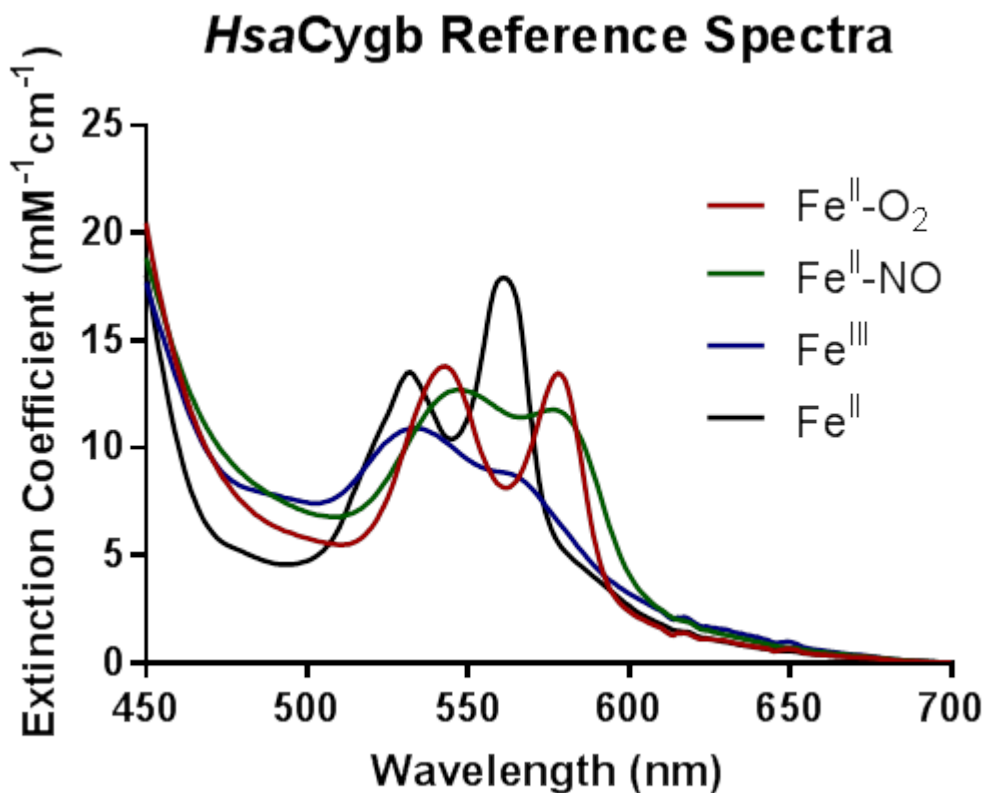


Figure 10: Spectra for four pure species of *HsaCygb*

All globins have characteristic spectra like these; by measuring these pure spectra, mathematical deconvolution can be used to determine the specific components of any mixture of different redox and binding states. This is an invaluable tool for analyzing globin function and reactivity and will be used extensively throughout this work. More information about this process, including the MATLAB code and reference spectra used to perform deconvolution, can be found in Appendix A.

1.3 CYTOGLOBIN: STRUCTURE AND FUNCTION

Among the many heme globins examined in this work, the primary focus of the work is Cytoglobin (Cygb). Cygb was first discovered around the year 2000 and was initially designated stellate cell activating protein (STAP), as it was initially found in stellate cells of the liver, and shown to be required for activation of these cells [21]. Subsequent work found that the protein was expressed in a wide variety of tissues and cell types, and given its similarity to other heme globins and its relatively ubiquitous expression, the protein was renamed Cytoglobin.

While human Cygb (*HsaCygb*) is prominently featured in this dissertation, two other Cygb proteins are studied in some detail as well: these are the two zebrafish (*Danio rerio*) Cygbs, designated Cygb1 (or *DreCygb1*) and Cygb2 (or *DreCygb2*). The presence of two Cygb proteins in zebrafish is relatively rare, and is seen only in the teleost fishes, as most organisms possess only one Cygb gene. This is thought to arise from an ancient gene duplication event and

subsequent divergence. These three proteins, while similar in many ways, also exhibit some significant differences that make the study of these proteins a compelling topic.

1.3.1 Cytoglobin Structure

All three Cygbs studied in this work are, at first glance, broadly similar. All three have similar molecular weights, around 20-21 kDa. The crystal structure is known only for *HsaCyg*b; it has been shown earlier and is shown again in figure 11.

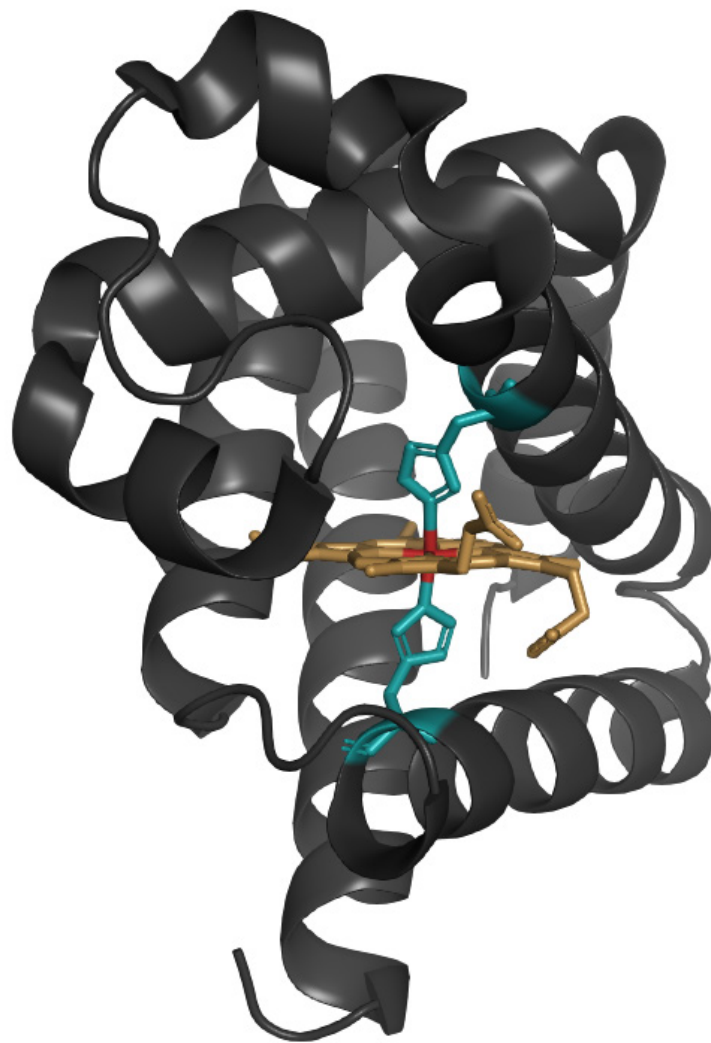


Figure 11: Crystal structure of *HsaCyg*b

Because only one of the three Cygbs of interest has had its crystal structure solved, very detailed comparisons of protein structure cannot be made. Nonetheless, comparing amino acid sequences and UV-Vis spectra has revealed numerous important insights into the structural variations between these proteins, which can then be related to observed differences in protein function.

In general, *DreCygb2* is homologous to *HsaCygb*, as well as other mammalian Cygbs; of the three proteins, *DreCygb1* is the least similar to the others, despite the great evolutionary separation between humans and zebrafish. This has led to speculation that *DreCygb2* and *HsaCygb* have evolved to perform similar roles, while *DreCygb1*, which arose from a gene duplication event and exists only in teleost fish, may have evolved to perform a different, distinct function.

Perhaps the most obvious discrepancy between the proteins is found in the heme coordination state of the ferrous proteins. While *Cygb2* and *HsaCygb* are both six-coordinate hemes, *Cygb1* is five-coordinate. Of note, this is thus far the only pentacoordinate *Cygb* that has been observed in any organism, and in fact may be the only pentacoordinate globin to be found in any hexacoordinate clade thus far [4]. The exact cause of this change is unclear, but may result from changes in the loop between the protein's C and D helices, a region where *DreCygb1* more closely resembles the pentacoordinate globins Hb and Mb than other *Cygb* proteins.

Another prominent structural variation between the three *Cygb* proteins studied here relates to the surface cysteine residues on the proteins, as discussed earlier. *HsaCygb* possesses two cysteines at positions 38 and 83 that are close enough together to form an intramolecular disulfide bridge, which are now being shown to exert a significant effect on the function of the

protein. The zebrafish Cygb proteins do not show any residues that could form a disulfide, and thus this effect is not expected to be present for the zebrafish proteins.

1.3.2 Cytoglobin Functional Characteristics

Like all heme globins, the Cygb proteins studied in this work have been shown to participate in the prototypical heme globin reactions. They bind and release O₂, CO, and NO, and they reduce nitrite to NO. The exact rates at which these reactions occur varies substantially between the three proteins and provides potential clues to the function of each protein.

All three Cygb proteins studied in this work are able to form a stable oxygen-bound species. The affinity of *HsaCygb* has been reported to be relatively high, with a P₅₀ around 1 to 2 mmHg, which is comparable to Mb. The oxygen affinity has not been directly measured for *DreCygb1* or *DreCygb2* prior to attempts to do so in this work (to be detailed later). Based on structure and homology, it was expected that both zebrafish cytoglobins would have fairly high affinity, likely similar to that of *HsaCygb* (a homolog of *DreCygb2*) and Mb (a rough homolog of *DreCygb1*). Like all other globins, they were found to autoxidize, spontaneously converting from the Fe^{II}-O₂ form to the Fe^{III} ferric form at characteristic rates. These rates are summarized in table 2.

Table 2: Autoxidation rate constants of vertebrate Cygb proteins

<i>Protein</i>	k_{autox} , 25° C (min^{-1})	k_{autox} , 37° C (min^{-1})	<i>Source</i>
<i>HsaCygb</i>	0.107 ± 0.015	0.270 ± 0.02	Corti et al. 2016 [4]
<i>DreCygb1</i>	0.0165 ± 0.0011	0.0239 ± .0024	Corti et al. 2016 [4]
<i>DreCygb2</i>	0.55 ± 0.13	1.44 ± 0.15	Corti et al. 2016 [4]

The autoxidation rate constants of these proteins vary by nearly two orders of magnitude, with very slow autoxidation by the five-coordinate *DreCygb1* and very rapid autoxidation by *DreCygb2*. This can provide some clue as to globin function, as slow autoxidation suggests a role involving oxygen storage or transport, whereas rapid autoxidation means oxygen binding is unlikely (as oxygen-bound *DreCygb2* would be rapidly oxidized).

Likewise, the Cygbs all reduce nitrite to NO at characteristic rates. These rates vary widely, with *DreCygb1* exhibiting nitrite reductase rates faster than most other globins. Nitrite reduction by *HsaCygb* proves particularly interesting, as recently published work has shown that the rate of nitrite reduction by *HsaCygb* varies substantially based on the redox state of the protein's surface thiols. Specifically, monomeric *HsaCygb* with an intramolecular disulfide between its cysteine residues (S-S monomer) has been reported to reduce nitrite very quickly, on par with *DreCygb1*. In the absence of the intramolecular disulfide, however, nitrite reduction by *HsaCygb* becomes relatively very slow. Table 3 summarizes the previously published rate constants for nitrite reduction for these three Cygb proteins, as well as human Hb for comparison.

Table 3: Nitrite reduction rate constants for select vertebrate globins

<i>Protein</i>	k_{nitrite} , 25°C ($M^{-1}s^{-1}$)	k_{nitrite} , 37°C ($M^{-1}s^{-1}$)	<i>Source</i>
<i>HsaCygb</i>	0.40 ± 0.08	1.14 ± 0.07	Corti et al. 2016 [4]
<i>HsaCygb</i>	0.26 (S-S dimer) 0.63 (S-H monomer) 32.3 (S-S monomer)	Not determined	Reeder et al. 2018 [15]
<i>DreCygb1</i>	14.2 ± 1.4	28.6 ± 3.1	Corti et al. 2016 [4]
<i>DreCygb2</i>	0.31 ± 0.04	0.94 ± 0.18	Corti et al. 2016 [4]
<i>HsaHbA</i> (T state)	0.12	Not determined	Huang et al. 2005 [22]
<i>HsaHbA</i> (R state)	6	Not determined	Huang et al. 2005 [22]

In terms of nitrite reduction, *DreCygb1* exhibits very rapid nitrite reductase activity, far greater than that of even R state Hb, while *DreCygb2* is relatively slow. Perhaps the most interesting data relates to *HsaCygb*. Initial publications reported a single rate constant for nitrite reduction by *HsaCygb*, but a very recent (early 2018) paper suggests the rate of nitrite reduction by *HsaCygb* varies greatly depending on the redox state of the protein's surface thiols, found at residues C38 and C83 and discussed in a prior section. Both the reduced thiol form and the intermolecular disulfide reduce nitrite fairly slowly, roughly similar to *DreCygb2* or T state Hb. When the intramolecular disulfide forms, however, the nitrite reductase activity of the protein becomes nearly two orders of magnitude faster, outstripping even *DreCygb1* [15]. This has implications both for the understanding of this protein's function *in vivo* (as a potential redox-sensitive NO donor) and for the creation of therapeutic molecules based on *HsaCygb* (as thiol manipulation may provide another way to fine-tune protein function).

Cygb also exhibits two specific activities that have not been previously discussed, as they have minimal relevance to the work performed for this dissertation. Nevertheless, they provide some insight into the potential functions of Cygb, and thus merit a brief discussion. The first such activity is peroxidase activity. This reaction can occur with any peroxide, but the simplest form comes from a reaction with hydrogen peroxide (H_2O_2), and converts that peroxide to water and oxygen. There are numerous specialized peroxidase enzymes, but Cygb (and other globins) are also able to perform this activity, which is thought to participate in protecting from oxidative stress. Cygb is thought to play a role in the cellular response to oxidative stress, and so this particular activity is likely important for this protein.

Cygb has also been found to exhibit lipid-binding properties, although this is mostly limited to *HsaCygb*. Multiple sources have reported that oleic acid can bind *HsaCygb* with relatively high affinity, and that this binding event triggers a change in the heme coordination of Fe^{III} Cygb, with the protein shifting from the hexacoordinate state to the pentacoordinate state (the distal histidine is replaced by a water molecule). This change in heme coordination has specific ramifications for globin function and has been shown to modulate the peroxidase activity of *HsaCygb* [20]. Furthermore, this effect seems to vary depending on which lipid is bound, with highly anionic phospholipids appearing to be the strongest activators of peroxidase activity [23]. The implications of this interaction in the search for Cygb's role in normal physiology are significant and will be discussed further in section 1.3.4.

1.3.3 Cytoglobin Localization

One area of particular interest to Cygb researchers since its discovery has been the localization of the protein, both within an organism and within the cell. In both cases, where the protein is found

can provide important insight into possible functions, as specific organs, tissues, and subcellular compartments typically play host to specific biological processes.

As has previously been mentioned, Cygb was initially discovered in the stellate cells of the liver in rats, where it was found to be expressed throughout the cytoplasm [21]. One year later, another group found that the protein was expressed relatively ubiquitously in human tissues, with the highest expression in the heart, stomach, bladder, and small intestine [24]. Based on this pattern of expression, they renamed the protein Cytoglobin. One year later, a study was published that used immunocytochemistry to examine the subcellular localization of Cygb, and found the protein exclusively in the nucleus [25].

Subsequent studies began to refine the understanding of Cygb's localization, reporting high expression of Cygb in connective tissue fibroblasts of all splanchnic organs, explaining its relatively ubiquitous expression pattern in previous studies. Cygb was also found in dermal fibroblasts and related cells like osteoblasts, chondroblasts, and hepatic stellate cells, as well as certain neuronal populations in the brain and the retina [26]. One of these same studies also examined subcellular localization, and found Cygb in the cytoplasm, the nucleus, or both, depending on the specific cell type.

Interestingly, in amphibians that do not express Mb, Cygb has been located in the heart (where it was found in cell nuclei) and skeletal muscles (in the cytoplasm). This led to the hypothesis that Cygb may compensate for the lack of Mb by providing oxygen storage within muscle tissue in these amphibians [27].

In 2009, Cygb was found in the vascular wall, both in adventitial fibroblasts and in smooth muscle cells from various species, as well as in the adventitia and media of intact rat

aortas [28]. Cygb has also been found in the myocardium, specifically in conditions of hypoxia-induced hypertrophy [29].

In zebrafish, the two Cygbs localize to different tissues. *DreCygb2*, the homolog of *HsaCygb*, was found in high levels in the eye and brain, and at lower levels in the heart and liver. *DreCygb1*, on the other hand, was found in the blood and in all other tissues analyzed; however, as hemoglobin was also found in all tissues, the ubiquitous presence of *DreCygb1* may be evidence of blood contamination rather than genuine expression in all tissues [4].

1.3.4 Putative Functions of Cygb *in vivo*

Despite extensive functional and structural characterization efforts, the role (or roles) of Cygb *in vivo* are still not definitively known. Numerous studies in cell and animal models have been undertaken, and numerous possible roles have been put forward, but to some extent the results remain inconclusive. Generally speaking, there is a growing body of evidence suggesting that Cygb can exert strong cytoprotective effects, protecting cells and tissues from a variety of different insults. There is also evidence that Cygb may support tissue regeneration and healing after injury, as well as inhibit fibrosis.

Animal models have demonstrated cytoprotective effects arising from Cygb overexpression in a variety of different tissues and pathologic conditions. Specifically, Cygb overexpression has been shown to reduce fibrosis in mouse models of both liver and kidney injury [30, 31]. Cygb knockout mice do not exhibit any phenotype at birth, but as they age they do appear to develop abnormalities in numerous organ systems at higher rates than wild-type mice [32]. These effects are thought to arise from a potential role for Cygb in the modulation of oxidative stress and consequent limiting of oxidative tissue damage [33].

More specific animal studies, most often in mice, have explored the effect of Cygb knockout or overexpression on various pathways, and found that Cygb affects a number of different pathological processes. Specifically, Cygb overexpression has been shown to reduce fibrosis in both the kidneys and the liver after injury, and even protect against radiation-induced toxicity [34]. It has also been identified as a candidate tumor suppressor that may be able to suppress carcinogenesis [35].

A variety of stimuli and pathways have been found to increase expression of Cygb in both cell and animal studies. Conditions such as hypoxia (via a HIF-1 α dependent mechanism), elevated blood glucose, and high levels of oxidant species have all been shown to induce upregulation of Cygb, again suggesting a role for Cygb in responding to oxidative stress [33, 36-39]. Cygb has been shown to be upregulated in activated myoprogenitors and proliferating myoblasts, where it seems to play an antiapoptotic role and contribute to regeneration of injured muscle [30, 40]. It is also expressed in heart muscle and has been shown to be upregulated during hypoxia-induced hypertrophy, again suggesting it plays a role both in response to hypoxia and in proliferation of muscle tissue [29].

One important mechanism by which Cygb may respond to oxidative stress is through its peroxidase activity. A recent paper conducted by members of our research group and others identified that Cygb's peroxidase activity can be greatly increased by the binding of oxidized lipids to the protein. While the peroxidase activity of Cygb had previously been shown at supraphysiologic levels of H₂O₂, this work demonstrated that anionic phospholipids can strongly activate Cygb's peroxidase activity at normal physiologic concentrations [23]. This suggests that binding of these lipids by Cygb is an important part of Cygb's ability to protect

against oxidative stress and suggests that reactive oxygen species (ROS) detoxification is a feasible and potentially important function of Cygb *in vivo*.

One of the most extensively-studied potential functions of Cygb relates to the protein's role in controlling nitric oxide signaling via its NO dioxygenase activity. Cygb is expressed in smooth muscle of the vascular wall, where it has been suggested to play a major role in the diffusion of NO through the vessel wall. By consuming NO, Cygb limits the ability of NO to promote relaxation of the vascular smooth muscle, maintaining vascular tone and blood pressure by limiting vasodilation [28]. Studies of Cygb knockout mice have shown significantly decreased mean arterial blood pressure compared to wild-type mice, and *ex vivo* arteries from Cygb knockout mice show much greater diffusion of NO through the vascular wall [41]. Conversely, while it has not been explored as extensively, in hypoxic conditions Cygb may also contribute to vasodilation via nitrite reduction in the vessel wall. Because Cygb has a notably higher oxygen affinity than Hb, this particular pathway would require very low oxygenation before NO production by Cygb becomes physiologically significant.

Furthermore, Cygb has shown an important role in the response to vascular injury, with Cygb knockout impairing formation of a new endothelium in vessels that had been denuded [42]. In the absence of Cygb, the cells of the vessel wall showed increased apoptosis following injury, but proliferation was unaffected by the loss of Cygb. This suggests that anti-apoptotic functions are the primary mechanism by which Cygb promotes healing after a vascular injury. Further experiments revealed that inhibition of nitric oxide synthase (NOS) enzymes prevented this increase in apoptosis, suggesting Cygb prevents NO-dependent apoptosis, likely through rapid NO consumption. Because NO consumption occurs via a dioxygenation reaction that oxidizes Cygb, catalytic NO consumption likely requires a system that can rapidly reduce oxidized Cygb.

Finally, one relatively controversial potential function for Cygb has been suggested, primarily as a consequence of studies showing nuclear localization of the protein in certain cell types. Cygb's presence in the nucleus suggests a possible role as a transcription factor, which under certain conditions could translocate to the nucleus and influence transcription of certain genes [25].

While the above discussion holds true for *HsaCygb* and homologous proteins, including *DreCygb2*, the different functional characteristics of *DreCygb1*, as well as its different pattern of localization, suggest it may perform a different function. Specifically, its pentacoordinate nature and slow autoxidation, as well as its presence in the blood of zebrafish, suggest that the protein may have evolved to perform a respiratory function, in which oxygen storage or transport are key functions. Studies of other fish have shown that hypoxia increases Cygb1 mRNA levels without concurrent increases in Cygb2 mRNA [43]. A large increase in Cygb1 mRNA is also observed around 18 to 31 hours post-fertilization in developing zebrafish, which is consistent with the timeline of erythropoiesis (red blood cell synthesis) [44]. This all suggests a role for *DreCygb1*, and indeed Cygb1 in other fish species, as an oxygen carrier in red blood cells, specifically one that may be specialized for oxygen transport at low oxygen tensions, as the Cygb's typically exhibit high oxygen affinity when compared to Hb.

While the specific function or functions of the Cygb's remain unknown, there is mounting evidence that Cygb seems to exhibit cytoprotective effects in a wide variety of different situations via interaction with numerous different biochemical pathways. This not only has compelling implications for the study of Cygb's role in normal physiology, but also suggests that exogenous therapeutic compounds based on Cygb may also be able to provide cytoprotective benefits beyond the specific targeted effect of the therapy.

1.4 DEVELOPMENT OF HEME GLOBINS FOR CLINICAL USE

The study of heme globins has proceeded in two primary directions. The first is concerned with the native biochemistry and physiology of the heme globins: their functional characteristics, their evolutionary history, and their potential roles in normal physiology. This field has seen notable progress, with the discovery and characterization of three new human globins (and myriad non-human ones) occurring within the last twenty years alone.

The second focuses instead on the potential non-native applications of heme globins. For at least the past century, researchers have considered that heme globins might be usable as therapeutic compounds, primarily to provide additional oxygen transport in cases of severe blood loss or anemia. Recently, however, the spectrum of potential clinical uses of heme globins has broadened, with the potential of globin-based antidotal therapies, most prominently for carbon monoxide (CO) poisoning, emerging as a new area of investigation. While this side of the field has seen very limited progress, with no FDA-approved therapies based on heme globins, ongoing advancements in technology continue to expand the potential clinical applications of heme globins to treat a variety of conditions.

1.4.1 Carbon monoxide poisoning, blood loss, anemia, and hemoglobin

While blood loss and carbon monoxide poisoning may seem distinct and largely unrelated, in many ways the pathophysiology that underlies the two conditions is remarkably similar. In both cases, one of the primary defects that arises is reducing carrying capacity for oxygen in the blood, although this common problem arises for different reasons.

Blood loss reduces the total oxygen carrying capacity of the blood by, quite simply, reducing the amount of blood present. As red blood cells are lost, the total amount of oxygen that can be transported in the blood likewise decreases. The same pathology is present after blood loss but also in cases of severe anemia, which reduces the number of red blood cells present. In the case of acute blood loss, as in cases of trauma, this is usually further compounded by a loss of blood volume, resulting in decreased blood pressure. If the pressure falls far enough, the body may be incapable of adequately perfusing the organs, and thus be unable to provide even oxygen-poor blood, further increasing the risk of tissue damage.

CO poisoning, on the other hand, reduces the number of available binding sites for oxygen on Hb while leaving total Hb and red blood cell levels unchanged. Hb typically has much greater affinity for CO than for oxygen; as such, CO will tend to displace oxygen from Hb, and once bound, the CO is very unlikely to be replaced by oxygen. As more CO enters the blood and binds to Hb, the total amount of oxygen that can be transported by Hb will continue to decrease. Furthermore, CO binding to one subunit of the Hb tetramer stabilizes the R state of the other subunits, increasing their affinity for oxygen. This results in delayed release of any oxygen that is still able to bind Hb. Notably, this is not the only mechanism of toxicity for CO poisoning. CO is also able to enter the mitochondria, where it can bind to components of the mitochondrial electron transport chain, greatly slowing (or completely stopping) electron transport and ATP production. The exact contribution of these two pathways to the negative outcomes of CO poisoning remains unclear.

To better understand the mechanisms of these conditions, we can consider again a saturation curve, as was depicted earlier in figure 7. In this case, however, the y-axis represents the total amount of oxygen in the blood, rather than the fractional saturation, and the x-axis

represents the oxygen partial pressure. In blood loss or anemia, the individual Hb molecules behave the exact same as they do under normal conditions, but there are fewer of them. This results in an equilibrium curve that is the same shape as that seen under normal conditions, but with a much lower maximum value. The fractional saturation will be unchanged from normal conditions, but because so much less Hb is present, far less oxygen is being transported at a given saturation level.

CO poisoning also decreases the maximum amount of total oxygen by occupying binding sites on the Hb and preventing oxygen binding. In addition, it also “left shifts” the equilibrium curve by stabilizing the R state and increasing the oxygen affinity of the available binding sites. This means that even the oxygen that does still bind will not be released until the oxygen partial pressure becomes very low, potentially compounding the problem of insufficient oxygen delivery to tissues. Figure 12 summarizes these effects, showing the equilibrium curves in cases of blood loss or anemia (red curve) and CO poisoning (blue curve) compared to normal physiology (black curve).

Pathology Affecting Blood Oxygenation

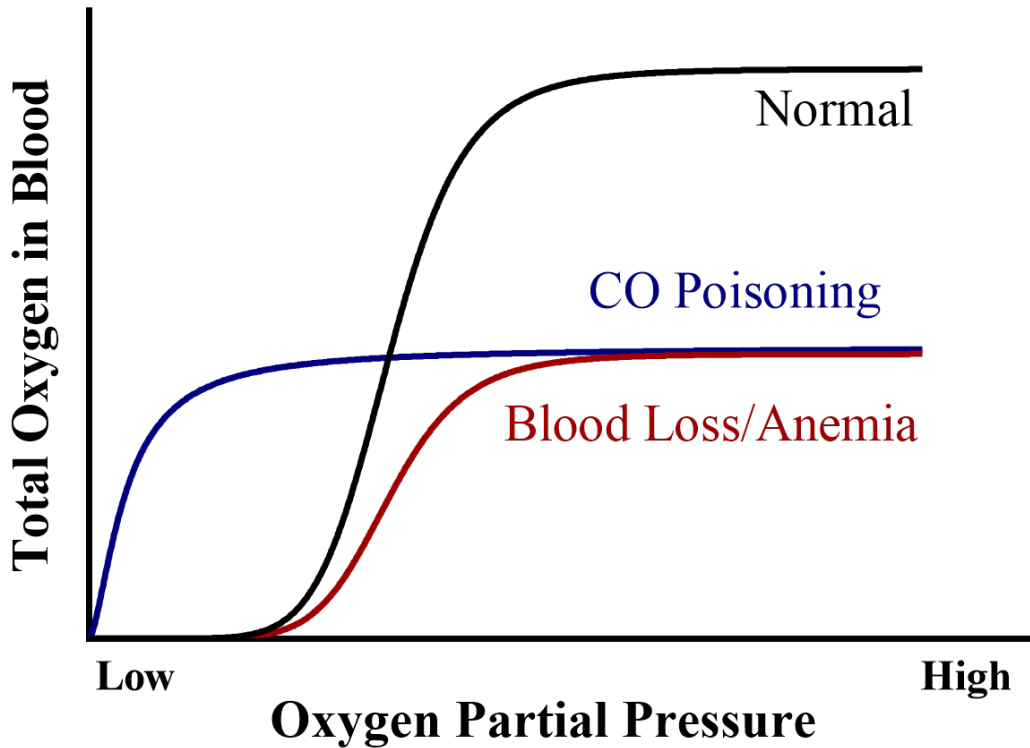


Figure 12: Effects of CO poisoning, blood loss, and anemia on blood oxygen capacity

These two conditions both have the potential to be treated by globin-based therapeutics. In cases of blood loss, infusion of heme globin could provide more oxygen binding sites, increasing the oxygen capacity of the blood and oxygen delivery to the tissues. In this case, an infusion of heme globin would function very similarly to a blood transfusion. In CO poisoning, an infused globin could either provide more oxygen binding sites or, if it possesses a higher affinity for CO than Hb, could remove the CO from the native Hb, allowing for the patient's own Hb to transport and deliver more oxygen.

1.4.2 Hemoglobin-based Oxygen Carriers (HBOCs)

One potential clinical use of heme globins is to use infusion of globins in place of blood transfusions. Blood transfusions are a very common medical procedure, used worldwide to sustain life in a variety of clinical scenarios. Unfortunately, blood products have a relatively short storage life, and combined with high demand, shortages of blood products are not uncommon, especially in developing regions. These shortages can become far worse following events like natural disasters or terrorist attacks, where a large number of people require transfusions in a short amount of time.

Furthermore, even when blood products are readily available, blood transfusions also carry some risks that have not been entirely eliminated. Extensive screening has greatly reduced the frequency of transfusion-transmitted infections like hepatitis and HIV, but these diseases exhibit a “window period”, in which the causative organism is present but cannot be detected with diagnostic tests. As a result, even the most aggressive testing cannot lower the risk of transfusion-related infections to zero. Blood transfusions also require the blood to be typed and crossmatched before treatment, as the recipient may otherwise mount an immune reaction

against the donor blood. It is also now becoming clear that even properly typed and crossmatched transfusions can have immunomodulatory effects, and may predispose patients to infection, acute lung injury, and development of autoimmune disease. These risks are of particular concern to patients who receive repeated blood transfusions, such as those with sickle cell anemia or hemophilia.

In light of these risks, there has long been a focus on developing an alternative to blood transfusions that can mitigate some or all of these adverse effects. One potential approach to this problem is the use of cell-free hemoglobin, and the hemoglobin-based oxygen carriers (HBOCs) derived from it. As a purified protein solution, cell-free Hb is less able to harbor infectious organisms than intact cells, and also does not express cell-surface antigens that can provoke an immune reaction. Purified protein can also be kept stable in storage for years, either at -80°C or as a lyophilized powder. It can also be produced from sources other than human donors (bovine RBCs, recombinant techniques), thus removing the dual issues of a short storage life and the constant need for willing human donors. All of these potential advantages have spurred extensive efforts to develop a successful HBOC, although various drawbacks have thus far prevented any from reaching widespread clinical use.

In the effort to develop a successful HBOC, numerous different strategies for Hb preparation and modification have been explored. These strategies, and the specific products developed using each strategy, are summarized in table 4, and will be discussed in more detail in subsequent sections.

Table 4: HBOC development strategies and products developed using each strategy

HBOC Strategy	Prominent Examples
Stroma-free Hb	None (not commercially developed)
Diaspirin-crosslinked Hb	HemAssist
Polymerized Hb	Polyheme HBOC-201 (Hemopure) Hemolink
PEGylated Hb	Hemospan (MP4)

1.4.2.1 The First HBOCs: Stroma-free Hemoglobin

As early as 1918, researchers had begun to explore whether a solution of purified, cell-free Hb could provide oxygen to tissues in place of blood. These solutions were prepared by lysing red blood cells and removing the membrane components (referred to as the stroma) to create “stroma-free hemoglobin” (SFHb) which was, in a sense, the first HBOC. A very early study replaced the entire blood volume of several cats with SFHb. The researchers reported that, for a brief period of time, the cats behaved mostly normally, with several even exploring the lab space after the exchange transfusion was completed, showing no apparent discomfort or complications. The half-life of circulating stroma-free Hb, however, was discovered to be very short, as the cats uniformly died of respiratory failure within the span of a few hours [45]. One year later, the same researchers showed rapid excretion of the administered protein in the urine, as well as some evidence of renal dysfunction. They also showed that nephrectomy did not slow the rate at which protein was lost from the plasma, suggesting an alternative pathway for protein elimination. Perhaps most relevant to future studies, they also saw an increase in blood pressure following SFHb infusion, one that they calculated to exceed what would be expected from the oncotic effect of protein administration [46, 47].

About 15 years later, around 1950, researchers began to explore the effects of stroma-free Hb when administered to humans rather than animals. In this case, the Hb was infused into euvoletic adults, rather than exchanged for an equal amount of blood. Much like the previous animal studies, these studies found an increase in blood pressure beyond what would be predicted from the oncotic effect of the protein. They also observed sharp but temporary reductions in urine output and renal plasma flow, including a complete cessation of urine production in at least one patient, following SFHb infusion. They concluded that SFHb causes substantial vasoconstriction in the kidneys, and while they saw only reversible effects on kidney function, they nonetheless acknowledged that “one must admit the possibility of hemoglobin acting as a severe nephrotoxic substance” [48].

The next few decades saw continued work with SFHb. Animal studies showed only temporary perturbations after SFHb administration, and concluded that SFHb did show promise as a potential blood substitute. At this early stage human trials were limited, but the few that were conducted showed temporary side-effects including hypertension, abdominal pain, hemoglobinuria, and temporary decreases in kidney function [49].

1.4.2.2 Established Methods for HBOC Development

As the drawbacks of SFHb became apparent, subsequent efforts began to focus on various ways to increase the plasma half-life of SFHb, as well as address some of the adverse effects that were seen after SFHb infusion. Rather than simply isolate Hb, researchers turned their efforts to modifying it. Most of these modifications focused on modulating the size of the molecule, as most of the problems seen with SFHb were attributed to extravasation of Hb dimers from the plasma.

The first such strategy was to cross-link the Hb tetramer, preventing dissociation of the tetramer into smaller dimers. This was intended to keep the protein within the intravascular space, and was initially developed mostly to prolong the plasma half-life of SFHb, as the causes of the adverse effects was not yet well understood. A variety of different compounds were used to perform this crosslinking, but the most commonly used were diaspirins, resulting in a product referred to as diaspirin cross-linked hemoglobin (DCLHb). The most prominent DCLHb, HemAssist, was developed by Baxter Therapeutics, and used bis(3,5-dibromosalicyl) fumarate as its diaspirin crosslinker [50].

After early tests of DCLHb suggested that even tetrameric Hb was able to extravasate, other researchers began searching for a way to increase the size of Hb beyond that of the unmodified tetramer. The first such technique to become widely used was chemical polymerization, a process in which multiple Hb tetramers were linked together into larger molecules. This not only increased the size and plasma half-life of the molecule, but was also found to reduce both the oxygen affinity and vasoactivity of the molecule; this effect was thought to arise from decreased availability of binding sites, as ligands had relatively little access to the proteins in the center of the large polymers that were formed.. Numerous commercial products were developed based on polymerized Hb, with Hemolink, Hemopure (also known as HBOC-201), and Polyheme being perhaps the most prominent.

Another approach developed to increase the size of the Hb tetramer was PEGylation, the attachment of poly-(ethylene glycol) chains to the surface of the Hb molecule. The most prominent example of PEGylated Hb was Hemospan, a product developed by Sangart [51]. Compared to the 64 kDa size of unmodified Hb, Hemospan had an average size of just under 100 kDa; in animal models, this size increase was shown to reduce extravasation of the molecule,

increasing its plasma half-life and blunting the hypertensive response after infusion [51]. PEGylation has also been shown to increase oxygen affinity and nitrite reductase activity.

Figure 13 provides a visual summary of the different HBOC development strategies. Three of these strategies (crosslinking, polymerization, and PEGylation), have seen products reach (and fail) large clinical trials, while the other two (recombinant modification and lipid encapsulation) have not yet had products reach large clinical studies.

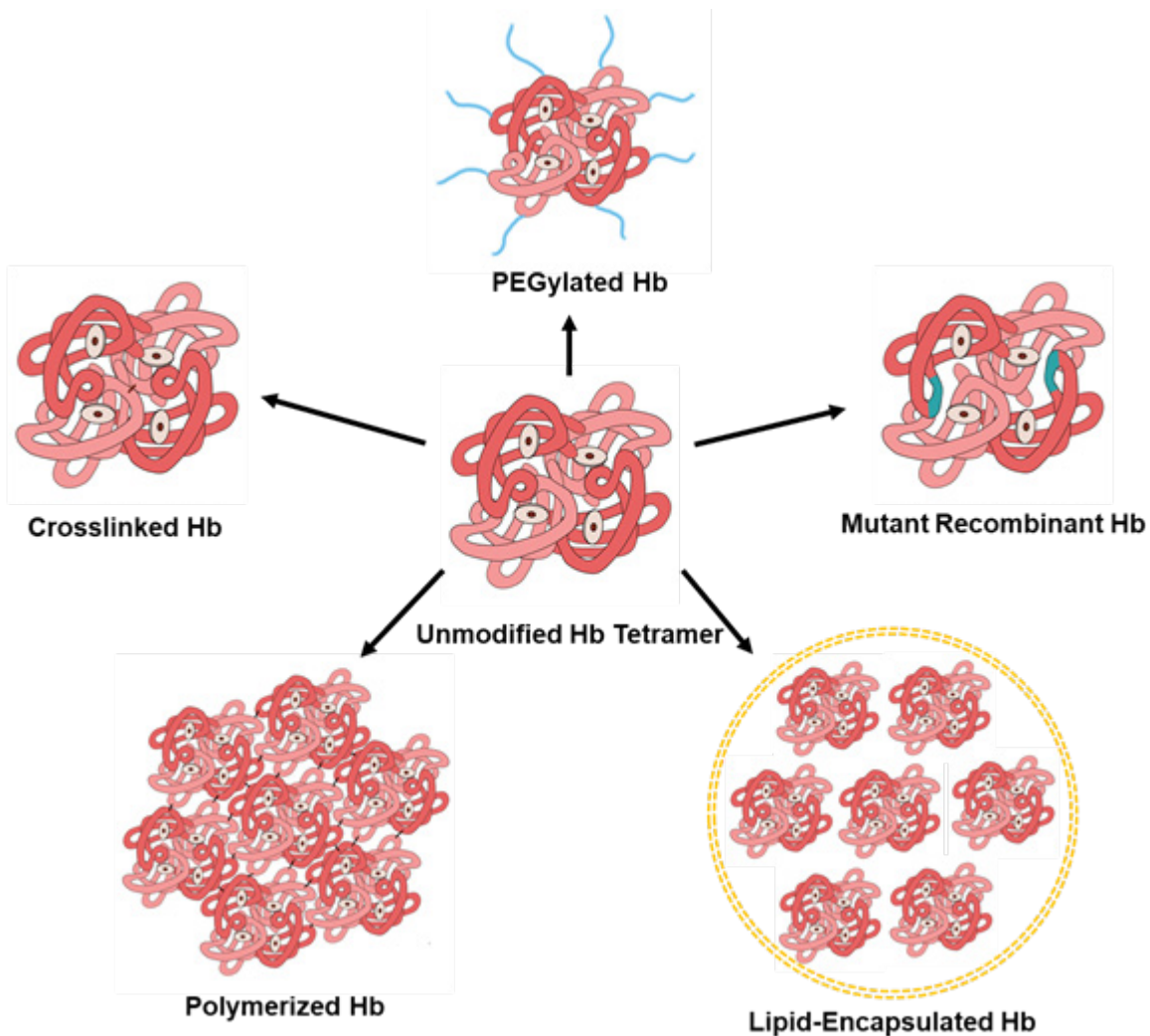


Figure 13: Summary of HBOC development strategies

1.4.3 HBOCs in clinical trials

Unfortunately, despite a long history of HBOC development and numerous novel strategies, HBOCs have uniformly failed to meet their desired endpoints in clinical trials. Throughout these trials, the same few mechanisms of toxicity have continued to arise, causing similar adverse effects in numerous trials. To date, no HBOC has performed well enough in a clinical trial to receive FDA approval, although HBOC-201 has been approved for use in South Africa and Russia due to concerns over infectious risks (specifically HIV) and/or inconsistent blood supplies, both of which make widespread use of blood transfusions less viable.

The earliest human trials of HBOCs used SFH. The first studies, in the late 1940s and early 1950s, have already been discussed, and saw temporary alterations in renal function following SFH infusion. A subsequent study with SFH in 1978 saw not only changes in renal function, but also mild hypertension and abdominal pain [49]. Perhaps as a result of these early trials, SFH never progressed to large-scale clinical trials.

The next HBOC to be put through clinical trials was HemAssist, the DCLHb developed by Baxter Therapeutics. Phase I testing of HemAssist was rather promising, with no serious adverse events in healthy volunteers given doses up to 100 mg/kg [50]. A later study gave doses up to 200 mL of 10% DCLHb to patients with hypovolemic shock, saw no increase in the rate of adverse events compared to saline treatment [52]. From here, HemAssist moved to a larger trial, which was planned to enroll 850 patients who would be treated with either up to 1L of 10% DCLHb or saline. This trial was halted after only 112 patients, as the mortality rate in the HemAssist-treated group was at 46%, vs. 17% in the saline group ($p = .003$) [53]. A second multicenter trial gave doses up to 750 mL and did find a reduction in transfusions needed with

DCLHb treatment, but was also stopped early due to increased adverse event rates [54]. A third trial in Europe treated 121 patients with up to 1L of 10% DCLHb and saw no increase in adverse events, but the two suspended trials marked the end of clinical studies using DCLHb [55].

Following the move away from DCLHb, polymerized Hb became the focus of numerous clinical trials. Hemopure (HBOC-201) was evaluated in a trial of 688 orthopedic surgery patients. Of those patients receiving Hemopure in doses from 65g up to 325g, 59.4% did not require any transfusion of packed RBCs. However, the patients receiving Hemopure also showed elevated rates of hypertension, high liver enzyme, lipase, and troponin levels, and cardiac-related adverse events, as well as a trend toward increased likelihood of stroke [56]. Further analysis of these data also suggested that Hemopure may have caused mild platelet dysfunction [57]. These concerns prevented FDA approval, but Hemopure is used clinically in Russia and South Africa, and some reports suggest it is typically well-tolerated in clinical use [58]. There is currently an ongoing clinical trial in the United States (NCT01881503) that is using Hemopure to treat patients with life-threatening anemia for whom blood transfusions are not an option. A case report has also been published detailing the use of Hemopure to treat a massively-burned patient with a religious objection to receiving blood transfusions [59].

Polyheme, another polymerized Hb product, was also the subject of several clinical trials. The first Polyheme trial, in 44 trauma patients, showed that doses up to 300g maintained the patients' total Hb concentration in the blood despite decreased red blood cell Hb, and reduced the need for blood transfusions [60]. A later trial with doses up to 1000g confirmed that Polyheme could maintain total blood Hb levels, and also reported improved survival with Polyheme treatment compared to "historical controls", which referred to published data on patients with severe post-operative anemia who refused blood transfusions [61]. The largest Polyheme trial

examined Polyheme's utility in cases of hemorrhagic shock where blood is not available. This trial, which treated a total of 714 trauma patients, used doses up to 300g of protein and found that Polyheme treatment yielded mortality rates similar to those seen with the standard of care, which in this trial was defined as treatment with a crystalloid plasma expander. This study did, however, document an increase in the rate of adverse events with Polyheme treatment, and the authors concluded that Polyheme showed clinical utility when blood transfusions were unavailable, but not as a replacement for blood transfusions [62]. In May 2009, citing the trial's failure to meet its primary efficacy endpoint, the FDA did not grant approval for clinical use to Polyheme [63]. The Polyheme trials later became the center of an ethical controversy, as the trials were granted an "Emergency Research Waiver", allowing treatment of badly injured trauma patients who were unable to provide informed consent at the time of treatment. While this process is not unheard of, critics identified several irregularities in the IRB approval process for this trial, and concluded that the trials were conducted in a way that should have prevented regulatory approval [64-66].

Hemospan, a PEGylated Hb developed by Sangart, was the most recent HBOC to reach a large clinical trial. An initial study used up to 42g of protein and found minimal side effects, with only one patient out of 20 showing elevated mean arterial pressure [67, 68]. A larger, double-blinded trial in hip arthroplasty patients showed a reduction in hypotensive episodes, but also significant increases in hypertension, nausea, and elevation of liver enzymes, lipase, and troponin [69]. The authors of the study concluded that Hemospan use in low-risk surgery patients was not indicated, and the FDA later decline to approve Hemospan for clinical use.

1.4.4 Mechanisms of toxicity observed in HBOC clinical trials

As shown above, the adverse effects seen in HBOC clinical trials have varied widely, affecting numerous organ systems and ranging from mild to life-threatening and even fatal. While the manifestations of HBOC toxicity can be very different, these adverse effects tend to arise from a small number of different underlying mechanisms. These mechanisms are all, in one way or another, related to high plasma concentrations of free, extracellular heme proteins. As such, they closely align with those observed in conditions that result in hemolysis and high concentrations of plasma heme proteins, such as sickle cell anemia and thalassemia. These mechanisms are summarized in figure 14.

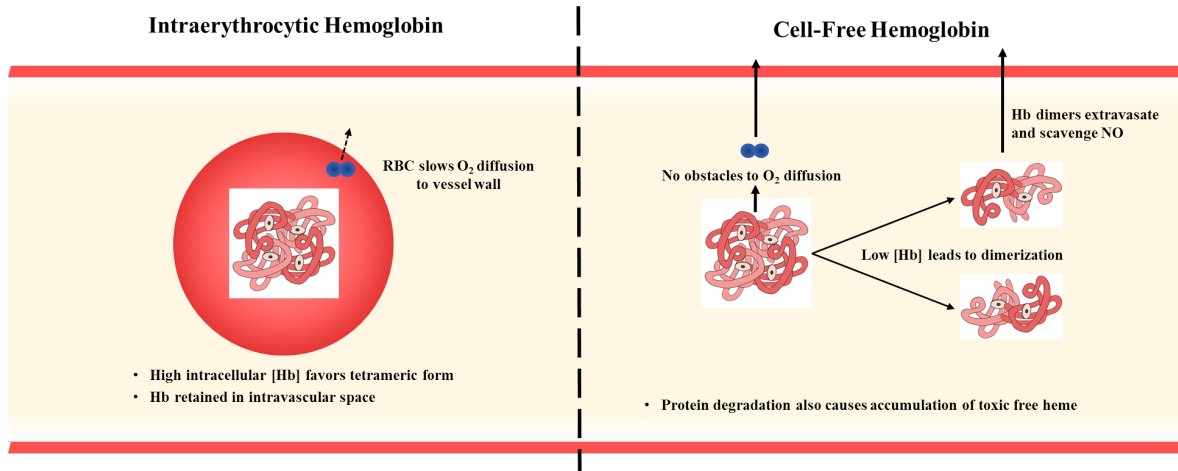


Figure 14: Mechanisms of cell-free hemoglobin toxicity

The most common, and arguably most injurious, mechanism of HBOC-related toxicity is pathologic arterial and arteriolar vasoconstriction, arising from excess NO consumption via NO dioxygenation reactions. While Hb in red blood cells can also consume NO, the red blood cell

has numerous adaptations that limit how much NO can be consumed, mostly related to spatial restriction of Hb. During normal laminar blood flow, shear causes the red blood cells to concentrate in the middle of the vessel; near the vascular wall is a “cell-free zone”, where no red blood cells are present. Cell-free Hb is small enough to diffuse freely, unaffected by shear, and thus can reach the vascular wall. When this occurs, any NO produced in the endothelium that diffuses into the vessel lumen will be rapidly consumed. Another contributor to vasoconstriction is the Hb tetramer’s ability to dissociate into two dimers. In the erythrocyte, the high concentration of Hb (in excess of 30 g/dL) favors the tetramer. In the plasma, however, the concentration is notably lower, even after infusion of large amounts of HBOCs or substantial hemolysis. This lower concentration favors the breakup of tetramers into dimers. These dimers can relatively easily extravasate, diffusing from the lumen through the vascular endothelium into the tissue of the vessel wall. While this is also possible for Hb tetramers, the rate of extravasation is higher for dimers. Once out of the lumen, the protein enters the smooth muscle of the vessel’s medial layer. In vascular smooth muscle, NO is a potent signaling molecule, promoting smooth muscle relaxation and subsequent vasodilation and decreased blood pressure. Some amount of NO is always present in vascular smooth muscle, where it plays an important role in maintaining vascular tone and preventing hypertension by inducing some level of relaxation of smooth muscle. Oxygenated heme globins, as discussed previously, are able to rapidly consume NO via dioxygenation reactions. Once the globins reach the smooth muscle, they rapidly consume the NO that is present, skewing the balance of smooth muscle tone towards constriction and resulting in hypertension and decreased perfusion. In addition to systemic hypertension, pulmonary hypertension is becoming increasingly recognized as a complication of elevated plasma Hb concentrations, although this has been observed more in hemolytic anemias than in

HBOC clinical trials. NO relaxes smooth muscle outside the vasculature as well, and as a result of NO scavenging, HBOC clinical trials have seen disorders of gastrointestinal smooth muscle, resulting in unopposed contraction and symptoms such as abdominal pain, esophageal spasms, and dysphagia.

Another mechanism that has been implicated in HBOC-associated vasoconstriction is early oxygen release. This theory states that cell-free Hb delivers oxygen to the vessel wall far more quickly than red blood cells. After Hb in a red blood cell releases oxygen, in order to reach the vessel wall, that oxygen must first cross the red blood cell membrane, which acts as a barrier of sorts and slows the movement of the oxygen. Once outside the cell, the cell-free layer ensures that the oxygen will have to diffuse a significant distance before reaching the vessel wall. It was suggested that HBOCs with oxygen affinity similar to unmodified Hb would thus have its oxygen reach the vascular wall too soon. There was concern that this early oxygen delivery would activate the same oxygen-sensing pathways as an oversupply of oxygen and cause reflex vasoconstriction. Increasing the oxygen affinity to delay oxygen reaching the vessel wall was the guiding principle in the development of Hemospan; while the adverse effects of Hemospan did seem more manageable than some earlier-generation HBOCs, the PEGylation process also increased the size of the molecule and modulated other activities, including NO production via nitrite reduction. As such, it is difficult to determine what role, if any, is played by early oxygen release in promoting vasoconstriction.

In addition to vasoconstriction, adverse effects have arisen from the delivery of a large amount of protein all at once. A large infusion of protein can cause stress on the kidneys, and numerous studies in animals and humans have seen renal function decline sharply after Hb administration. Hb is typically reabsorbed in the proximal tubule, where it is catabolized and

releases iron as hemosiderin. Above a certain Hb concentration, hemoglobinuria results, and there is some evidence that persistent hemoglobinuria and hemosiderin deposition in the kidney can progress to the development of chronic renal failure.

With a large amount of Hb present in the plasma, some amount of the protein is almost certain to degrade. Hb degradation can often result in release of the heme prosthetic group from the protein. Free heme has been shown to promote systemic inflammation, directly activating toll-like receptor 4 and driving the innate immune response, leading to sterile inflammation [70]. Heme also promotes the expression of adhesion molecules on the surface of endothelial cells *in vitro*, promoting activation and recruitment of inflammatory cells such as neutrophils. Both free heme and cell-free Hb can also form hydroxyl and superoxide radicals, which increase vascular permeability and can cause oxidative tissue damage, both of which can worsen an inflammatory reaction.

Finally, high levels of Hb in the plasma have been shown to activate platelets and promote clot formation. Hb itself stimulates platelet activity by binding to GP1b α on the platelet surface, and an *in vivo* study of cross-linked Hb showed increased platelet aggregation on prothrombotic surfaces. Here again NO consumption by free Hb plays a role as well, as NO is a potent inhibitor of platelet aggregation and adhesion, and also inhibits factor XIII in the coagulation cascade. Decreased NO is thus expected to enhance clot formation and stability, and in animal models loss of NO signaling has been seen to promote fibrin deposition and thrombus formation.

1.4.5 Ongoing efforts in HBOC development

As HBOCs have continued to fail in clinical trials, and the mechanisms underlying these failures have become better understood, novel methods have been used to create another new generation of potential HBOCs. These emerging technologies have not yet reach large scale clinical testing, but show promise for potentially improving performance compared to previous HBOCs.

While previous trials of chemically polymerized Hb showed drawbacks, a new product has been developed that uses a novel process referred to as “zero-link polymerization”. This product, OxyVita, uses a chemical agent that induces direct linkages between Hb molecules, forming polymers with an average weight of 17 MDa and leaving no chemical linker behind that might be able to perform side reactions [71]. Pre-clinical studies in animal models have found decreased extravasation and did not cause the vasoconstriction seen with smaller HBOCs [72, 73]. Recent studies have also found that OxyVita is stable as a powder and should have a long storage life, and that OxyVita is less likely to degrade and release free heme under oxidative stress than unmodified Hb [74, 75].

Another novel method of HBOC preparation takes inspiration from the role of the red blood cell membrane in regulating oxygen diffusion. By suspending Hb along with a mixture of two lipids (cholesterol and distearoylphosphatidylcholine) and subsequently homogenizing the solution, researchers have created a series of small (roughly 100 nm) vesicles containing Hb [76]. These vesicles resemble very small red blood cells, but lack any of the additional components present in RBCs. This includes desired components, like reducing enzymes, but also avoids undesirable components of RBCs, including antigens that allow for immune reactions. The developers of this method have also been able to increase the stability of these Hb vesicles by storing them under carbon monoxide gas. CO-bound globin does not oxidize, and is stable for

a long period of time; while this at first seems like a safety risk, small amounts of CO can have a potentially beneficial vasodilatory effect. In animal studies, these vesicles have been shown to exhibit reduced vasoactivity and an extended plasma half-life compared to unencapsulated Hb [77].

Recombinant modification is another technique that has long been explored for HBOC development, but continues to be used today. Previous studies have explored the ability of site-directed mutagenesis of Hb to reduce the protein's rate of NO deoxygenation, hoping that this alteration would cause less vasoconstriction. Confirming the validity of this approach, it has been shown that the magnitude of hypertension after globin infusion correlates directly to the NO dioxygenation rate of the globin. Other recombinant mutant globins have shown very high rates of nitrite reduction to NO, presenting another alternative for preventing vasoconstriction. If a globin could be designed that generates more NO than it consumes, the primary driver of globin-induced hypertension would be removed, ideally yielding improved outcomes in animal (or human) studies. Recombinant techniques have also been able to modulate other globin characteristics, such as oxygen affinity, autoxidation rates, and redox potential. By characterizing and combining mutations, a novel mutant globin with ideal characteristics as an HBOC may be attainable.

1.4.6 Heme Globins as Antidotal Therapies

In the past several years, our lab group has begun to explore the potential clinical applications of heme globins as antidotal therapies for carbon monoxide (CO) poisoning.

A heme globin-based CO antidote functions by binding CO in the plasma, thus reducing the amount of CO that is present to bind red cell Hb. Ideally, the globin used as an antidote will

have a much higher affinity for CO than native Hb, as this will allow the antidote to outcompete Hb for any available CO. One globin that has been evaluated for this usage is recombinant Ngb in which the distal histidine has been mutated to a glutamine residue (referred to as H64Q Ngb). When the distal histidine is replaced by a smaller residue that cannot directly coordinate with the heme iron, the rates of CO binding to the iron increase greatly, and the resultant protein exhibits a CO affinity much greater than that of Hb. This mutant has been shown to rapidly remove CO from free Hb as well as red blood cells *in vitro*. Furthermore, in a mouse model of severe CO poisoning, treatment with H64Q Ngb was reported to significantly increase survival compared to treatment with phosphate-buffered saline, seemingly by preventing the precipitous declines in heart rate and blood pressure seen in the untreated, CO-poisoned mice [78]. Other ongoing work is also exploring the ability of heme globin treatment to reverse the mitochondrial effects of CO poisoning.

One additional benefit of this protein is that, once CO is bound to H64Q Ngb, the rate of CO dissociation from the heme iron is slow enough that the binding is almost irreversible. This not only effectively removes the CO from the plasma, preventing it from binding Hb again, but also results in a largely inert, CO-bound form of Ngb. Because the heme iron is essentially irreversibly bound to CO, it is unable to perform other potentially harmful reactions that require the heme iron. For example, NO consumption via dioxygenation activity, as well as superoxide generation via autoxidation, are impossible for the CO-bound form of the protein. In this way, many of the well-established mechanisms of toxicity seen in HBOC clinical trials should be greatly reduced in cases of CO poisoning. Nonetheless, in cases of overadministration or misdiagnosis, where heme globin is administered in excess compared to CO, these potential

causes of toxicity would again become a concern. As such, a molecule that exhibits reduced toxicity when not bound to CO would be optimal.

While this molecule shows great promise as a CO scavenger, certain characteristics could still benefit from further optimization. One persistent problem is the difficulty of keeping the protein in the Fe^{II} redox state, which is required for CO binding. Unfortunately, like wild-type Ngb, H64Q Ngb has proven fairly difficult to reduce, with common reducing agents like ascorbate or CYB5 only very slowly reducing the oxidized form of the protein. This poses a potential barrier to clinical use, as storage of the protein under oxygenated conditions would lead to accumulation of the oxidized form of the protein (via autoxidation), which would subsequently be very difficult to reverse before administration to a patient. A high-affinity CO scavenger that can be rapidly reduced back to the ferrous form would offer a significant advantage over H64Q Ngb, and potentially offer even better outcomes in reversing CO poisoning.

A more recent area of focus for our lab is in a potential antidote for cyanide (CN⁻) poisoning. Victims of building fires often inhale significant amounts of both CO and cyanide, which is produced primarily by burning plastics. Interestingly, as discussed earlier, CN⁻ is typically bound by the oxidized, Fe^{III} form of heme globins. This suggests that optimization of a globin-based CO antidote, which in large part focuses on maximizing the ligand-binding affinity of the Fe^{II} form, may not be sufficient to yield an optimal cyanide scavenger as well. As a result, an ideal antidotal therapy for victims of building fires and smoke inhalation would bind both CO and cyanide with high affinity, although there is relatively little existing insight into how to design a molecule that will exhibit both characteristics.

2.0 MATERIALS AND METHODS

This section details materials and methods used throughout the work in this dissertation, rather than those used for specific projects. These widely used methods mostly relate to the expression and purification of recombinant heme globins. Most of the experimental methods, in contrast, were associated with one of four specific projects that are the subjects of chapters 3 through 6. Any methods specific to a single project are not included in this chapter, but rather at the beginning of the chapter detailing the relevant project.

2.1 RECOMBINANT PROTEIN EXPRESSION IN *E. COLI*

For the work detailed in this dissertation, nearly all proteins that were analyzed were expressed in and purified from *E. coli* using recombinant techniques. Depending on the exact identity of the protein, as well as other factors like desired yield, the specific expression vectors, growth conditions, and purification process varied significantly.

In general terms, proteins were expressed using one of two methods, hereafter referred to as the “soluble” method and the “inclusion bodies” method. The soluble method supplements the bacteria with δ -aminolevulinic acid (δ -ALA), a heme precursor, which allows the bacteria to generate properly folded, fully functional protein with the heme prosthetic group in place. Various purification techniques are then used to separate the recombinant protein from the native

bacterial proteins. The inclusion body method withholds this precursor, resulting in the generation of misfolded and aggregated heme-free protein. This protein can subsequently be isolated, denatured, and allowed to refold in the presence of heme to generate protein at much higher yields than the soluble method, albeit with some increase in the required number of processing steps.

2.1.1 Expression Vectors

The genes for all recombinant proteins utilized in this work are inserted into *E. coli* as a component of specific expression vectors. These vectors are specialized plasmids that contain a site for insertion of the protein, as well as other sites to allow for selective antibiotic resistance, control of protein expression, and ease of sequencing to confirm proper gene insertion.

Far and away the most commonly used expression vector in this work is the pET-28a plasmid. This plasmid has been developed for high levels of expression in bacteria, and contains a number of key elements required for optimal function. First, all forms of pET-28a contain a gene for resistance to the antibiotic Kanamycin, allowing for selective culture of plasmid-containing bacteria in Kanamycin-containing media. The vector also contains the lac operator just upstream of the gene for the protein. This operator typically represses protein expression, but initiates transcription following addition of the allolactose mimic isopropyl β -D-1-thiogalactopyranoside (IPTG) to the culture media. This allows for induction of protein expression after sufficient replication to reach a large number of bacteria, ultimately increasing protein yield. Also just upstream of the protein is the T7 promoter DNA sequence, which provides a starting point for the sequencing reactions necessary to confirm the proper protein sequence before performing protein expression.

One protein that is studied in this work, human Cytochrome B5 type B (CYB5B), is instead in a pET11 plasmid, as it was prepared this way by Dr. Mario Rivera at the University of Kansas, who generously provided the plasmid. This vector functions very similarly to the pET-28a, but confers resistance to the antibiotic Ampicillin rather than Kanamycin. Induction of expression via IPTG is carried out in the same fashion, as is sequencing from the T7 promoter region.

2.1.2 Bacterial Culture and Protein Expression: Soluble Method

The expression of soluble protein proceeds in similar fashion for all proteins studied, with some small variations that have been made to optimize protein yields. Initial preparation includes the preparation of 300 mL of LB media (25 g/L) in a 2 L Erlenmeyer flask, as well as four liters of TB media (47.6 g/L) in four 5 L Erlenmeyer flasks (one liter per flask). All media is autoclaved for 30 minutes, and once cool, Kanamycin at 30 mg/mL is added to all media to a final concentration of 30 µg/mL. The only change in this protocol occurs when expressing human Cytochrome b5, in which case 100 mg/mL Ampicillin is added to a final concentration of 100 µg/mL in lieu of Kanamycin.

Bacterial culture begins with inoculation of the LB media with a small amount of *E. coli* containing a vector that includes the gene for the protein to be produced. Typically, these *E. coli* are a strain referred to as SoluBL-21, which was developed as a modified form of BL-21 *E. coli* intended specifically for the expression of soluble protein. In one specific instance, which will be discussed further later, standard BL-21 *E. coli* are used instead. These bacteria are obtained from either a colony of plated bacteria (if a newly-cloned protein; the mutagenesis section below will provide more detail on this process) or a previously-made glycerol stock of frozen bacteria.

Inoculation is followed by incubation overnight at 37°C with shaking at 225 rpm. The following morning, 50 mL of the LB culture is added to each liter of TB media, and returned to 37°C with 225 rpm shaking. Bacterial density is monitored via measurement of the optical density of the culture medium measured at a wavelength of 600nm (OD_{600nm}); the remainder of the protocol varies depending on which protein is being expressed.

2.1.2.1 Cytoglobins and Cytoglobin Mutants

Once the optical density of the bacterial cultures reaches roughly 0.8, bacterial induction is induced via addition of 1 mL of 1M IPTG to each liter of culture. 1 mL of 0.4M δ -ALA is also added at this time to provide a precursor for heme synthesis.

At this point, the bacteria begin to synthesize both heme and the protein itself. Expressing Cymb in the same conditions used for bacterial growth (five liter flasks, 37° and 225 rpm) was shown to result in largely nonfunctioning protein, potentially due to protein production outpacing the rate of heme cofactor synthesis. In order to slow down protein synthesis, following the addition of IPTG and δ -ALA, the cultures are transferred into one liter Erlenmeyer flasks. These flasks are then incubated overnight at 30°C and 100 rpm shaking. The combination of the lower temperature and relatively lower oxygen levels in media (due to a nearly full flask and slower shaking, decreasing the surface area available for gas exchange) restores the balance between protein and cofactor synthesis, and leads to high-quality, functional protein.

2.1.2.2 Neuroglobin, Neuroglobin Mutants, and Globin X

For the other globins expressed recombinantly, IPTG is used to induce bacterial expression at an OD₆₀₀ of anywhere from 0.6 to 0.8, with 1 mL of 0.4 M δ -ALA being added concurrently. These proteins did not exhibit the problems with poor cofactor incorporation that were observed with

the cytoglobins, and so can be left in five liter flasks at 37 deg and 225 rpm overnight while producing protein.

2.1.2.3 Cytochrome b5

For cytochrome b5, induction of protein expression with IPTG and supplementation with δ -ALA is performed when the optical density at 600 nm reaches a value of 0.8 to 1.0; a higher optical density is chosen because this protein requires a shorter time period for expression. The bacteria are kept in five liter flasks at 37° and 225 rpm throughout the protein expression process. It was observed early on that overnight expression of this protein resulted in greatly reduced bacterial yields and thus small amounts of recoverable protein, presumably via some still unknown mechanism of toxicity. In fact, peak bacterial and protein yields were found to be obtained roughly four hours after bacterial induction. As such, these bacteria are harvested (see below) four hours after induction of protein expression, rather than the following day.

2.1.2.4 Cytochrome b5 reductase

Cytochrome b5 reductase (CYB5R) is expressed very similarly to the neuroglobins and globin X, but as this protein does not include a heme prosthetic group, no δ -ALA is added. In every other regard, expression of this protein proceeds in the same fashion.

2.1.2.5 Final Common Step: Bacterial Harvesting

Regardless of the protein expressed, or the exact conditions used for protein expression, the final step of expression is always the same. The culture media is subjected to 10 minutes of centrifugation at 10,000x g and 4°C. Typically, this centrifugation is performed two liters at a time, with approximately 330 mL in each of 6 500 mL bottles. This process forms a pellet of

bacteria at the bottom of the container; after decanting off the media, this bacterial pellet can be removed and subjected to further processing. Depending on the specific protein and growth conditions, one liter of media can yield anywhere from 1 to roughly 10 grams of bacteria. In general, four liters of soluble prep culture yields anywhere from 0.5 to 3 micromoles of protein.

2.1.3 Bacterial Culture and Protein Expression: Inclusion Body Method

As our group began to move from *in vitro* protein work to animal models, a protein expression method that was able to yield larger amounts of protein became necessary. For example, certain animal experiments performed in our lab required three to five micromoles of protein. In order to increase protein yields, protein expression in inclusion bodies was explored as an alternative method. Inclusion bodies are insoluble aggregates of misfolded protein; while production of functional protein from these inclusion bodies requires some additional steps, the overall yield of protein per liter of bacterial culture tends to be much greater.

Unlike the soluble method of protein expression, the expression of protein in inclusion bodies is always performed the same way, regardless of the specific protein being expressed. The process begins the same way as the soluble prep, with inoculation of 300 mL of LB media containing 30 $\mu\text{g}/\text{mL}$ of Kanamycin, followed by overnight culture at 37° C with 225 rpm shaking. The following day, 50 mL of this culture is added to four separate five-liter flasks, each containing one liter of TB media with 30 $\mu\text{g}/\text{mL}$ Kanamycin. These flasks are returned to the incubator, where they are monitored until the OD₆₀₀ reaches 0.6 to 0.8. At this point, protein expression is induced via addition of 1 mL of 1M IPTG to each liter of culture, but the δ -ALA is omitted; this is intended to prevent heme synthesis, resulting in the production of nonfunctional inclusion body protein. Following induction, the cultures (still in five liter flasks) are returned to

37°C and 225 rpm and left there overnight. The following morning, the bacteria are pelleted via centrifugation at 10,000x g for 10 minutes at 4°C. This process yields 5-7 grams of off-white bacterial pellet per liter of culture.

While Solu-BL21 cells were typically capable of producing inclusion bodies when cultured under these conditions, in the case of one specific mutant Cygb, the V85I single mutant, no inclusion bodies were obtained from SoluBL-21 cells. To address this, the plasmid containing the gene for this specific mutant was inserted into standard BL21 *E. coli*, which are not optimized for soluble protein expression. This change resulted in the expression of large amounts of inclusion body protein. Even for mutants that are expressed in inclusion bodies in Solu-BL21 cells, the change to standard BL21 cells would likely greatly increase the amount of inclusion bodies produced. This may become necessary for other mutants in the future, especially for tests in animals larger than mice, which will require large amounts of protein.

2.2 PROTEIN PURIFICATION

2.2.1 Lysis of bacteria

Before protein can be isolated from bacteria, the bacteria must first be lysed. This is accomplished in two steps. First, following expression and harvest, all bacterial pellets are placed in a freezer kept at -80° C. This freezing and subsequent thawing before purification results in some lysis. After being thawed, the pellets are resuspended to a volume of roughly 20 mL per liter of initial bacterial culture. This resuspension is performed into whatever buffer is used for the first step of subsequent purification, which varies based on the purification method being

used. The specific resuspension buffers will be listed below in the corresponding purification sections. These resuspended bacteria then undergo sonication on a Qsonix sonicator. Using a ½ inch flat tip and an amplitude setting of 5 on the sonicator, the bacteria are sonicated for a grand total of 30 minutes in 15-second pulses, each with 30 seconds of inactivity in between. During this process, the bacteria are kept on ice (to prevent excessive heating and protein denaturation) and constantly stirred via a magnetic stir plate.

Following lysis, the lysate is centrifuged for 1 hour at 18,000x g and 4°. This process separates out insoluble components, mostly membrane fragments and other cellular debris, from the soluble protein, which is recovered in the supernatant. The supernatant is then filtered through a filter with a 0.22 µm pore size to remove large contaminants. In some cases, the supernatant is unable to pass through the filter due to significant contamination, often with residual bacterial DNA. Treatment with polyethyleneimine (PEI), a positively-charged compound that binds DNA and renders it less soluble, can ameliorate this issue. While the supernatant is kept on ice and actively being stirred, 1 to 3 mL of 10% PEI is added into the solution, which prompts the virtually immediate and clearly visible precipitation of nucleic acids. 20 minutes of additional centrifugation results in formation of a DNA pellet and a protein-containing supernatant that is far easier to filter and process further. The “clarified lysate” that results from this process consists largely of soluble proteins, but additional purification is required to separate the protein of interest from all the bacterial proteins present. These further steps are carried out using an AKTApurifier system (GE) and a variety of different chromatography columns that allow for the separation of different proteins for soluble proteins. The inclusion body proteins are purified via a different process that does not rely on

chromatography, but instead isolates inclusion bodies via a series of centrifugation steps, followed by denaturation and subsequent refolding of the protein of interest.

2.2.2 Nickel-based affinity purification

For most of the proteins studied in this work, specifically all cytoglobins, globin X, and cytochrome b5 reductase, the protein has been modified to include a region that contains numerous histidine residues. This “histidine tag” does not affect protein function, but simplifies the process of protein purification. The tag causes the protein to have very high affinity for nickel ions that can be immobilized on a specialized Ni-NTA resin.

The Ni-NTA column is prepared by pumping 100 mM nickel sulfate (NiSO_4) through a column containing Ni-NTA resin. Repeated purifications can decrease the effectiveness of the column, so following every use, the column is regenerated via addition of 100 mM EDTA to strip out old nickel ions. water to remove residual EDTA, and finally more nickel sulfate to reload the column.

If this purification method is to be used, the initial resuspension of the bacteria is performed in a buffer containing 50 mM sodium phosphate (NaPO_4) pH 8.0, 300 mM sodium chloride (NaCl), and 10 mM imidazole. The column is also equilibrated with this buffer before protein is loaded onto the column. After protein loading, 100-200 mL of this buffer is used to wash the column. The imidazole present in the buffer displaces proteins with low affinity for the nickel ions, but high affinity proteins, like those with histidine tags, remain bound to the column.

Protein is eluted via a gradient of increasing imidazole, from the initial 10 mM concentration up to a final concentration of 200 mM, a concentration high enough to displace virtually any protein from the resin. As the imidazole is increased, the purification system

measures the absorbance of the column outflow at 280 nm (general protein peak) and 410 nm (heme-specific peak). At some point during the gradient, usually around 80-100 mM imidazole, the absorbance at 410 rapidly increases to a high level, indicating the elution of the heme protein of interest. During this period, the outflow from the column is collected, and is a relatively pure solution of the desired protein. The very high level of imidazole present, however, would dramatically affect protein function and must be reduced. This is accomplished via concentration of the protein solution in a 10 kDa molecular weight cutoff centrifugal filter and subsequent redilution of the protein in 100 mM NaPO₄, pH 7.4. This process is repeated until the concentration of imidazole has been reduced to low nanomolar levels, at which point the protein is concentrated a final time, divided into 30-50 µL aliquots, and stored at -80° C.

2.2.3 Anion exchange purification

A small number of the recombinant proteins produced in our lab do not include a poly-histidine tag, as this tag was found to influence the structure or function of these proteins. The most prominent example is CYB5. Because these proteins lack the His tag, they cannot be purified by Ni-NTA affinity chromatography. Instead, they are purified through two successive chromatography columns. The first column is an anion exchange column, loaded with DE-32 resin. This resin is positively charged, and thus allows negatively charged molecules, including CYB5 (which has significant concentrations of negative charge on its surface), to bind to the resin. Elution is performed by a gradient from low salt to high salt; the increasing salt concentration floods the column with anions, displacing proteins as the anion concentration increases. Proteins with more negative charge will be eluted later, as higher anion concentrations are required to displace them from the resin.

For this purification, a buffer containing 50 mM Tris and 1 mM EDTA at pH 8.0 is used to both resuspend the bacterial pellet and equilibrate the column. Following lysis and clarification of the lysate (centrifugation, PEI treatment, and filtering), the protein is loaded on to the column, which is then washed with addition 50 mM Tris, 1 mM EDTA, pH 8.0. Protein elution is initiated by slowly switching the flow (via the AKTA purifier's gradient function) to 100% 50 mM Tris, 1 mM EDTA, 200 mM NaCl, pH 8.0. As the salt concentration increases, proteins will elute from the column. CYB5 elution is detected by observing an absorbance peak at 410nm in the eluent (corresponding to heme, as CYB5 is a heme protein). All fractions containing CYB5 are collected and concentrated in 10 kDa MWCO centrifugal concentrators to a total volume of no more than 1.5 mL. This small volume of protein is ready for further purification on a second chromatography column.

2.2.4 Size-exclusion purification

The second column uses size exclusion chromatography, also referred to as gel filtration, to further purify CYB5. Size exclusion resin contains pores of many different sizes, and relies on these pores to change the transit time for proteins through the resin. Because smaller proteins can enter more pores than larger ones, they will be retained longer, and elute from the column later. In order to maximize the separation during this step, the resin is kept in a very long chromatography column.

This column is equilibrated with 50 mM Tris, 1 mM EDTA, 200 mM NaCl, pH 8.0, as the protein is already in this buffer, and the process of size exclusion is largely unaffected by the specific buffer used. Elution does not require any changes in the buffer, simply time and continued washing. Once again, eluent showing an absorbance peak at 410nm is collected into

fractions, and these fractions are pooled and concentrated using 10 kDA centrifugal concentrators. The final protein solution is typically buffer exchanged into 100 mM Tris or sodium phosphate, pH 7.4, before separation into aliquots and storage at -80°C. Compared to protein purified via Ni-NTA purification, this buffer exchange process is far less extensive, as no component of the purification buffers can affect protein behavior the way imidazole can. One or two cycles of concentration and resuspension in the desired storage buffer are sufficient to ready protein purified in this way for storage.

2.2.5 Inclusion body purification

For purification of inclusion bodies, the pelleted bacteria are resuspended in 100 mM Tris pH 7.4 to undergo sonication and lysis. Following bacterial lysis, the inclusion bodies are isolated via a series of centrifugation and resuspension steps. All centrifugation steps are performed at 4°C. Initially, the lysate is centrifuged at 6900x g for 30 minutes. The supernatant resulting from this step should contain the soluble portions of the bacteria, including all protein not in inclusion bodies. This supernatant is discarded, and the pellet, which is composed primarily of inclusion bodies and membrane debris, is resuspended in a solution of 50 mM Tris pH 7.5, 5 mM EDTA, and 2% deoxycholic acid. Deoxycholic acid is a bile salt, which readily solubilizes the lipids that make up the membrane debris present in the pellet. After sonicating to resuspend the pellet, the solution is spun again, this time for 10 minutes at 10,700x g. During this spin, the membrane debris remains soluble, while the inclusion bodies again form an insoluble pellet. This process of resuspension in Tris+EDTA+deoxycholic acid and subsequent centrifugation is repeated 2-4 times, until the supernatant following centrifugation appears completely colorless. The pellet is then resuspended one time in filtered millipure water, and spun a final time, again for 10 minutes

at 10,700x g. The resultant pellet should contain the desired inclusion bodies and virtually nothing else.

To obtain usable protein from the misfolded, aggregated inclusion bodies, the first step is to denature all of the inclusion body protein. To do this, the pellet is resuspended in a solution of 50 mM Tris pH 7.5 containing 6M guanidinium HCl, a potent chaotropic agent that induces complete protein denaturation. Just before resuspension, dithiothreitol (DTT) is added to the guanidinium solution to a final concentration of 36 mM. This level of DTT, a potent reducing agent, acts to keep any surface thiols on the protein reduced during denaturation and refolding, thus ideally preventing any aggregation via intramolecular disulfide formation. At this stage, the protein is resuspended into a volume of 5 mL for each original liter of culture from which the inclusion bodies were obtained. As protein was typically expressed in four liters of media at a time, this step usually saw resuspension into a total volume of 20 mL.

Once the protein has been completely denatured, the absorbance of the protein solution at 280 nm is measured. Using the extinction coefficient at 280nm for the specific protein expressed (which can be calculated from the number of tryptophan residues present in the protein, with additional minor contributions by tyrosine, phenylalanine, and cysteine), the concentration of the unfolded protein can be calculated.

The steps described above to isolate and denature inclusion body protein have been well-documented in the literature, and are virtually identical for all proteins. Following denaturation, however, the protein must then be refolded, and here the literature becomes far less clear. Ample protocols have been developed for refolding denatured protein, but the vast majority of these proteins do not require any additional cofactors for proper refolding or function, resulting in a relatively simple process. When refolding heme proteins, because the inclusion body form of the

protein does not include the heme prosthetic group, the process is complicated by the need to provide supplementary hemin to the protein as it refolds. Obtaining heme proteins from inclusion bodies is not unheard of, but the process is most commonly used to create peroxidase enzymes.

A key difference between peroxidases and globins is that peroxidases are stable in the “apo” form, with no heme group present; as a result, peroxidases are simply refolded like any other protein, with heme being added as a final step. Globins, in contrast, are typically very unstable in the apo form, and thus require heme to be present during the process of refolding. There have been some published protocols documenting the refolding of globins from inclusion bodies, but attempts to replicate these protocols did not result in the recovery of any functional protein. The protocol documented here has been developed via adaptation of published protocols for refolding of globins, peroxidases, and even non-heme-containing proteins.

In general, protein refolding has two main priorities: promoting proper refolding and minimizing aggregation. This protocol aims to satisfy those criteria, providing conditions that promote refolding but not aggregation. Aggregation is limited by performing all steps at 4°C, either in refrigerated centrifuges or a cold room. The initial steps of refolding are also allowed to proceed in a buffer that contains several components that either promote refolding or inhibit aggregation.

Once the protein has been completely denatured, the absorbance of the protein solution at 280 nm is measured. Using the extinction coefficient at 280nm for the specific protein expressed (which can be calculated from the number of tryptophan and tyrosine residues present in the protein), the concentration of the unfolded protein can be calculated.

The first step is dilution of the denatured protein into a refolding buffer. The basis of the buffer is 50 mM Tris pH 7.5, to which numerous other components are added, all of which are

chosen either to stabilize the refolding protein, prevent unwanted aggregation, or both. The first component is guanidinium HCl, at a concentration chosen to ensure a final concentration between 0.6 and 0.7 M once the denatured protein is added. While very high guanidinium completely denatures protein, this intermediate concentration is high enough to prevent immediate aggregation of the protein, but low enough to still allow refolding to occur over time. Also present in the refolding buffer are glycerol (10% by volume) and NaCl (300 mM final concentration). These compounds have both been reported to act as stabilizers during protein refolding, keeping the partially folded protein intact and decreasing the rate of misfolding[79]. In isolation, however, these stabilizers are not able to prevent the partially folded proteins from coming together as insoluble and nonfunctional aggregates. As such, stabilizers should always be accompanied by another agent which can serve as an aggregation inhibitor, a role filled here by the amino acid glycine (final concentration 500 mM). Glycine, like other amino acids, is thought to bind to the surface of partially folded proteins near hydrophobic residues, increasing the protein's mobility and likely encouraging proper refolding while preventing aggregation [80]. The final component of the refolding buffer is hemin. Based on the measured concentration of the protein, hemin is added such that the total amount of hemin is in roughly 20% excess compared to the total amount of protein. The hemin must first be solubilized in a small volume of 50 mM Tris pH 7.5 with 10 mM NaOH; these basic conditions allow the hemin to enter solution, at which point it can be added to the refolding buffer. Interestingly, once added to the refolding buffer, the hemin (which is obtained as a black powder) rapidly takes on a strong green color.

Typically, the volume of refolding buffer is chosen such that the denatured protein is diluted 20 to 30-fold upon addition to the refolding buffer. For 20 mL of denatured protein, 480

mL of refolding buffer is prepared, resulting in a 25-fold dilution of the protein into the refolding buffer. The protein is not added to the refolding buffer all at once, but is slowly dispensed into the solution using a P-1 peristaltic pump (GE Healthcare) set to the lowest setting (1x flow mode, dial set to 1). During the addition of the protein, the refolding buffer is on a magnetic stir plate with constant stirring. This slow addition and immediate mixing of the protein results in a very low initial protein concentration. Because refolding is a zero-order process (intrinsic to a single molecule), but aggregation is higher order (stems from interaction of multiple molecules), a low protein concentration promotes refolding over aggregation. It has been suggested that adding the protein gradually allows progressive refolding, with protein added early in the process folding into a state that is less likely to aggregate before addition of the remainder of the protein. Once the entirety of the protein has been added, the solution quickly turns from green to brownish-red, indicating rapid heme binding by the protein.

At this point the protein is left to refold, stirring in the cold room, for at least 48 hours¹. By this time, the initially clear solution has typically become very turbid as a result of the formation of insoluble aggregates. The next step of the process is to dilute the protein further, but first the volume must be reduced (as diluting from an initial volume of 500 mL would rapidly become unworkable). Before concentrating the protein, the solution is centrifuged at 24,000x g for 45 minutes to remove insoluble material, then filtered through a 0.45 μm filter. The solution is then concentrated down to a final volume of 10 mL or less using Amicon centrifugal protein concentrators with a MWCO of 10 kDa. This is achieved via repeat centrifugation at 4,000x g

¹ While 48 hours is the minimum time recommended for this step, longer times seem to have no negative effect. This step has been allowed to proceed as long as a week with no appreciable loss in final protein yield, and in fact, as this time is extended, the aggregation seen in the subsequent concentration step seems to decrease.

and 4°C. As the protein concentration increases, some protein aggregation is observed as a film deposited on the concentrator membranes, but the end result is a highly concentrated solution of (presumably) partially-refolded protein.

The next step is to dilute this protein roughly 40 times into 50 mM Tris, pH 7.5, with addition of DTT to a final concentration of 1 mM just before protein dilution. Protein addition is once again performed with a P-1 peristaltic pump on the lowest setting, in the cold room, with constant stirring of the solution. Once again, this solution is left in the cold room for at least 48 hours to allow refolding to proceed.² This solution is then concentrated again, using 10 kDa MWCO centrifugal concentrators. At this point, the concentration of guanidinium HCl has become low enough that slow dilution is no longer necessary, as the protein should be nearly finished refolding. The centrifugal concentrators are then used to buffer exchange the protein into 100 mM Tris, pH 7.4, with buffer exchange continuing until guanidinium concentrations are down to the nanomolar range. The resultant protein can be aliquoted and stored at -80°C.

2.3 SITE-DIRECTED PROTEIN MUTAGENESIS

A major component of this project centered on the generation and characterization of novel Cygb mutants with the goal of turning them into potential therapeutic molecules. This section details how specific mutants were identified for therapeutic potential, as well as how these novel mutants were then produced.

² As with the previous refolding step, this time has been extended out to one week or more with no negative effects observed.

2.3.1 Selection of Desired Mutants

The first step in generating mutant proteins for therapeutic use is to identify which residues represent potentially beneficial targets for alteration. This requires that the desired characteristics for different clinical applications be defined in advance, based on the specific pathophysiology of the condition the molecule is intended to treat. Once these ideal characteristics have been enumerated, the next step is to review previous globin mutagenesis work to determine which mutations might yield the desired effects. Once promising mutants have been identified, the process of generating these mutants can begin.

2.3.1.1 Desired functional characteristics

For proper function as an oxygen carrier, important characteristics include oxygen affinity, autoxidation rates, potential for rapid reduction by CYB5 or ascorbate, and nitrite reduction. The oxygen affinity must be high enough to pick up oxygen in the pulmonary circulation, but also low enough to release bound oxygen in the peripheral tissues. Previous work in HBOC engineering suggests an oxygen P_{50} (partial pressure of oxygen at which 50% of the globin is oxygen-bound) between 1 and 10 mmHg is likely the ideal range for an acellular oxygen carrier [29, 30]. Autoxidation is the spontaneous conversion of the oxygen-bound form of the protein to the non-functional oxidized “met” form, which occurs at different rates for all heme globins. An ideal oxygen carrier would autoxidize slowly: hemoglobin, for example, autoxidizes at a rate of roughly 2% per day, and this is quickly reversed by CYB5-mediated reduction. As a bare minimum, autoxidation should be slow enough that the CYB5 system or millimolar levels of ascorbate are able to prevent any accumulation of the oxidized protein in normoxic conditions. Nitrite reduction allows globins to create nitric oxide from nitrite, potentially eliminating the

harmful vasoconstriction that results from nitric oxide scavenging. Rapid nitrite reductase activity is desirable in this application, as it will increase the potential for vasodilation with nitrite infusion.

For a carbon monoxide scavenger, the most important characteristics are carbon monoxide affinity and autoxidation rates. As discussed above, slow autoxidation is necessary to preserve the protein in the functional reduced state. Like an oxygen carrier, a CO scavenger that can easily be reduced is also ideal; even H64Q Ngb, which autoxidizes very slowly compared to most hexacoordinate globins, can oxidize to an undesirable degree within a relatively short period of time. This autoxidation is difficult to reverse, and has posed a challenge to my colleagues as they attempt to prepare this protein. Perhaps most importantly, a protein-based carbon monoxide scavenger needs a sufficiently high affinity for carbon monoxide to outcompete red cell hemoglobin for carbon monoxide and provide a therapeutic effect.

The requirements for a cyanide scavenger are even simpler. Because globins bind cyanide in the ferric form rather than the ferrous, autoxidation rates and reduction by CYB5 or ascorbate are effectively irrelevant. Essentially the only important characteristics for a potential cyanide scavenger are the protein's affinity for cyanide and kinetics of cyanide binding. An ideal cyanide antidote would bind cyanide rapidly and more or less irreversibly, preventing it from reaching other potential targets that would lead to toxicity.

2.3.1.2 Identifying promising mutations

As the development of therapeutic molecules from recombinant heme globins became a priority, both Ngb and Cygb were initially considered as potential starting points. As data was obtained characterizing the reduction of globins by Asc and CYB5, however (see chapter 3 for results), the focus of these efforts shifted primarily to Cygb. Because the ferrous form is so important for

function as an oxygen carrier, NO donor, and CO scavenger, Cygb's rapid reduction by various reducing agents made it an appealing starting point, especially when compared to Ngb's comparatively very slow reduction by both CYB5 and Asc.

Once Cygb had been identified as the desired backbone for any novel therapeutic mutants, the next step was to identify specific mutations that had the potential to optimize the functional characteristics of Cygb for one or more of the previously discussed clinical roles. Previous Cygb mutagenesis has focused primarily on the distal histidine (H81) and the protein's surface cysteines (C38 and C83). Distal histidine mutations show some desirable characteristics, including very high nitrite reductase activity and ligand affinity. This suggests they may function as ideal antidotes, capable of very tightly binding CO or cyanide. This is the principle behind H64Q Ngb, which has been developed by other members of our lab as a potential CO antidote [78].

Unpublished data from our lab shows that the oxygen affinity of hexacoordinate globins is also dramatically increased by mutating away the distal histidine, with estimates that H64Q Ngb has an oxygen P_{50} of 0.01 mmHg or lower. This would prevent meaningful oxygen release in the tissues, and suggests that distal histidine mutant globins would not function well as oxygen carriers. This prompted an examination of other residues, primarily in the distal heme pocket, that might increase nitrite reduction and slow autoxidation without dramatically increasing oxygen affinity. In this search, two frontrunners emerged in the B10 and E11 residues, which had been the subject of mutagenesis studies in Mb and Ngb [5, 81-83]. The most applicable study, published by other members of the Gladwin research group, focused on the effect of mutations at the B10, E7 (distal histidine), and E11 sites in Ngb, a protein with close structural similarity to Cygb. As such, these residues were chosen as the mutation sites for development of Cygb-based

therapeutics. The positions of these three residues with respect to the heme group in *HsaCygb* can be seen in figure 15.

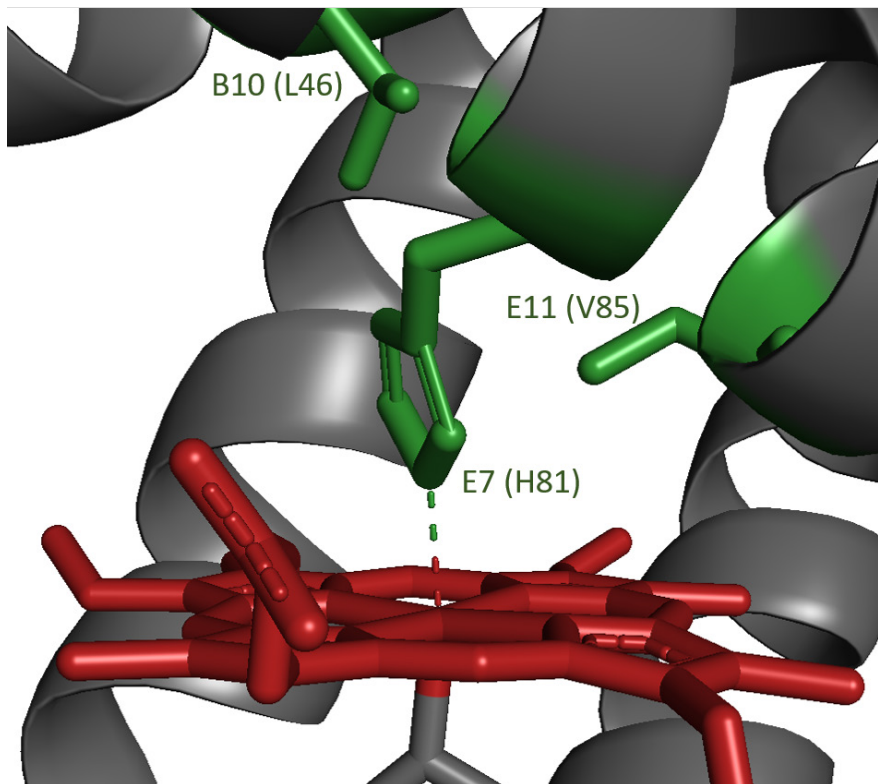


Figure 15: Distal heme pocket of Cygb, showing primary mutagenesis targets

Based on the results found in *Ngb* mutants, specific mutations were identified that it was believed may yield *Cygb* mutants with ideal properties for clinical use. The first such mutation was L46(B10)F, the replacement of the leucine at position 46 with phenylalanine. The B10 residue is natively a phenylalanine in *Ngb*, and mutating it to a leucine was seen to increase the rate of autoxidation 7 to 8-fold while speeding nitrite reduction roughly 5-fold. The reverse mutation in *Cygb* was expected to yield roughly opposite effects, slowing autoxidation and nitrite reduction. This mutation was chosen for addition to the wild-type protein, which may slow

autoxidation enough to have potential as an oxygen carrier, but also in the H81(E7)Q mutant, as slower autoxidation combined with the loss of the distal histidine has the potential to yield a powerful antidote to CO poisoning that also autoxidizes more slowly than the distal histidine single mutant.

The other two mutants that were found to be particularly intriguing were both mutants at the E11 site, which is occupied by residue V85 in Cygb. In Ngb, V68F and V68I mutants exhibited decreased autoxidation and increased nitrite reduction when compared to the wild-type protein. These were the only two mutants with the distal histidine intact that preserved both of these desirable characteristics. It was hoped that the combination of these two effects, if they could be replicated in the equivalent Cygb mutants, might yield a protein that could function well as an oxygen carrier and NO donor. Most of the mutations selected at this stage appeared to have fairly small effects on redox potential in Ngb, and so this was not a significant factor in my decisions at the time. The highest-priority mutations that were identified, and tentative predictions of their effects based on the characterization of corresponding Ngb mutants, are summarized in table 5.

Table 5: Predicted effect of chosen Cygb mutations on important functional characteristics

Mutation(s)	Expected effect of mutation(s) on:		
	Autoxidation	Nitrite Reduction	Redox Potential
L46F	↓ vs. wild-type	↓ vs. wild-type	↑ vs. wild-type
L46F + H81Q	↓ vs. H81Q	↓ vs. H81Q	↑ vs. H81Q
V85F	↓ vs. wild-type	↑ vs. wild-type	↔ vs. wild-type
V85I	↓ vs. wild-type	↑ vs. wild-type	↔ vs. wild-type

At this point, as preparation began to generate these mutants of Cygb, it was also decided to generate several other arguably less promising mutants at the B10 and E11 sites. While these additional mutants were considered less likely to result in a molecule with potential clinical use, mutagenesis studies still provide valuable information regarding structure-function relationships in protein. These other mutants included L46H, L46H + H81Q, V85A, and V85H mutants.

2.3.2 Generation of mutant plasmids

Once a desired mutation was identified, the plasmid containing the gene for the corresponding wild-type template protein had to be modified to include the mutation of choice. This was accomplished via a multi-step process, which is summarized here.

2.3.2.1 Primer Design

The mutagenesis reaction is essentially a polymerase chain reaction, but requires the introduction of a deliberate change in one or more base pairs. This is accomplished via the use of primers with a deliberate change in their DNA sequence.

For this specific reaction, the primers have a number of different criteria that must be met. First, each mismatched base pair (pair that has been changed between the primer and the template) should be flanked by at least 10 to 12 correct base pairs, to ensure the primer still binds the template. Second, the melting temperature (temperature at which the primer separates from the template) should be fairly high, typically around 78 to 80° C. Primers that met these criteria were designed using the QuikChange primer design tool, developed by Agilent and available online. Upon inputting the template gene, as well as the desired base pair changes, the program would output custom primers for that desired mutagenesis reaction.

2.3.2.2 Mutagenesis Reaction

Once primers were obtained, the next step was to carry out the site-directed mutagenesis. The reaction was performed in Phusion High-Fidelity PCR Master Mix (New England Biolabs, Ipswich, MA). 10 ng of template DNA and 125 ng of each primer (forward and reverse) were added to 25 µL of Master Mix, with nuclease-free water used to adjust the total volume for each reaction up to 50 µL.

The reaction was carried out in a BioRad C1000 thermal cycler (BioRad, Laboratories, Hercules, CA) according to the following protocol.

Step 1: 30 seconds at 95°C

Step 2: 18 consecutive cycles of the following three steps:

15 seconds at 95°C

30 seconds at 55°C

180 seconds at 72°C

Step 3: 10 minutes at 72°C

Step 4: Hold at 4°C indefinitely

Once the reaction was complete, 1.25 μL of DpnI were added to the 50 μL reaction volume. DpnI is a restriction enzyme that preferentially degrades methylated DNA. In this case, the template DNA was obtained from a bacterial source, where it was subject to methylation. The new mutant plasmid, on the other hand, has not been methylated, and thus DpnI selectively degrades the template, leaving only the mutant plasmid. This reaction is allowed to proceed for 90 minutes to 2 hours at 37° C. This time is sufficient to ensure complete or near-complete degradation of the non-mutant template plasmid while preserving the newly generated mutant plasmid.

2.3.2.3 Transformation into competent bacteria and plasmid isolation

In order to generate more plasmid, the product of the mutagenesis reaction had to be transformed into XL-10 Gold Ultracompetent *E. coli*. These bacteria have been optimized to efficiently take up and replicate large pieces of DNA, including plasmids. 50 μL of these cells were taken from storage at -80°C and put on ice. Once thawed, they were transferred to a 14 mL round-bottomed tube, at which point 2 μL of β -mercaptoethanol was added. The tube was then left on ice for 10 minutes, during which time it was swirled gently by hand every two minutes.

Plasmid transformation was initiated by the addition of 2 μL of DpnI-treated DNA to the cells, after which the tube was again swirled gently and left on ice for 30 minutes. This was followed by a heat pulse lasting exactly 45 seconds at 42°C, then returning the cells to ice for 2 minutes. After 2 minutes on ice, 500 μL of SOC media was added to the tube, and the tube was

moved to 37°C with 225 rpm shaking for one hour. After one hour, 300 µL of the cells were plated onto LB-Agar plates (25 g/L LB media and 20 g/L agar, roughly 25-30 mL per plate) containing 30 mg/mL Kanamycin and left to grow at 37° C overnight.

The following morning, the plate was checked for bacterial colonies: the presence of colonies suggested successful transformation, as survival on a Kanamycin-containing plate would be unlikely for non-transformed bacteria. If colonies were present, four isolated colonies (each presumed to arise from a single bacterium, and thus to express the same plasmid within the colony) were selected at random, and each was used to inoculate a 5 mL culture of LB media (25 g/L) containing 30 mg/mL Kanamycin. These cultures were left at 37° with 225 rpm for 12-16 hours.

Following this growth period, the bacteria were pelleted via 15 minutes of centrifugation at 3000 rpm and 3°C in an Allegra X-15R centrifuge (Beckman Coulter, Brea, CA). From these pelleted bacteria, plasmid DNA was isolated using a MiniPrep plasmid isolation kit (Qiagen, Hilden, Germany). Throughout this process, the samples were kept separate, to ensure that each product was obtained from a single bacterial colony.

Following plasmid isolation via the miniprep kit, the presence of DNA was confirmed via an ethidium bromide gel. A gel of 1% agarose in Tris-Acetate-EDTA (TAE) buffer was prepared and mixed via heating. Once slightly cooled but still liquid, 2 drops of ethidium bromide (EtBr) were added to the gel, after which it was poured into its mold and allowed to cool. Once the gel was completely cool, it was immersed in TAE buffer, and each well was loaded with 5 µL of sample (4 µL MiniPrep product from a single colony + 1 µL 5x nucleic acid sample buffer). The gel was then run at 90 V for 30-40 minutes, and imaged using a BioRad ChemiDoc Imager. The

presence of a band when the gel was imaged was indicative of DNA, and suggested successful recovery of the plasmid.

2.3.2.4 Sequence confirmation

The final step in generating a novel mutant plasmid was to confirm that the mutation had been properly incorporated into the gene. Samples of the plasmid were submitted to the Genomics Research Core (GRC) at the University of Pittsburgh for Sanger Sequencing. All samples were composed of 50-100 ng of plasmid DNA and 0.8 picomoles of T7 forward promoter in a final volume of 15 μ L. After 2-3 business days, the GRC would provide the complete sequence of the *Cygb* gene (placed after the T7 promoter in the plasmid) present in the sample, which could be compared to the desired mutant sequence to confirm successful mutagenesis.

2.3.3 Transformation into expression bacteria

Before the confirmed mutant plasmid can be used to make recombinant protein, it must be transformed into a second type of *E. coli*, one ideal for expression of proteins. For this step we use Solu-BL21 cells, already mentioned in a previous section, which are optimized to express soluble proteins.

The process of Solu-BL21 transformation is similar to transformation of XL-10 Gold cells, but somewhat simpler. Once again, 50 μ L of bacteria are removed from storage at -80° C and moved to a 14 mL round-bottom flask once thawed. 5-10 ng of plasmid DNA is then added, mixed gently but thoroughly, and the cells are left on ice for 15 minutes. This is followed by a 45 second heat shock at 42° C, and the subsequent addition of 250 μ L of SOC media, after which the bacteria are moved to 37° C with 225 rpm shaking for one hour. At the conclusion of this hour,

the entire volume (300 μ L) is plated onto LB-Agar plates containing Kanamycin, and left overnight at 37° C. If colonies are present in the morning, one of these colonies is used to inoculate a larger (usually 300 mL) culture of LB media containing 30 mg/mL Kanamycin. This represents the first step of expression of soluble protein, which can then proceed as detailed above in section 2.1.

2.3.3.1 Glycerol stock production

The first time bacteria containing the plasmid for a new mutant protein are cultured, they are first grown in a single 300 mL culture of LB media containing the appropriate antibiotic. A total of 200 mL of this culture are used to seed larger 1 L cultures, leaving 100 mL left over. From this leftover volume, 500 μ L is removed and mixed in a small cryo-tube with an equal volume of 50% glycerol. This process results in a 1 mL glycerol stock, which is then stored at -80°C. If expression of that mutant is desired again in the future, the glycerol stock can be used to inoculate the 300 mL culture in LB media. This task is typically performed by using a small plastic pipette tip to scrape up a small amount of the frozen glycerol stock, then dropping the entire tip into the culture media. For each new mutant generated, three glycerol stocks were generated and stored at -80°C, facilitating repeat expression of these novel mutants.

3.0 REDUCTION OF HEME GLOBINS BY CELLULAR REDUCTANTS

This work has already been published in the journal *Biochemistry*. While the text has been rewritten for this work (but with a very similar structure), rather than directly copied, the figures shown in this chapter are largely unchanged from those previously published. With occasional modifications or adaptations, all figures are reprinted (adapted) with permission from:

Amdahl MB, Sparacino-Watkins CE, Corti P, Gladwin MT, Tejero J. Efficient Reduction of Vertebrate Cytoglobins by the Cytochrome b/Cytochrome b Reductase/NADH System. *Biochemistry*. 2017;56(30):3993-4004. Copyright 2017 American Chemical Society.

Rationale and aims

A major question for both the development of globin-based therapeutics and the search for the *in vivo* functions of the hexacoordinate globins is how the heme iron can be kept in the reduced Fe^{II} state. Binding of oxygen or CO requires the reduced iron, but autoxidation, nitrite reduction, and NO dioxygenation all oxidize the iron. In order to guide both our development of therapeutic globins and our understanding of potential *in vivo* signaling pathways for various globins, it was important to characterize how a wide variety of heme globins are reduced by two common globin reducing systems.

The first is the CYB5/CYB5R/NADH system, known to be primarily responsible for the reduction of Hb in red blood cells and numerous other targets. The second is ascorbate (vitamin C), also responsible for reducing a wide range of targets, including extracellular Hb in the plasma. It was hoped that, by identifying particularly efficient reductant-globin pairings, it would be possible to identify a way to keep therapeutic globins reduced, as well as gain insight into how potential globin functions requiring rapid electron transfer might be supported *in vivo*.

3.1 MATERIALS AND METHODS

3.1.1 Pseudo-physiologic reduction

Initially, the ability of both the CYB5 system and ascorbate to reduce globins was assessed at concentrations that simulate those found in physiologic conditions. These reactions were all performed in 100 mM sodium phosphate (NaPO₄) buffer at 37°C in anaerobic conditions. This test was performed for *HsaCygb*, *DreCygb1*, *DreCygb2*, human *Ngb*, human Hb, zebrafish globin X, and equine Mb (obtained from Sigma-Aldrich, St. Louis, MO).

The globin was reduced with excess potassium ferricyanide (KFeCN, Sigma-Aldrich), then passed through a G-25 desalting column to remove the ferricyanide. The protein was then diluted to 20 μM within a 1.7 mL optical glass cuvette (Starna Cell, Atascadero, CA). The reducing system was then added, and reduction was followed on an Agilent 8453 UV-Vis spectrophotometer (Agilent Technologies, Santa Clara, CA). The spectrum of the protein solution was measured between 450 and 700 nm, (the Q band region) once per second, for at least 900 seconds.

To assess reduction by the CYB5 system, CYB5, CYB5R, and NADH were pre-mixed to ensure complete reduction of the CYB5 prior to addition. Because CYB5 is a hexacoordinate heme protein, reduction of CYB5 produces spectral changes similar to those seen during reduction of a heme globin; premixing allows this reduction to occur before spectral measurements begin. This mixture was then added to the oxidized globin to final concentrations of 2 μM CYB5, 0.2 μM CYB5R, and 100 μM NADH. These concentrations roughly approximate those that can be found in certain cell types, and replicate the roughly 10:1 CYB5:CYB5R ratio that has been documented in liver tissue [84].

Tissue concentrations of ascorbate vary widely, from tens of micromolar to as high as several millimolar in certain tissues. After initial experiments revealed the reduction by ascorbate to proceed fairly slowly, a final concentration of 5 mM ascorbate was chosen, which represents the upper end of levels observed *in vivo*.

3.1.2 Kinetic analysis of reduction

While the pseudo-physiologic reduction provides valuable qualitative data, and suggests which globins are reduced most quickly (or most slowly) by cellular reductants, a qualitative analysis of the underlying kinetics provides a more direct comparison to other proteins and reactions. Based on the results of the pseudo-physiologic reduction tests, which showed rapid reduction of all the Cygbs, we set out to determine the kinetics for the reduction of all three Cygb proteins by both CYB5 and ascorbate.

3.1.2.1 Kinetics of ferric globin reduction by ascorbate

Kinetic characterization of the reduction by ascorbate was fairly simple. Each of the three Cygb's studied, as well as Mb (for comparison), were oxidized as described above, and reduction was then tested with a wide range of ascorbate concentrations (from 100 μM up to 50 mM). The reduction was again followed in anaerobic conditions for at least 900 seconds at 37°C in 100 mM NaPO_4 pH 7.4. When the observed reduction did not follow a single exponential as had been initially expected (see the results section for more details), the decision was made to instead calculate the initial rate of reduction at each concentration of ascorbate. For a bimolecular reaction, the reaction rate at any point in time is given by equation 3-1:

$$\text{Rate} = k * [\text{reactant 1}] * [\text{reactant 2}] \quad \text{Equation 3-1}$$

Where k represents the overall rate constant for the reaction in units of $\text{M}^{-1}\text{s}^{-1}$ and, in this case, the two reactants are the ferric globin and ascorbate. At the beginning of the reaction, the concentrations of both reactants (globin and Asc) are known. By holding the initial globin concentration constant and varying [Asc], a plot of initial reaction rate vs. [Asc] should have slope k, allowing calculation of the bimolecular rate constant.

3.1.2.2 Kinetics of ferric globin reduction by CYB5

The kinetics of CYB5-mediated reduction proved more complex. The pseudo-physiologic reduction experiment used not two but four separate chemical species (globin and CYB5, but also CYB5R and NADH). In order to measure the kinetics for the bimolecular reaction between CYB5 and globins, the two species needed to be isolated. This was accomplished by oxidizing the globin with ferricyanide and reducing the CYB5 with excess sodium dithionite. KFeCN and

dithionite were both removed via Sephadex G25 desalting columns (PD-10, GE Healthcare) equilibrated with 100 mM sodium phosphate pH 7.4. This step and all subsequent steps were performed in anaerobic conditions.

These reactions occur very quickly, and so were followed on an SX-20 stopped flow spectrophotometer (Applied Photophysics, Leatherhead, UK). This instrument uses pressurized gas to drive two separate samples into a mixing chamber, allowing for incredibly rapid (1 ms or less) mixing and measurement of spectra. This allows for the measurement of reactions that are completed within one second or less, which is impossible on most spectrophotometers.

For all globins, the final concentration of oxidized globin was held constant between 5 and 10 μM . The concentration of reduced CYB5 was varied from as high as 60 μM to less than 10 μM . Reactions were followed at 25°C in 100 mM sodium phosphate, pH 7.4. The time for the reactions varied from 1 second (for very fast pairings) out to 100 seconds or more (for the slowest reactions).

Once the data for these reactions had been obtained, the next step was to derive kinetic parameters from it. All kinetic calculations were performed using the measured absorbance at 568nm, as only the globin changes absorbance between the ferrous and ferric states at this wavelength. The reaction between a globin and CYB5 is a simple bimolecular reaction, which can be described by equation 3-2:



This reaction can proceed in either direction, governed by the bimolecular rate constants k_{fwd} for the forward reaction (globin reduction) and k_{rev} for the reverse reaction (globin oxidation).

First, the initial rate of reduction at each concentration of CYB5 was determined by calculating the slope of the linear portion of the absorbance data, usually the first 5 to 10 points. This yielded the initial velocity of the reaction in units of abs/s. By comparing the molar extinction coefficients at 568nm between the ferrous and ferric form of each globin, this value was converted to a velocity in $\mu\text{M/s}$, and subsequently divided by the concentration of the globin to obtain a rate in units of s^{-1} . A plot of initial rate vs. the concentration of CYB5 should be linear, with a slope initial to the k_{fwd} value.

Additional analysis of these data was performed according to the method described by Malatesta for non-pseudo-first-order conditions. The absorbance traces at 568nm were first fit to equation 3-3:

$$\Delta A_{\lambda} = \Delta A_{\text{eq}} \frac{1 - e^{-\eta t}}{1 + \omega e^{-\eta t}} + C \quad \text{Equation 3-3}$$

Where ΔA_{λ} equals the absorbance change at a given point in time for a specific wavelength (568nm in this case), ΔA_{eq} is the equilibrium absorbance change (the absorbance change at long time values where no change in the absorbance is still occurring) at the same wavelength, η is the observed rate constant for the reaction, ω is a constant between -1 and 1 that represents the data's deviation from first-order behavior, and C is a constant.

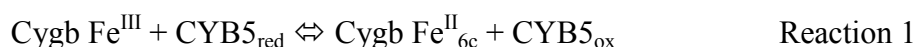
These observed rate constants (η values calculated from equation 6) can be plotted against the concentration of CYB5 and used to calculate the forward and reverse reactions via an additional fitting process, this time to equation 3-4:

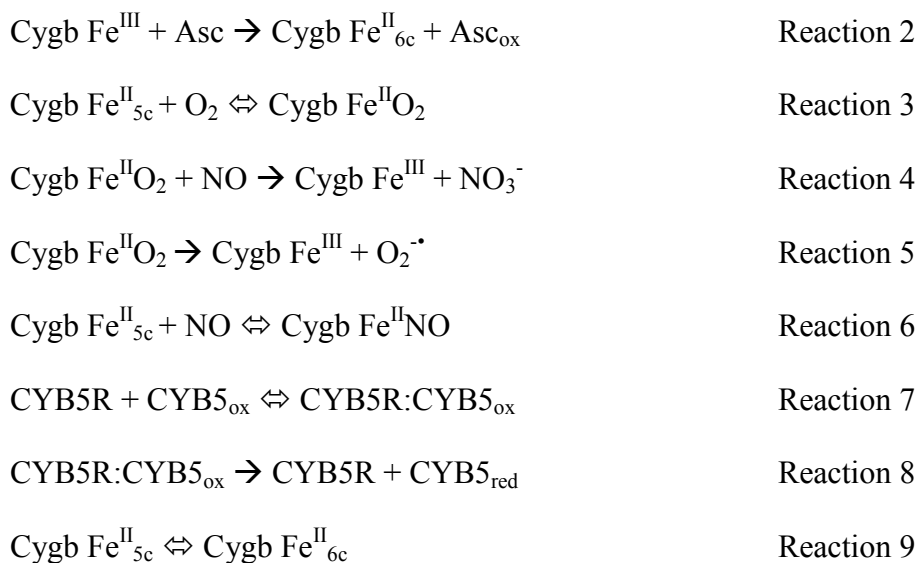
$$\eta = \sqrt{k_{fwd}^2([globin] - [CYB5])^2 + 4k_{fwd}k_{rev}[globin][CYB5]} \quad \text{Equation 3-4}$$

where η is again the observed rate constant at a given point, k_{fwd} and k_{rev} are the forward and reverse rate constants for the reaction, and $[globin]$ and $[CYB5]$ are the total concentrations of both the globin and CYB5 present in the reaction. Fitting to these two equations produced parameters with high standard deviation and very high dependency. In order to estimate values more accurately, the k_{fwd} values calculated from the initial rates were substituted into equation 7. All data analysis was performed using Origin 8.0 (OriginLab Corp.).

3.1.3 Support of NO dioxygenation activity

Dr. Jesús Tejero, an Assistant Professor in the Gladwin lab group, used the kinetic parameters derived in the first portion of this work to develop a mathematical model of CYB5 and ascorbate's interactions with Cygb. Using COPASI software, version 4.19, Dr. Tejero generated a model that incorporated nine reactions to calculate the time course of different Cygb species during Cygb reduction and NO dioxygenation reactions in oxygenated conditions. Those nine reactions are listed here:





In these reactions, $\text{Cygb-Fe}^{\text{II}}_{6\text{c}}$ denotes six-coordinate ferrous Cygb, $\text{Cygb-Fe}^{\text{II}}_{5\text{c}}$ indicates five-coordinate ferrous Cygb, $\text{Cygb-Fe}^{\text{III}}$ is ferric (met) Cygb, and $\text{CYB5R}:\text{CYB5}_{\text{ox}}$ is the Michaelis complex between CYB5R and CYB5_{ox} . In reaction 2, Asc_{ox} indicates the oxidation product of Asc, which could be the ascorbate radical or dehydroascorbate. To simplify the model, and because a high concentration of NADH is present during the experiment, CYB5R was assumed to be fully reduced throughout the reaction, allowing for the use of the approximation $[\text{CYB5R}]_{\text{red}} \approx [\text{CYB5R}]_{\text{Total}}$.

As a final test of the ability of reducing systems to support rapid redox cycling by *Hsa*Cygb, and to compare the *in vitro* experimental results against those predicted by Dr. Tejero's model, both the CYB5 system and ascorbate for their ability to support NO dioxygenation *in vitro*. This reaction, in which ferrous-oxy Cygb converts nitric oxide to nitrate and is oxidized in the process, occurs at near diffusion-limited rates, and has been implicated in many of the functions of Cygb [28, 42, 85]. Because Cygb is typically found in relatively low concentrations, this reaction is almost certainly catalytic, with each molecule of Cygb consuming many

molecules of NO. This requires a way to rapidly regenerate reduced Cygb following its oxidation.

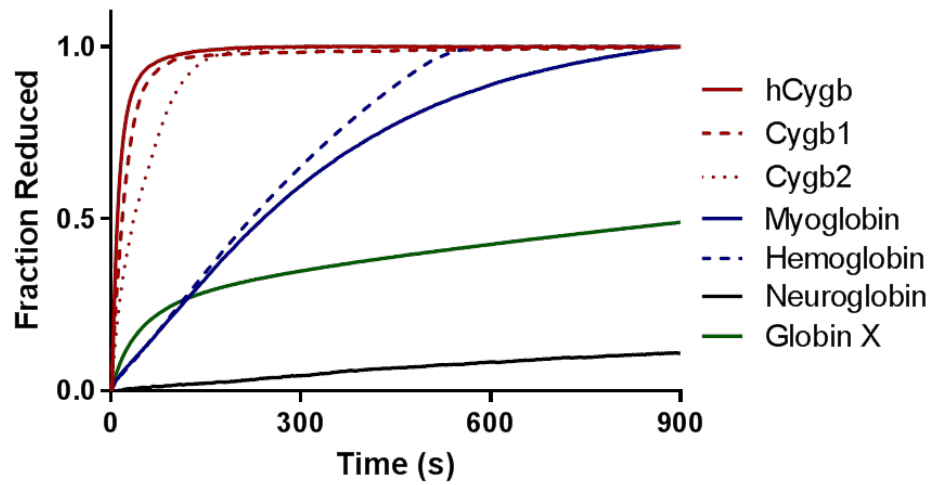
These reactions were carried out in a 1 mL cuvette, closed tightly with a screw cap and rubber septum. Inside the cuvette, in buffer saturated with 100% oxygen, 20 μ M ferric *HsaCygb* was mixed with either the CYB5 system (2 μ M CYB5, 0.2 μ M CYB5R, and 200 μ M NADH) or 5 mM Asc. The mixture was monitored via UV-Vis spectroscopy on an Agilent HP8453 until the characteristic peaks for the ferrous-oxy form of *HsaCygb* were apparent. NO dioxygenation was initiated via addition of NO-saturated buffer to a final NO concentration of 5-10 μ M. Once the spectra showed a return to the stable ferrous-oxy species, this process was repeated 3-5 more times. Spectral deconvolution using standard spectra for both *HsaCygb* and CYB5 was then used to determine the concentration of all species at each time point. These reactions were followed at 37°C in 100 mM sodium phosphate, pH 7.4.

3.2 RESULTS

3.2.1 Pseudo-physiologic reduction

The first experiment performed in this section examined the ability of both CYB5 (2 μ M) + CYB5R (0.2 μ M) + NADH (100 μ M) and ascorbate (5 mM) to reduce a variety of ferric vertebrate globins (all 20 μ M). In both cases, there was wide variation in the rates of reduction depending on the specific globin that was being examined. For both the CYB5 reducing system and Asc, the initial reduction of Cygb was very rapid when compared to that of all other globins. These results are depicted in figure 16.

A. Globin Reduction by CYB5 + CYB5R + NADH



B. Globin Reduction by Ascorbate

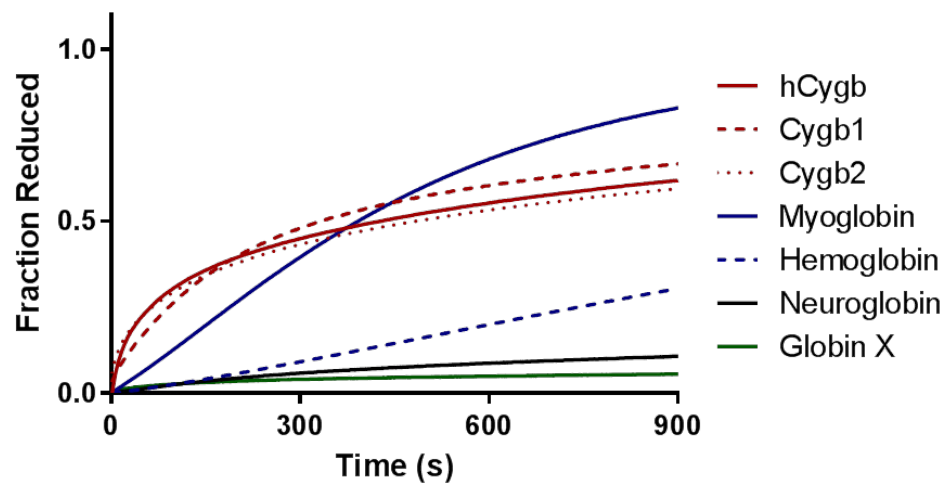


Figure 16: Pseudo-physiologic reduction of globins by the CYB5 system and Ascorbate

For the CYB5 system, the reduction of the Cygbs remained rapid throughout the reaction, as the Cygbs were all completely reduced within 100-200 seconds. Hb and Mb were reduced at intermediate rates, with complete reduction of both globins achieved at roughly 600 (Hb) or 900 (Mb) s. Globin X showed a rapid initial rate of reduction, but quickly slowed down, and by 900 s was only about 50% reduced. Ngb was reduced slowest throughout the reaction time, with only 10-15% reduction after 15 minutes. The reasons for this variation are not entirely clear: Ngb and GbX have very negative redox potentials, and so it is expected that they would be reduced most slowly. Hb and Mb, however, have redox potentials that are significantly more positive than those of the Cygbs, and yet are reduced significantly slower. This suggests that a factor other than redox potential of the heme iron may exert a strong influence on the redox interaction between CYB5 and the globins.

Reduction by ascorbate shows a similar trend in terms of initial rates, with the Cygbs exhibiting initial rates far faster than any other globins. Interestingly, this pattern does not persist as the reaction proceeds, with the rate of Cygb reduction declining as the protein approaches 50% reduced. Similar behavior is not seen for Mb, the reduction of which proceeds well beyond the point where Cygb reduction has almost entirely stopped, despite a slower initial rate. In fact, the reduction of Mb by Asc and by the CYB5 system look remarkably similar. The behavior observed for Cygb could be the result of a reversible reaction, likely involving an intermediate with Asc bound to ferric Cygb [86].

While the reduction of the Cygbs by the CYB5 system was clearly very fast, it was not clear from these first results which components of the reducing system were most important. Direct reduction of heme-based enzymes (such as sGC) by CYB5R, apparently without the need for CYB5 as an intermediary electron transporter, has been reported. When CYB5 was removed

from the experimental setup used to obtain figure 16a, reduction of the Cygb's and Mb did still proceed, as shown in figure 17. The rates, however, were much lower, and in most cases quickly leveled off, suggesting a backwards reaction (electron transfer from globin to b5r) at rates comparable to that of the forward. CYB5R exhibits a very negative redox potential, and so some ability to reduce the globins was to be expected, but it is clear that this reduction becomes far more effective when CYB5 is present. Removal of either NADH or CYB5R from the reaction mixture resulted in no reduction of the globin at all (data not shown).

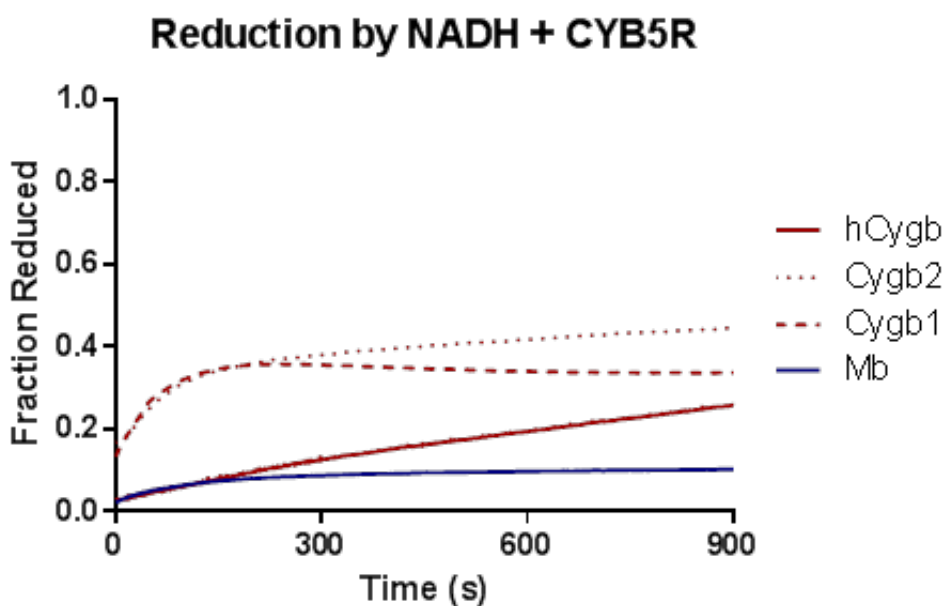


Figure 17: Globin reduction by NADH and CYB5R without CYB5

To further explore the interaction between the CYB5 reducing system and the Cygb's, the next experiment attempted to determine an apparent K_M for the reduction of Cygb.³ This was achieved by varying the concentration of the heme globins while holding the concentrations of the CYB5 system components at the same levels used for previous experiments. The resulting data, as well as fits of the data to the Michaelis-Menten equation, are shown in figure 18. All three Cygb's show relatively low K_M values of 3.6 ± 2.5 , 14 ± 2 , 1.6 ± 0.8 μM for *HsaCygb*, *DreCygb1*, and *DreCygb2*, respectively. These values tend to closely approximate the observed concentration of Cygb *in vivo*, which is typically in the micromolar range [87]. The V_{max} , or maximal reaction rate, was calculated as 5.0 ± 3.0 , 3.7 ± 1.0 and 5.0 ± 2.5 $\mu\text{M/s}$, again for *HsaCygb*, *DreCygb1*, and *DreCygb2*, respectively. It is worth noting that these values are likely to vary heavily depending on the specific concentrations of the reducing system components used, and in this specific case, the close proximity of the calculated K_M values to the CYB5 concentration (2 μM) suggests these values may vary significantly if the CYB5 concentration is changed. Nonetheless, these values indicate a very high affinity compared to other globins. The K_M of CYB5 for Hb has been reported to be between 0.11 and 2.2 mM, which seems to be very low affinity, but is still well below the typical concentration of Hb in erythrocytes [88]. For Mb, the relationship between globin concentration and initial reaction velocity remains mostly linear even up to 500 μM globin, at which point the absorbance limits of our spectrophotometers prevented further increase in the globin concentration. The relative linearity of the data within

³ K_M is the concentration of substrate (globin in this case) at which the rate of enzyme (the CYB5 system in this case) activity is one-half its maximal rate. A high affinity interaction will show high rates even at low substrate concentrations, which can be seen as a low value of K_M . A low calculated K_M thus indicates a high affinity of an enzyme for its substrate.

the measurable range lessens the quality of any Michaelis-Menten fit, but the analysis was nonetheless able to estimate a K_M of $790 \pm 250 \mu\text{M}$, which is consistent with both the reported affinity of CYB5 for Hb and the typical concentration of Mb in cells [89].

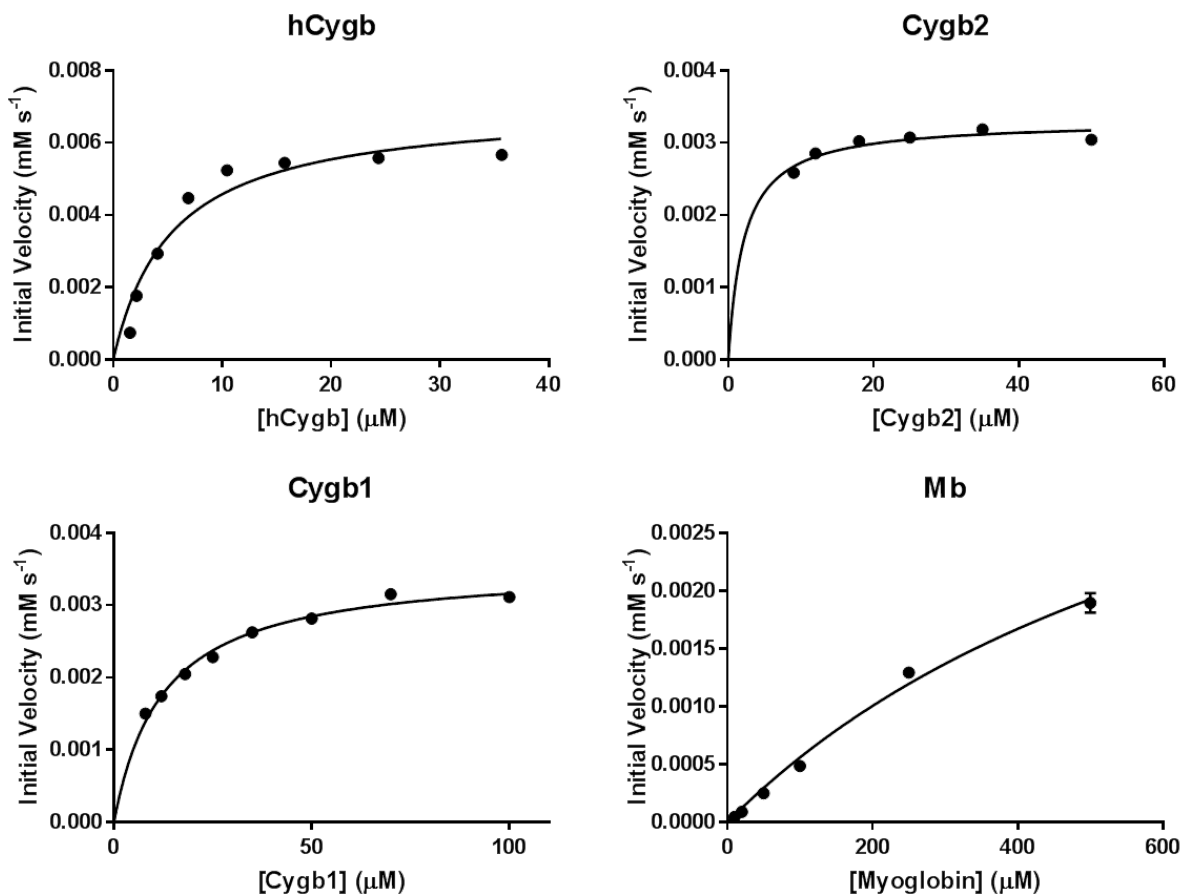


Figure 18: Michaelis-Menten kinetics of globin reduction by the CYB5 reducing system

3.2.2 Kinetic analysis of reduction

To begin analysis of the kinetics of globin reduction, the reduction of the Cygbs and Mb was first examined at ascorbate concentrations between 0.1 and 50 mM. The resulting reduction data are shown in figure 19. Even before kinetic analysis, several interesting qualitative trends can be observed. In all cases, the reduction proceeds with hyperbolic behavior, which has been previously reported for *HsaCygb* [86, 90, 91]. Second, even at extremely supraphysiologic levels of ascorbate (50 mM), none of the Cygbs reach 100% reduction after 15 minutes, even when the initial rate is very high. The behavior observed for the Cygbs could be the result of a reversible reaction, likely involving an intermediate with Asc bound to ferric Cygb [86]. This trend is not observed for Mb, which is essentially 100% reduced within 15 minutes by 10 mM or greater ascorbate.

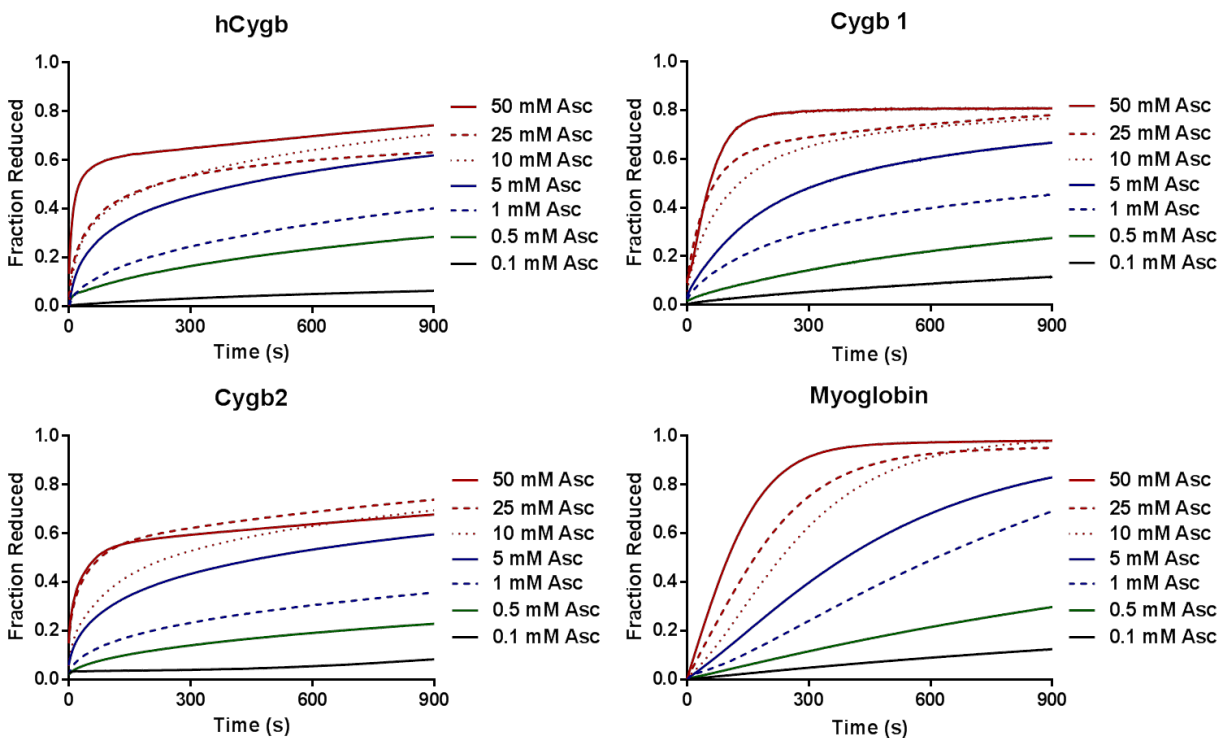


Figure 19: Reduction of heme globins by varying concentrations of ascorbate

Further trends become apparent when the initial velocity of reduction for each concentration of Asc is calculated. The calculated initial velocities at each concentration of Asc can be seen in figure 20. For the Cygb's, increasing concentrations of Asc above a certain point do not continue to yield linear increases in the initial rate of reduction. This behavior, which is not observed for Mb, has been documented previously for *HsaCygb* [90]. The linear relationship seen for Mb allows for calculation of the bimolecular rate constant for Asc-mediated Mb reduction, which comes to $0.124 \text{ M}^{-1}\text{s}^{-1}$. Within the approximate physiologic range of Asc concentrations (0-10 mM), the relationship between Asc concentration and initial rate is sufficiently linear for all three Cygb's to allow for calculation of bimolecular rate constants. Linear fits to these regions of each plot yield rate constants of $1.14 \pm 0.17 \text{ M}^{-1}\text{s}^{-1}$, $0.83 \pm 0.07 \text{ M}^{-1}\text{s}^{-1}$, and $0.83 \pm 0.07 \text{ M}^{-1}\text{s}^{-1}$ for hCygb, Cygb 1, and Cygb2, respectively.

$^1s^{-1}$, and $1.04 \pm 0.15 M^{-1}s^{-1}$ for *HsaCygb*, *DreCygb1*, and *DreCygb2*, respectively. These rates agree relatively well with previously published rates for *HsaCygb*[85, 92] and Mb [85, 86]. Another previously published rate for *HsaCygb*, however, is one order of magnitude higher [90]. A summary of my calculated rate constants, as well as related values previously published, can be found in table 6.

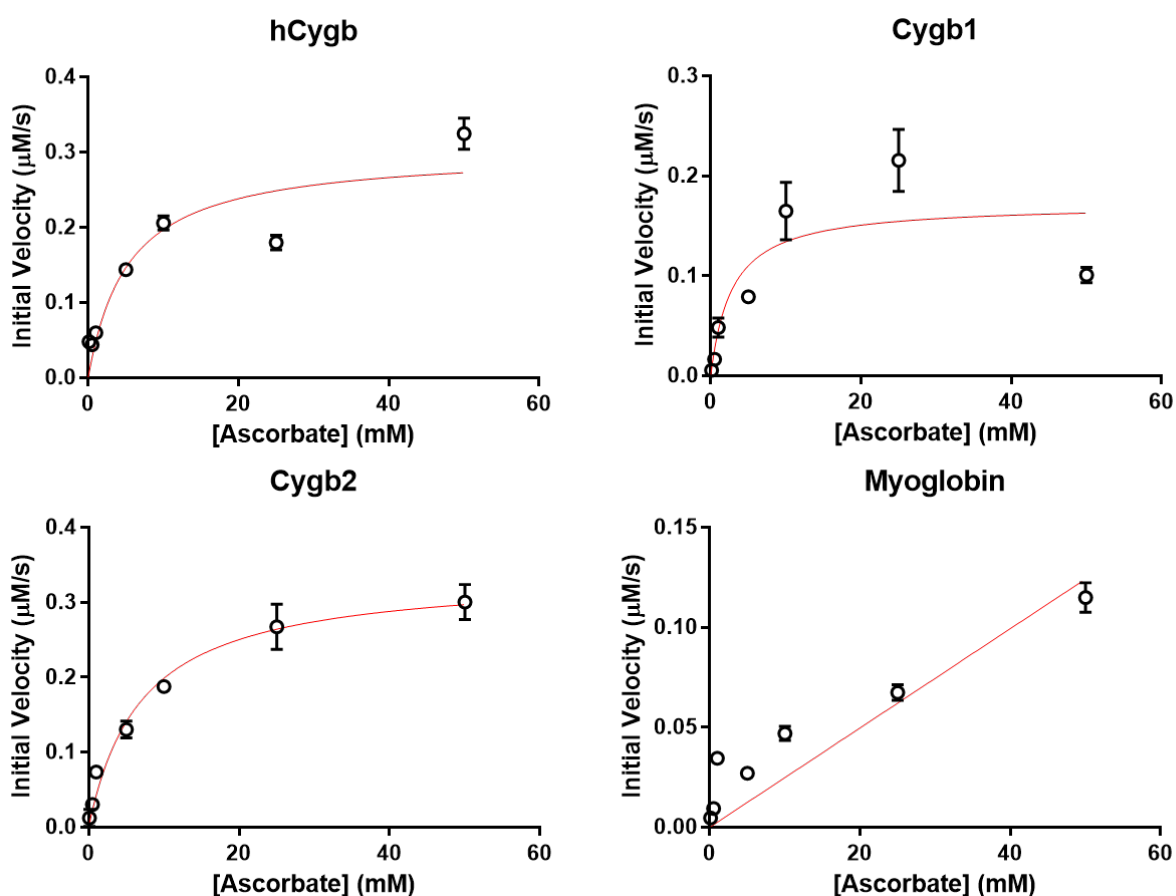


Figure 20: Initial velocity and kinetic fitting of globin reduction by ascorbate

Table 6: Bimolecular rate constants for the reduction of ferric globins by Asc

Protein	Bimolecular Reaction Rate Constant ($M^{-1}s^{-1}$)	Source
<i>HsaCygb</i>	1.14 ± 0.17	This work
<i>HsaCygb</i> (monomer)	2.68 ± 0.13	Ref [92]
<i>HsaCygb</i> (dimer)	1.58 ± 0.10	Ref [92]
<i>HsaCygb</i>	1.3 ± 0.2	Ref [85]
<i>HsaCygb</i>	36.1 ± 4.4	Ref [90]
<i>DreCygb1</i>	0.83 ± 0.07	This work
<i>DreCygb2</i>	1.04 ± 0.15	This work
Mb	0.124 ± 0.016	This work
Mb	0.13	Ref [85]
Mb	0.087 ± 0.003	Ref [86]

The kinetic analysis of CYB5-mediated reduction of ferric globins proved more complex for several reasons. Early data using the entire CYB5 reducing system (not shown) revealed transient oxidation of CYB5 during globin reduction early in the reaction. Kinetic analysis in this situation requires the electron transfer from CYB5 to the globin to be the rate-limiting step, with electron transfer from NADH to CYB5R to CYB5 always keeping up with the final electron transfer to the globin. It quickly became apparent that the CYB5 to globin electron transfer was too fast to rely upon this assumption, suggesting that an isolated reaction between ferrous CYB5 and ferric globin would need to be analyzed. Furthermore, the speed of this reaction would require the use of stopped-flow spectroscopy (detailed in the methods section).

The second problem arises from the similarity in the spectra of CYB5 and the globins. CYB5, *HsaCygb*, and *DreCygb2* are all hexacoordinate hemes, with remarkably similar spectra for the ferric (“met”) and unbound ferrous (“deoxy”) forms. Previous analyses have avoided this problem by allowing the reaction to proceed under excess carbon monoxide gas, resulting in saturation of the reaction buffer with CO [93]. CYB5, while a heme protein, exhibits no ligand binding properties, while globins must be reduced to the ferrous form before they can bind CO. Any globin that is reduced will rapidly bind CO, accompanied by a spectral shift to the easily distinguished CO-bound form. Once again, however, the speed of the reduction of Cygb posed a problem. Because two of the Cygbs are hexacoordinate, the distal histidine must dissociate before CO can be bound (if no distal histidine is present, CO binding occurs at roughly diffusion-limited rates). The reduction of Cygb appeared to proceed at rates similar to or faster than those of the distal histidine dissociation, roughly 2-5 s⁻¹ for *HsaCygb* [14, 94], again suggesting that a reaction other than Cygb reduction could prove rate-limiting. Were this the case, the measured rate of CO binding would correlate to distal histidine dissociation, providing no information about the rate of Cygb reduction.

A solution to this problem emerged from a detailed comparison of the spectra of the proteins. CYB5 exhibits an isosbestic point, where a change in redox state results in no change in absorbance, between its ferric and ferrous forms at 568nm. This can be clearly seen in figure 21, which depicts the ferric and ferrous reference spectra for CYB5.

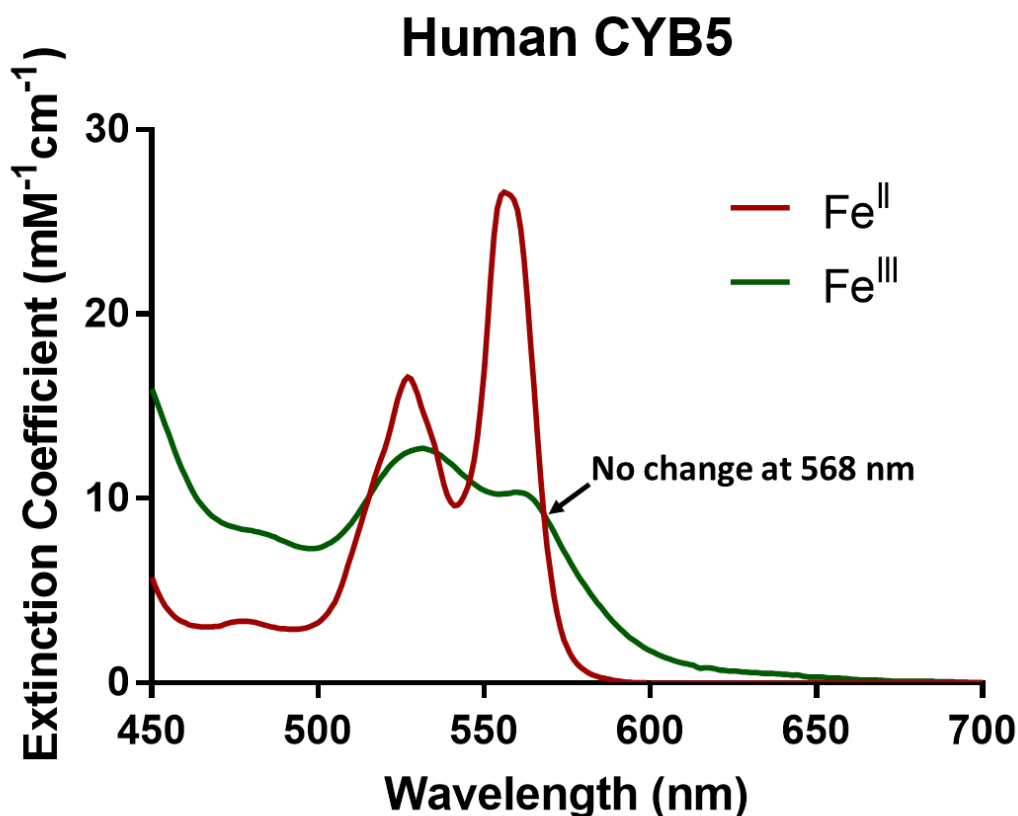


Figure 21: Reference spectra of ferric and ferrous CYB5 showing isosbestic point at 568nm

While *HsaCygb* and *DreCygb2* have very similar spectra, the isosbestic points of these proteins fall at slightly different wavelengths, and the ferric to ferrous transition of these proteins does slightly change the wavelength at 568 nm. This means that any measured absorbance change at 568nm arises only from the globin protein, and not CYB5.

The final challenge in these measurements also arose from the similar spectra of both CYB5 and the globins. Because both are heme proteins, both absorb strongly in the Q band region (500-600nm), and even more strongly at the Soret peak (around 400nm). Unfortunately, all spectrophotometers have an absorbance limit, above which they saturate and can no longer obtain meaningful information. Practically, this means that the total heme concentration in any

sample cannot exceed roughly 100 μM . Analysis of second-order reactions, such as this one, are often simpler in pseudo-first order conditions, where one reactant is in roughly 50-fold (or greater) excess compared to the other. Unfortunately, a 50-fold difference while keeping the total heme concentration to 100 μM or less would limit one species to no more than about 2 μM . The absorbance signal generated by a reaction of only 2 μM heme would likely be too small to be reliably detected. As a result, these reactions were performed in non-pseudo-first order conditions, with 8-10 μM globin held constant as the CYB5 concentration was varied from roughly 60 μM down to 4-5 μM , with a total of 7 to 9 different CYB5 concentrations.

All analysis of these data was performed on single wavelength absorbance traces measured at 568nm. Sample traces for each of the globins, representing an average of 5-7 individual experiments, can be seen in figure 22. As previously mentioned, the overall magnitude of the absorbance change at 568nm is fairly small for the 6-coordinate globins, somewhat larger for the 5-coordinate *DreCygb1*, and much larger for Mb. The time scale of these reactions can also be seen to vary greatly, with *HsaCygb* and *DreCygb2* reaching equilibrium in about half of one second, *DreCygb1* taking 1-2 seconds, and Mb taking over a minute. This is in partial contrast to the data obtained with the entire CYB5 reducing system, where *DreCygb1* was completely reduced more quickly than *DreCygb2*. It is also worth noting, though it cannot be seen from these data alone, that as the concentration of CYB5 decreased, the magnitude of the spectral change would also decrease, even when a significant excess of CYB5 vs. the globin remained. This suggests that the reverse reaction (ferrous globin transferring an electron to ferric CYB5) is not only possible but non-trivial, and these bimolecular reactions ceased not when the globin was completely reduced, but when the forward and reverse reactions reached equilibrium.

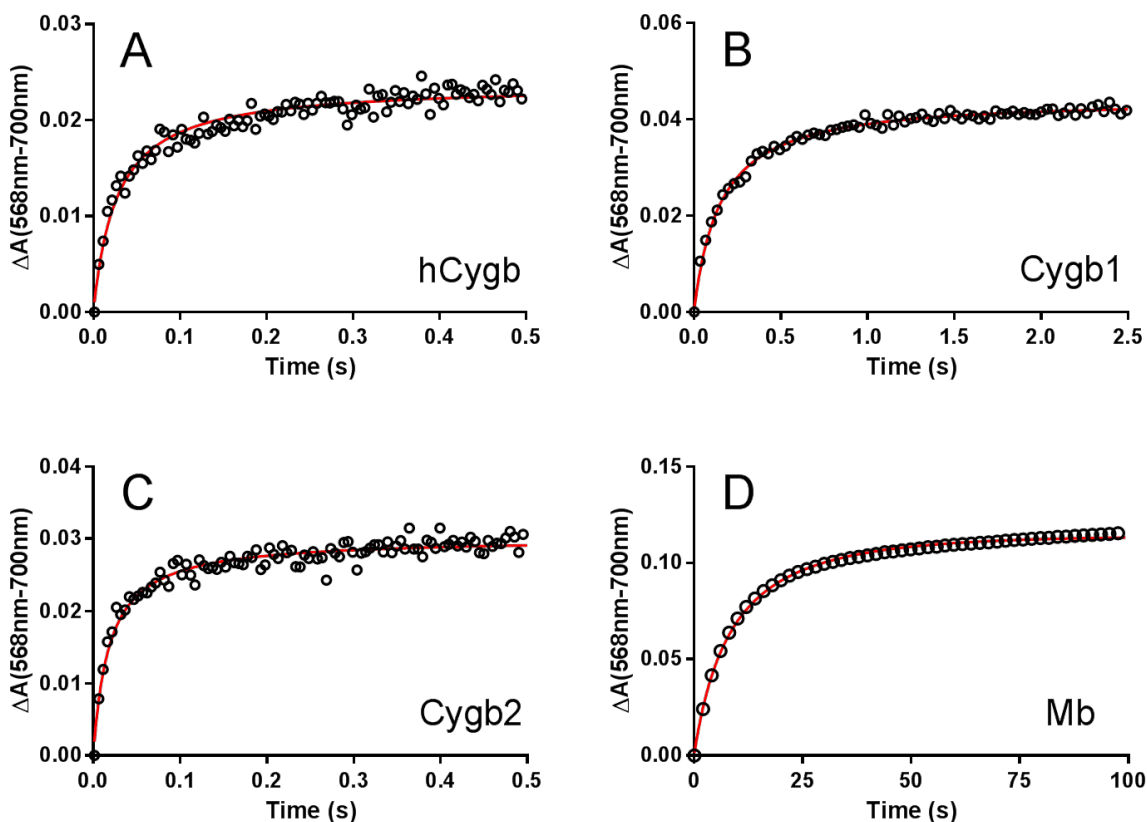


Figure 22: 568nm absorbance traces during the reaction of ferrous CYB5 with ferric globins

Kinetic analysis of these data was performed using two separate methods. First, the initial rate of reduction at each concentration of CYB5 was calculated and is shown in blue in figure 23. Second, the absorbance traces measured at 568nm for each concentration of CYB5 were fit to equation 6, which models second-order reactions under non-pseudo first order conditions. More information on this equation and its use can be found in section 3.1.2.2. Fits of representative traces to this equation are shown in red in figure 22. One parameter calculated as part of this fit is

an observed rate constant, k_{obs} , in units of s^{-1} , for each concentration of CYB5. These k_{obs} values are shown in black in figure 23.

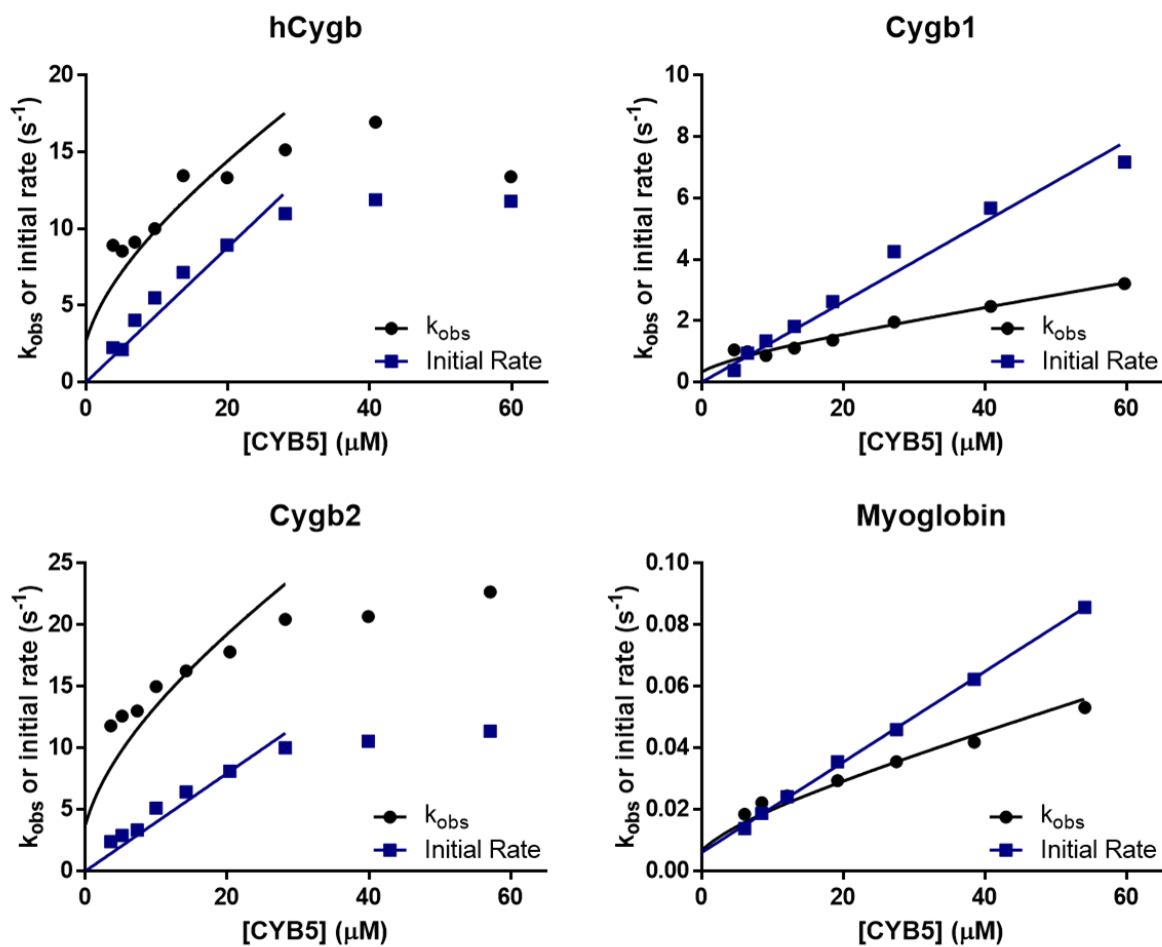


Figure 23: Determination of reaction rate constants between CYB5 and globins

The plots of initial reaction rate vs. CYB5 concentration are mostly linear, although both *HsaCygb* and *DreCygb2* show noticeable flattening of the data as the CYB5 concentration exceeds 30 μM . The same flattening can be seen for the k_{obs} values for these two proteins at high CYB5 levels. This seems likely to be a consequence of the very high values at these concentrations of CYB5 (note the different y-axis scales for the four globins). Interestingly, if an appreciable reverse reaction is present, k_{obs} is not expected to vary linearly with the CYB5 concentration, but rather to reach a minimum value when the two species are at equimolar concentrations, and increase as the concentration difference between the two species grows wider. This behavior can be seen in both the *HsaCygb* and the *DreCygb1* plots, with the point at the lowest CYB5 concentration not showing the lowest k_{obs} value.

By fitting a linear model to the initial rate data (shown as a solid blue line in figure 23), one estimate of the forward reaction rate constant in units of $\text{M}^{-1}\text{s}^{-1}$, which governs electron transfer from ferrous CYB5 to the ferric globin, was obtained.

For the k_{obs} plots, rather than a linear fit, the data were fit to equation 7 (see section 2.4.3.2) to separate out forward and reverse rate constants. The process of fitting the data to equation 7 was marked by a high degree of dependency between parameters, which gave unpredictable and inconsistent results. This was addressed by substitution of the forward rate constants measured from the initial rates into equation 7 and resulted in more reliable fitting. All estimated constants are listed in table 7.

Table 7: Calculated rate constants for the reactions between CYB5 and globins

Protein	<i>From initial rates</i>	<i>From k_{obs} plot</i>	
	Forward rate constant ($M^{-1}s^{-1}$)	Forward rate constant ($M^{-1}s^{-1}$)	Reverse rate constant ($M^{-1}s^{-1}$)
<i>HsaCygb</i>	$2.87 \pm 1.39 (x10^5)$	$2.49 \pm 0.29 (x10^5)$	$3.47 \pm 0.37 (x10^5)$
<i>DreCygb1</i>	$1.11 \pm 0.18 (x10^5)$	$0.95 \pm 0.15 (x10^5)$	$0.197 \pm 0.51 (x10^5)$
<i>DreCygb2</i>	$2.96 \pm 1.50 (x10^5)$	$2.53 \pm 0.73 (x10^5)$	$2.91 \pm 0.99 (x10^5)$
Mb	$16.1 \pm 0.38 (x10^2)$	$8.04 \pm 4.17 (x10^2)$	$5.34 \pm 2.66 (x10^2)$

These values indicate that CYB5 reacts most rapidly with *HsaCygb* and *DreCygb2*. Based on initial rate data, *DreCygb1* is reduced nearly three-fold slower than the other Cygbs, and Mb is reduced roughly 100-fold slower than the Cygbs. Our calculated values for Mb are comparable to a previously published value of 8.2×10^2 [95].

While the dependency of the fitting parameters in equation 7 does give some cause for caution regarding the exact values, the calculated rate constants do indicate that the reaction is reversible for all globins, with the reverse reaction proceeding even more rapidly than the forward reaction for *HsaCygb* and *DreCygb2*. This is consistent with my observation of incomplete reduction of the globins during the bimolecular reaction of ferric globin and ferrous CYB5. The reverse rate constants may also explain why *DreCygb1* is reduced more quickly by the entire CYB5 system than the forward rate constants would indicate; the reverse reaction is slow enough that CYB5R effectively outcompetes *DreCygb1* to reduced CYB5, leading to a largely unidirectional reaction.. Referring back to the redox potentials listed in table 1, the relatively small differences between the Cygbs and CYB5 may help explain the reversibility,

although Mb's relatively very positive redox potential makes it somewhat surprising that the reaction of CYB5 and Mb is also reversible.

3.2.3 Support of nitric oxide dioxygenation

Using the kinetic parameters calculated in the above sections and data available from published literature, Dr. Jesús Tejero in the Gladwin lab was able to develop a kinetic model describing the interactions of CYB5 and Asc with globins in an oxygenated environment. The reactions modelled, as well as the rate constants assigned to each reaction, are shown in table 8.

Table 8: Rate constants used for kinetic simulation of CYB5 and Cygb interactions

	Reaction	Forward rate		Reverse rate		Reference
1	$\text{Fe}^{\text{III}} + \text{CYB5}_{\text{rd}} \rightleftharpoons \text{Fe}^{\text{II}}_{6\text{c}} + \text{CYB5}_{\text{ox}}$	2.87×10^5	$\text{M}^{-1}\text{s}^{-1}$	3.47×10^5	$\text{M}^{-1}\text{s}^{-1}$	This work
2	$\text{Fe}^{\text{III}} + \text{Asc} \rightarrow \text{Fe}^{\text{II}}_{6\text{c}} + \text{Asc}_{\text{ox}}$	1.05	$\text{M}^{-1}\text{s}^{-1}$	<i>NA</i>		This work
3	$\text{Fe}^{\text{II}}_{5\text{c}} + \text{O}_2 \rightleftharpoons \text{Fe}^{\text{II}}\text{O}_2$	3×10^7	$\text{M}^{-1}\text{s}^{-1}$	3.5×10^{-1}	s^{-1}	[94]
4	$\text{Fe}^{\text{II}}\text{O}_2 + \text{NO} \rightarrow \text{Fe}^{\text{III}} + \text{NO}_3^-$	3×10^7	$\text{M}^{-1}\text{s}^{-1}$	<i>NA</i>		[90]
5	$\text{Fe}^{\text{II}}\text{O}_2 \rightarrow \text{Fe}^{\text{III}} + \text{O}_2^{\cdot-}$	4.5×10^{-3}	s^{-1}	<i>NA</i>		[4]
6	$\text{Fe}^{\text{II}}_{5\text{c}} + \text{NO} \rightleftharpoons \text{Fe}^{\text{II}}\text{NO}$	1×10^8	$\text{M}^{-1}\text{s}^{-1}$	8×10^{-4}	s^{-1}	[90]
7	$\text{CYB5R} + \text{CYB5}_{\text{ox}} \rightleftharpoons \text{CYB5R}:\text{CYB5}_{\text{ox}}$	6×10^6	$\text{M}^{-1}\text{s}^{-1}$	33	s^{-1}	[88]
8	$\text{CYB5R}:\text{CYB5}_{\text{ox}} \rightarrow \text{CYB5R} + \text{CYB5}_{\text{rd}}$	5.67×10^2	s^{-1}	<i>NA</i>		[88]
9	$\text{Fe}^{\text{II}}_{5\text{c}} \rightleftharpoons \text{Fe}^{\text{II}}_{6\text{c}}$	4.3×10^2	s^{-1}	5	s^{-1}	[94]

The results of the simulation are shown in the top half of figure 24, which depicts the concentration of ferrous oxy Cygb as a function of time for various concentrations of CYB5 or Asc. The model predicts that 1 μM CYB5 would be sufficient to fully reduce 20 μM Cygb in a very short time period, while even 10 mM Asc would level off well before 100% of the Cygb

had been reduced. In general, these results look fairly similar to those measured above in anaerobic conditions, with rapid complete reduction by CYB5 and slower, less thorough reduction by ascorbate. It is interesting that the model predicts the presence or absence of oxygen would have relatively little effect on the reduction of Cygb.

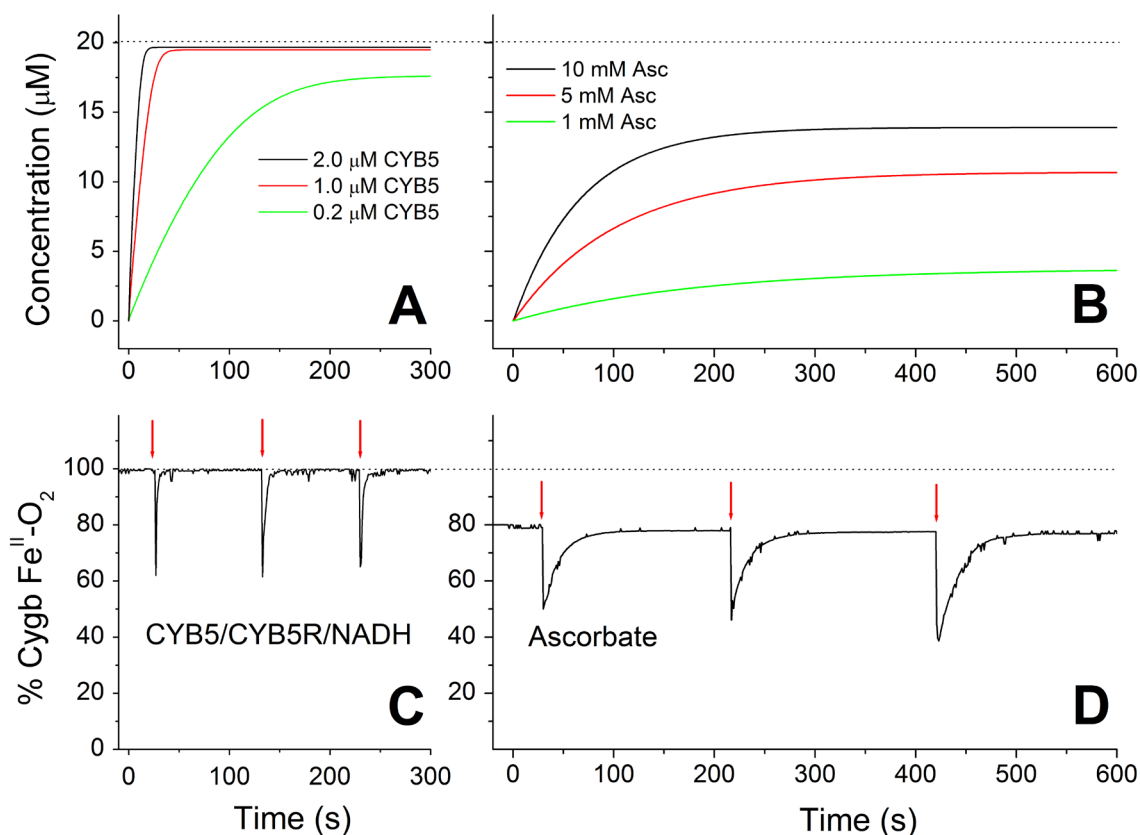


Figure 24: Simulated and measured reduction of *HsaCygb* by the CYB5 system and Asc

The bottom portion of figure 24 depicts the data measured during *in vitro* experiments that matched the conditions depicted in the model, with the red arrows depicting injections of NO-saturated buffer. The measured data for CYB5-mediated reduction are in relatively close

accordance with the data from the model. The CYB5 system is able to quickly and thoroughly restore complete reduction after the immediate protein oxidation caused by NO dioxygenation. Ascorbate, on the other hand, is seen to perform appreciably better *in vitro* than was predicted by the model. Recovery of the pre-NO level of reduced Cygb occurs 4 to 5-fold faster in the measured data than was predicted by the model, and the baseline level of reduction is also notably higher (roughly 75% measured vs. 55% predicted for 5 mM Asc). This supports a theory proposed by Gardner et al. that NO dioxygenation by Cygb produces a reaction intermediate that is reduced by Asc more rapidly than typical ferric Cygb [85]. On the whole, these results suggest that NO dioxygenation activity by Cygb would be better supported by the CYB5 system than by Asc, with CYB5-mediated reduction enabling faster turnover and a higher rate of NO consumption.

3.3 DISCUSSION

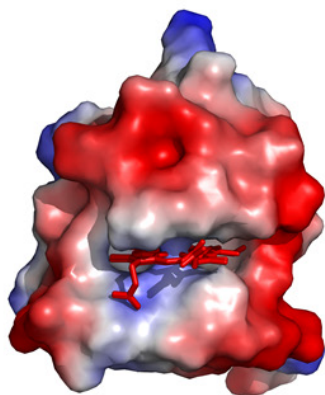
As has been repeatedly discussed in this work, the heme iron of a globin must be in the reduced ferrous state in order to carry out most of the globin's functions. Hb and Mb are known to have canonical redox partners that function to restore the reduced form of these proteins when they become oxidized. Such redox partners are presumably even more important for the hexacoordinate globins like Cygb, which autoxidize at much higher rates than the pentacoordinate globins Hb and Mb. Reduction of Cygb by Asc has been reported by numerous sources [85, 86, 90, 91], but the physiologic relevance of this interaction remains unknown. My results, shown above, suggest that the CYB5/CYB5R/NADH system represents a more efficient redox partner for Cygb *in vivo* than Asc. Even very high levels of Asc are outperformed by the

CYB5 system, with CYB5 maintaining complete reduction and rapidly reversing oxidation in a variety of *in vitro* settings.

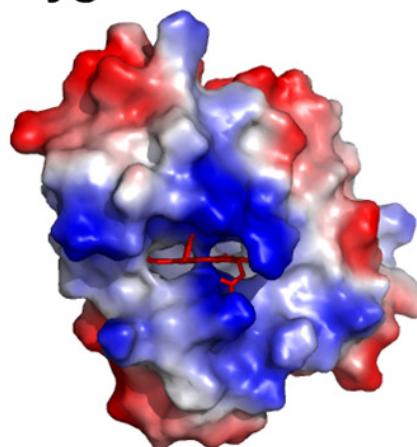
This does not, however, suggest that Asc is not involved in Cygb reduction *in vivo*. Some tissues that have been shown to express Cygb, including certain populations of neurons, have also been shown to contain very high levels of ascorbate (up to 10 mM) [96]. Most tissues, however, have notably lower Asc levels, usually below 1 mM [97]. Two tissues with particularly low levels of Asc are vascular smooth muscle (100-200 μ M) [98, 99] and red blood cells (40-80 nM) [97, 100]. At these levels, Asc is unlikely to efficiently reduce Cygb. Recent studies have shown that six-coordinate globins, including Ngb [101] and GbX [6], can be found in fish RBCs, and *DreCygb1* has been located in zebrafish blood as well, likely in the RBCs [4]. Since RBCs contain CYB5 and CYB5R at levels around 1 μ M (where they act as the primary reducing agent for erythrocyte Hb), the CYB5 system seems far more likely than ascorbate to be the natural reducing agent for hexacoordinate globins in red blood cells.

One question raised by this work is how CYB5 is able to reduce Cygb so much faster than it reduces Hb or Mb. Based on redox potentials, the driving force for electron transfer from CYB5 to Hb or Mb should be much greater and would be expected to lead to faster reduction. The interaction between CYB5 and Cygb may be favored through electrostatic interactions. As shown in Figure 25, the heme cavity of CYB5 is surrounded by a high density of negative charge. The heme cavities of Cygb and Mb, in contrast, are surrounded by numerous positively charged residues. While *HsaCygb* may have a slightly higher density of positive charge around its heme cavity, the strong preference of CYB5 for Cygb can likely not be explained without further analysis of docking interactions between the proteins.

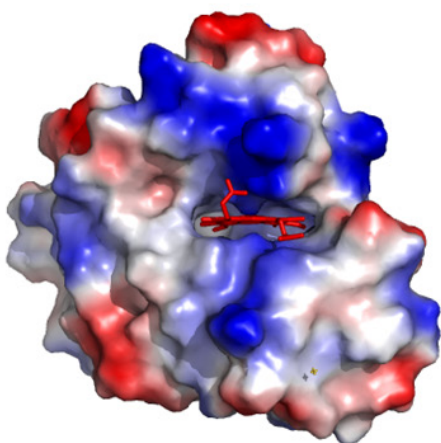
CYB5



HsaCygb



Mb



Ngb

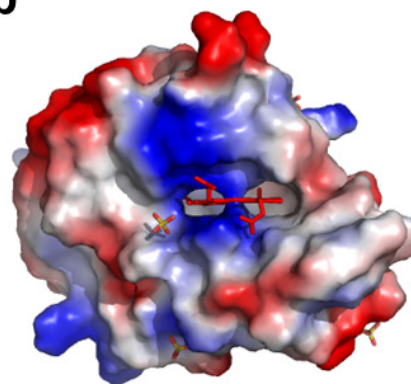


Figure 25: Electrostatic surface potentials of CYB5 and selected heme globins

The strong interaction between CYB5 and Cygb may arise simply from necessity, as Cygb and the other hexacoordinate globins autoxidize relatively quickly, resulting in increased electron demand compared to Hb or Mb. As mentioned in the introduction, Cygb predates Hb and Mb in the evolution of heme globins, and this rapid interaction introduces the possibility that CYB5 may have coevolved with Cygb, with evolution optimizing CYB5 for reduction of Cygb and not its canonical substrates Hb and Mb. The potential importance of CYB5-mediated reduction of Cygb is reinforced by the ability of human CYB5 to reduce *DreCygb1* and *DreCygb2* at rates comparable to the reduction of *HsaCygb*. This level of evolutionary conservation suggests an important physiologic function. Furthermore, as zebrafish and many other animals are known to express CYB5 as well as Cygb, the CYB5 system may serve as the primary physiologic reductant for Cygb in a variety of animals, not just humans.

Another potentially important observation is the CYB5 system's ability to support NO dioxygenation, reducing Cygb more rapidly and more thoroughly than 5 mM Asc, which is near the highest Asc concentration documented in human cells [97]. NO dioxygenation has been identified as a potentially very important role of Cygb, especially in the vascular wall, where this reaction is thought to contribute to blood pressure regulation and even healing and remodeling after vascular injury [28, 41, 42, 86, 90]. Considering the relatively low levels of Asc in vascular smooth muscle, this important activity is almost certainly supported by the CYB5 reducing system. More generally, Cygb has also been suggested to protect against oxidative stress or damage in a variety of contexts, and to exert broadly cytoprotective effects. If these effects are mediated via any sort of electron transfer reactions, not exclusively NO dioxygenation, the presence of a very efficient system to reduce Cygb would likely play a key role in supporting and enabling this activity.

3.4 CONCLUSIONS

These results suggest that CYB5 represents a more efficient system to reduce oxidized Cygb than ascorbate. The role of Asc as a cellular reducing agent for Cygb may be limited to tissues and cells with very high ascorbate, such as neurons, hepatocytes, and fibroblasts. The combination of CYB5R, CYB5, and Cygb may represent a functional nitric oxide metabolon in the vascular wall, performing catalytic consumption of NO to regulate vascular tone as long as NADH is present as an electron donor. Furthermore, it appears that high (mM) levels of ascorbate or small amounts of CYB5 and CYB5R with NADH may represent a way to keep Cygb-based therapeutics in the desired reduced state.

4.0 CYTOGLOBINS AND THE CYB5 SYSTEM IN ZEBRAFISH

Rationale and aims

During completion of the previously discussed experiments showing the reduction of heme globins, especially Cygbs, by CYB5 and ascorbate, several members of the Gladwin lab were performing in depth research into the zebrafish cytoglobins. Dr. Paola Corti has been at the forefront of characterizing these proteins, publishing a paper that documented their nitrite reductase activity, autoxidation rates, and redox potential. Along with several other lab members, she is also conducting a variety of in vivo studies aimed at elucidating the Cygbs' roles in normal zebrafish physiology, with hopes that these results may provide insight into mammalian physiology as well.

Given the laboratory's interest in the zebrafish globins and experience in studying the redox interactions of heme globins, a logical progression was to perform a similar analysis using the zebrafish CYB5 system with the zebrafish Cygb proteins. Plasmids were obtained for the zebrafish forms of CYB5R3, CYB5a and CYB5b, and all three proteins were successfully expressed in and purified from *E. coli*. Using exclusively zebrafish proteins, some of the same experiments performed in the previous chapter with the human CYB5 system were repeated with the homologous zebrafish proteins. This allowed for characterization of the reduction of the zebrafish Cygbs at roughly physiologic concentrations and during NO dioxygenation activity.

Because NO dioxygenation activity requires the oxygen bound form of the protein, Dr. Angela Fago, PhD, at the University of Aarhus, was recruited as a collaborator, and with her lab was able to measure the oxygen affinity of the two zebrafish Cygb's.

4.1 MATERIALS AND METHODS

4.1.1 Pseudo-physiologic reduction of zebrafish cytoglobins

These experiments closely replicated those previously performed using the human CYB5 reducing system, and which were detailed in section 2.4.2. Briefly, the experiment began with 20 μ M ferric globin in a 1.7 mL cuvette in an anaerobic environment. To this globin, a mixture CYB5 (to a final concentration of 2 μ M), CYB5R3 (final concentration 0.2 μ M), and NADH (final concentration 100 μ M) was added, and the subsequent reduction of the globin was followed using UV-Vis spectroscopy.

While previous work examined the reduction of many different globins by a single CYB5 protein at a single temperature, this work focused on only two globins: *DreCygb1* and *DreCygb2*. However, because zebrafish do not live at 37°C, these reactions were performed at both 37°C (for direct comparison to the previous data) and at 25°C (for better relevance to zebrafish physiology). Both CYB5a and CYB5b from the zebrafish were successfully expressed, and so both forms of CYB5 were tested separately. The CYB5R3 used in these experiments was also the zebrafish protein; no mammalian proteins were used for this analysis. All reactions were followed for at least 900 seconds (although all were complete within roughly 300 seconds, if not sooner) on an Agilent HP8453 UV-Vis spectrophotometer in 100 mM sodium phosphate, pH 7.4.

4.1.2 Oxygen affinity measurement

These experiments were performed by Elin Petersen and Dr. Angela Fago, PhD, at the University of Aarhus in Denmark. Our lab provided them with the *DreCygb1* and *DreCygb2* that they used, as well as the CYB5, CYB5R, FDH, and sodium formate that was used during the reaction. Standard spectra for the ferrous, ferrous-oxy, and ferric forms of the zebrafish Cygbs were also provided to Dr. Fago, and these spectra were used to calculate fractional saturation.

Briefly, these experiments were performed in a reaction volume of 140 μL containing 200 μM globin in 100 mM sodium phosphate buffer. A system is used that provides continuous gas flow over the globin solution and allows for stepwise control of the partial pressure of oxygen in the gas flow. This system's continuous addition of new oxygen via continuous flow prevents consumption of O_2 via autoxidation from affecting oxygen partial pressure, keeping the partial pressure at exactly the value in the inlet gas stream. This allows the oxygen tension to be kept steady long enough for oxygen binding by the globin to reach equilibrium, even for a rapid autoxidizer like *DreCygb2*, which is not possible in a closed system.

Oxidation of the globin was reversed via inclusion of the CYB5 reducing system. Because the globin concentration was 10-fold higher than what was typically used, it was suggested that the concentrations of CYB5 and CYB5R should also be increased ten-fold compared to my typical concentrations, to 20 μM and 2 μM respectively. NADH was freshly prepared and added to a final concentration of 300 μM , along with 10 mM sodium formate and 15 mU/mL of formate dehydrogenase (FDH) to regenerate the NADH.

This analysis was performed at pH 7.4 and 6.8, and at 25°C and 37°C for both Cygbs. The measured data was used to fit an equilibrium binding curve, which allowed for calculation of both the oxygen P_{50} (a measure of affinity) and the Hill coefficient (a measure of cooperativity).

4.1.3 Support of NO dioxygenation activity

As had been done in the previous section for *HsaCygb* with the human CYB5 reducing system, this experiment undertook to characterize the zebrafish CYB5 reducing system's ability to support the NO dioxygenation activity of the zebrafish cytoglobins.

Where the previous experiment with the mammalian proteins simply tested the CYB5 system and Asc in identical conditions, these experiments called for a greater number of conditions. For both *DreCygb1* and *DreCygb2*, reduction of the protein after NO dioxygenation by both CYB5a and CYB5b was measured at both 25 and 37°C. Once again, all proteins used, including the CYB5R3 present in all reactions, were the zebrafish forms of those proteins.

These reactions took place in 1 mL cuvettes, sealed with screw tops and rubber septa in buffer saturated with 100% oxygen. As in the earlier experiments with the mammalian proteins, 20 μM of ferric Cygb was mixed with 2 μM of CYB5, 0.2 μM CYB5R3, and 200 μM NADH. However, it quickly became apparent that the very rapid autoxidation of *DreCygb2* quickly consumed even 200 μM NADH; because high concentrations of NAD^+ can affect redox reaction rates, simply adding more NADH was not necessary. To prolong NADH availability, 10 mM sodium formate and 15 U/L of the enzyme formate dehydrogenase (FDH; both from Sigma-Aldrich), were added to the reaction mixture. FDH is able to consume formate and regenerate NADH, allowing the CYB5 system to keep Cygb2 reduced for a longer time period. Superoxide dismutase (SOD) was also added to a final concentration of 400 U/mL, in order to limit superoxide accumulation from ongoing autoxidation.

As before, once the ferrous-oxy spectrum for Cygb was observed, NO dioxygenation was initiated by addition of NO-saturated buffer to a final NO concentration of 5-10 μM . This resulted in virtually immediate oxidation of a significant portion of the Cygb and subsequent

monitoring of the recovery to the reduced form. The process of NO addition was repeated 3-5 times, with each addition occurring after the ferrous-oxy spectrum had stabilized again. Spectral deconvolution using standard spectra for the zebrafish proteins was used to calculate the concentrations of each globin species.

4.2 RESULTS

4.2.1 Pseudo-physiologic reduction

The first effort to characterize the reduction of the zebrafish Cygbs by the zebrafish CYB5 proteins closely resembled the pseudo-physiologic reduction experiments performed earlier with the human CYB5 system and various heme globins. In this case, however, the tests were performed for each of two Cygb proteins, two different CYB5 proteins, and at two different temperatures (37°C for direct comparison to previous data from mammalian proteins, 25°C because it more closely resembles the native temperature for zebrafish). This resulted in eight different experimental setups, allowing for numerous different comparisons to be made. The concentrations of each species (0.2 μM CYB5R, 2 μM CYB5, and 20 μM Cygb) were the same as previously utilized, and were held constant in every different set of conditions tested. The results of these experiments are shown in figure 26.

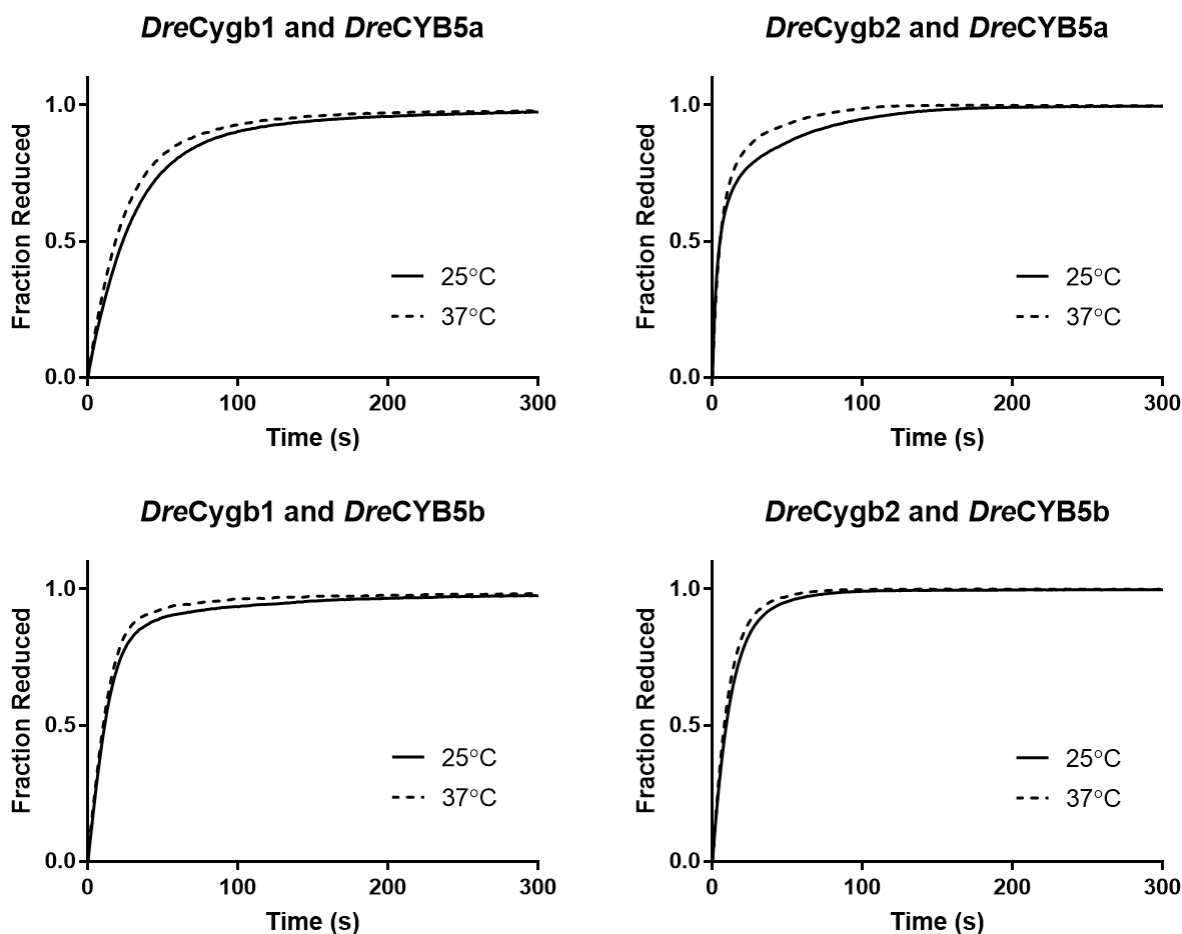


Figure 26: Pseudo-physiologic reduction of zebrafish Cygbs by the zebrafish CYB5 system

Consistent with previous observations of rapid electron transfer from CYB5 to Cygb, every pairing of CYB5 and Cygb results in complete reduction within a very short time, typically 100-200 seconds. It appears that CYB5b may mediate slightly faster reduction than CYB5a, while *DreCygb2* appears to be reduced slightly faster than *DreCygb1*. That said, these differences are far smaller than the wide range of rates seen in chapter 3 for the reduction of different globins by the human CYB5 system. The reduction of *DreCygb1* by the zebrafish CYB5s seems comparable to its reduction by the human CYB5 system, while the reduction of

DreCygb2, which was appreciably slower than *DreCygb1* when the human CYB5 system was used, is markedly faster with the zebrafish CYB5s. Interestingly, the temperature increase from 25 to 37°C resulted in relatively minimal increases in the rate of reduction in every case. As zebrafish tend to live closer to 25°C, this suggests that their specific CYB5 enzymes may have evolved for optimal function at this lower temperature. One potential explanation for this finding is the presence of a reverse reaction (globin oxidation by ferric CYB5); such a reaction was documented for the reduction of the zebrafish Cygbs by human CYB5, and if present here, an increase in the reverse reaction at high temperatures may keep the overall reaction rate the same even as the temperature increases.

4.2.2 Oxygen Affinity Measurement

All data presented in this section were measured by Elin Petersen and Dr. Angela Fago. The CYB5 reducing system, when combined with formate dehydrogenase and sodium formate to regenerate NADH, kept the Cygbs reduced long enough for the measurement of fractional oxygen saturation at enough partial pressures of oxygen to reach 70-80% saturation. This provides enough data to fit a saturation curve to the data, which provides estimates for both the P_{50} and the Hill coefficient (n), which is a measure of cooperativity. The data points measured at 37°C, as well as the calculated equilibrium curves, are shown in figure 27.

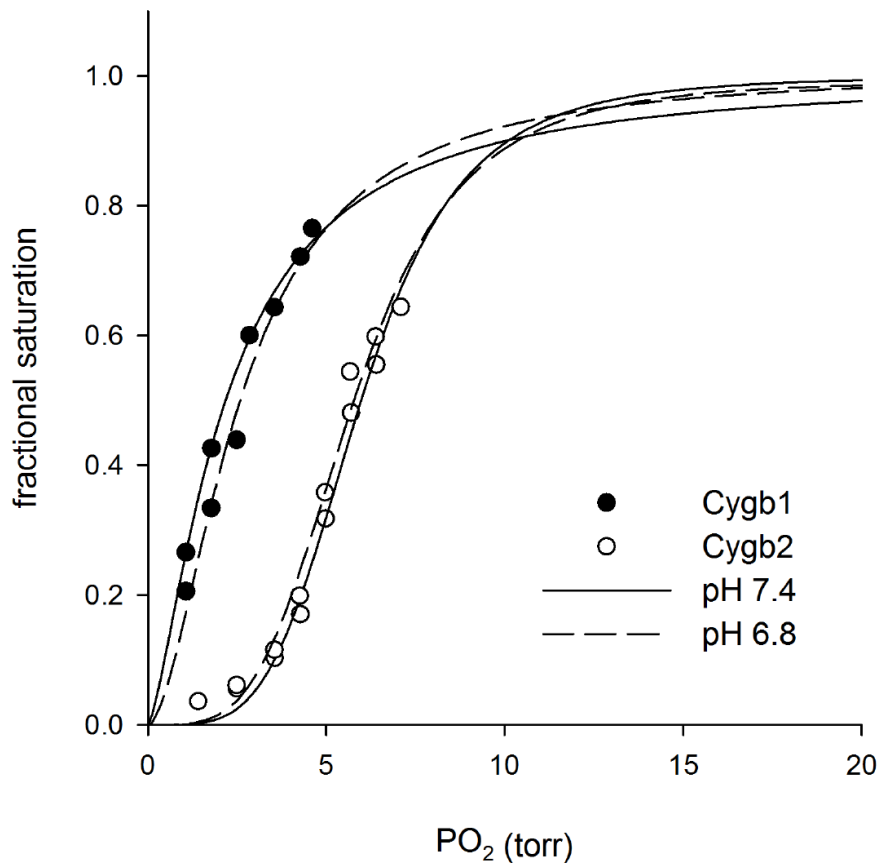


Figure 27: Oxygen-binding equilibrium curves for *DreCygb1* and *DreCygb2* at 37°C

From this graph, a few trends are immediately apparent. *DreCygb1* binds oxygen with a P_{50} of roughly 2 mmHg, indicating a higher affinity than *DreCygb2* (P_{50} roughly 6 mmHg). The binding of oxygen by both proteins appears largely unperturbed by a change in pH from 7.4 to 6.8, suggesting that the zebrafish Cygb's do not exhibit the Bohr Effect. Finally, *Cygb2* exhibits a sigmoidal shape, which suggests a significant degree of cooperativity. The most likely explanation for this observed data is the combination of multiple units of the protein into larger multimers.

Table 9 summarizes the calculated P_{50} and n values for both proteins at pH 7.4 and 6.8, as well as at both 25°C and 37°C. All values represent the average of values from two separate experiments, except for Cygb2 at pH 7.4 and 25°C, which was measured only once.

Table 9: Oxygen P_{50} values and Hill coefficients calculated for *DreCygb1* and *DreCygb2*

Protein	pH	Temp (°C)	P50 (torr)	n
Cygb1	7.4	37	2.2	1.4
Cygb1	7.4	25	0.53	1.4
Cygb1	6.8	37	2.5	1.8
Cygb1	6.8	25	0.39	1
Cygb2	7.4	37	6.1	4.3
Cygb2	7.4	25	4.4	3
Cygb2	6.8	37	5.7	3.8
Cygb2	6.8	25	3.6	3.4

In general, the trends observed at 37°C appear to also hold true at 25°C, although the oxygen affinity of both proteins is notably higher at 25°C, as expected. One other noteworthy trend is the value of n for Cygb2. While some cooperativity was apparent in the plot, these data make clear that the Hill coefficient indicates a very high degree of cooperativity for Cygb2, with values ranging from 3 to over 4. The Hill coefficient for Hb, which forms a tetramer, is typically between 2.5 and 3, suggesting that *DreCygb2* may form a tetramer or an even larger multimer, which has not been previously reported.

Finally, the calculated oxygen affinity values suggest that these proteins will almost always exist in the ferrous-oxy form in normal physiologic conditions, with the ferrous deoxy form appearing only at very low oxygen partial pressures. This has numerous implications for the potential functions of these proteins *in vivo*, as any physiologic role would likely need to be performed by the ferrous-oxy form of the protein.

4.2.3 Support of NO Dioxygenation Activity

The final experiment in this section replicated another experiment previously performed with human proteins, examining the CYB5 reducing system's ability to support NO dioxygenation reactions by reducing Cygb following NO consumption. As in section 4.1.1, the choice of two cytoglobins, two CYB5 proteins, and two temperatures resulted in eight different experimental conditions, each of which was expected to show slight variations compared to the others. In general, however, the reduction was expected to be rapid and thorough in all cases, as

Overall, the zebrafish CYB5 reducing system proved fairly efficient at returning Cygb to the $\text{Fe}^{\text{II}}\text{-O}_2$ form following oxidation caused by injections of NO. Figure 28 shows the results for all possible combinations of Cygb protein, CYB5 protein, and temperature. This variation in conditions allows for a number of interesting comparisons to be made.

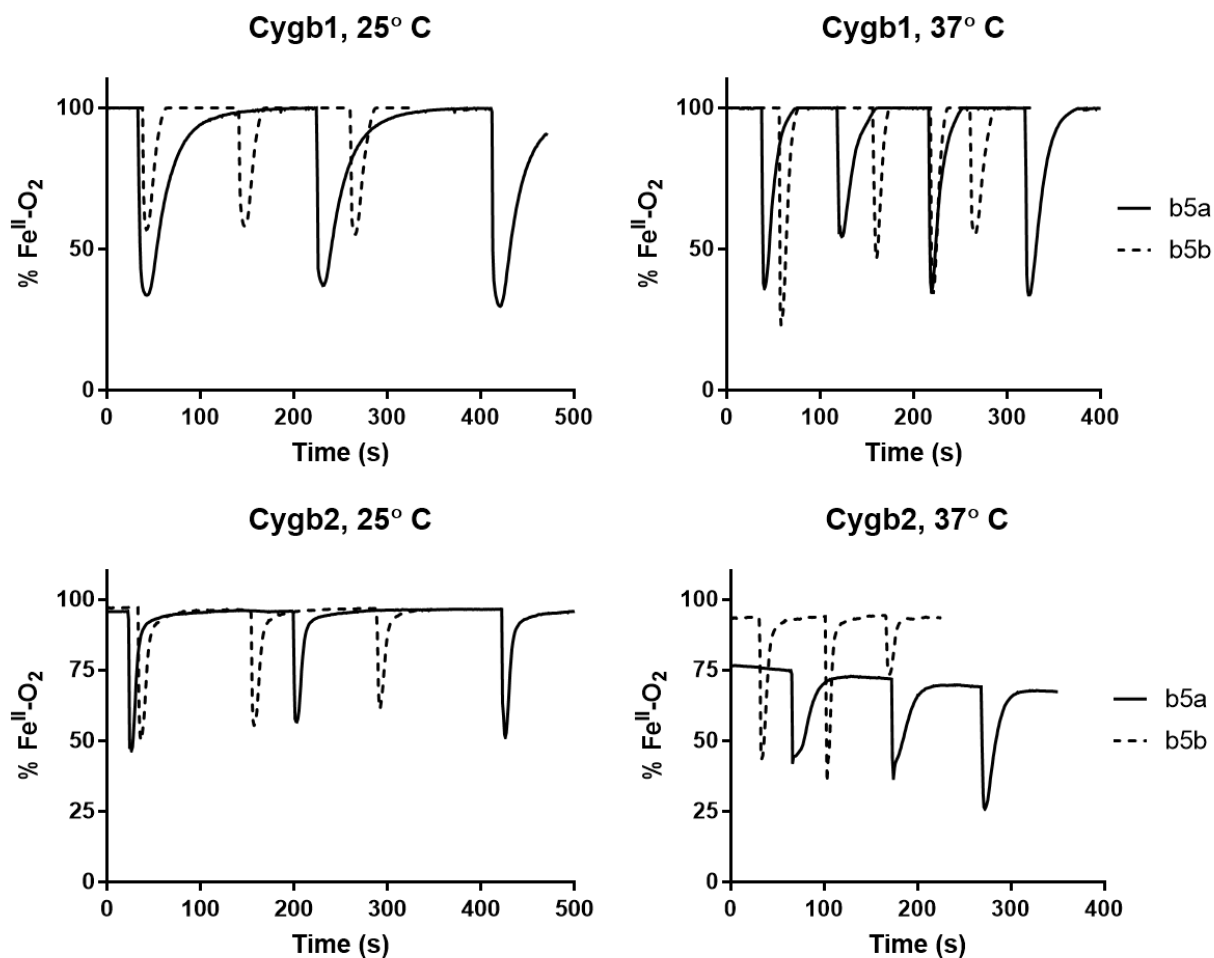


Figure 28: NO dioxygenation by zebrafish Cygbs supported by the zebrafish CYB5 system

Overall, the results resemble the previous data obtained using the human homologs of Cygb and the CYB5 reducing system. In nearly all conditions, the reduced state of the globin is restored within a fairly brief period of time (typically no more than 30-60 seconds). Nevertheless, in most conditions the rates of reduction seen here for the zebrafish proteins seem somewhat slower than the corresponding rates for the human proteins, which appeared to take no more than 10 seconds for *HsaCygb* to return to being 100% reduced.

There are appreciable differences based on the specific proteins and temperature examined, and these differences reveal some noteworthy trends. *DreCYB5b* seems, in general, to facilitate faster reduction of both *DreCygb1* and *DreCygb2* than *DreCYB5a*, regardless of temperature. This advantage seems especially pronounced with *Cygb1* at 25°, and with *DreCygb2* at 37°. In fact, for *Cygb2* at 37°C, *CYB5b* provides not only faster reduction, but also more thorough reduction, as *CYB5a* is unable to prevent slow accumulation of the oxidized form of the protein. Even *CYB5b*, however, is unable to maintain 100% reduction of the *Cygb2* under these conditions, likely as a result of the autoxidation rate of *DreCygb2*, which is extraordinarily high at 37°C (1.44 min⁻¹; refer back to table ATX). While an interesting result, the physiological applicability of this may be minimal, as zebrafish themselves will rarely be exposed to temperatures as high as 37°C. That said, while both forms of *CYB5* perform much better when reducing *DreCygb2* at 25°C, they are still unable to maintain complete reduction, suggesting that the rapid autoxidation of this protein may necessitate a rapid reducing system in any tissue where *Cygb2* is required to function in the presence of oxygen.

Reduction of *DreCygb1* by *DreCYB5a* in this setting appears notably slower at 25°C than at 37°C, which is somewhat unexpected given the minimal difference in *DreCygb1* reduction observed between 25° and 37° in the earlier steady-state reduction experiment. This difference appears to arise primarily from more rapid reduction of *DreCygb1* at 37° following NO dioxygenation, rather than any slowing of the reduction at 25°. One potential explanation for this discrepancy is a reversible reaction between *DreCYB5a* and *DreCygb1*, as was seen for the *Cygb*s with human *CYB5* in section 3.1.3. Because the ferrous-oxy form of *DreCygb1* is not free to transfer an electron to ferric *CYB5a*, the reverse reaction will be eliminated (or greatly reduced) in oxygenated conditions such as those used in the NO dioxygenation experiments. As

a result, the increase in the forward reaction rate due to the increase in temperature is largely unopposed in oxygenated conditions, whereas in anaerobic conditions a commensurate increase in the rate of the reverse reaction would likely also occur. In fact, the rates of reduction at 37° C almost always appear significantly faster in oxygenated conditions than in anaerobic conditions, suggesting a non-negligible reverse reaction that is prevented by oxygen binding to the Cygb heme iron.

4.3 DISCUSSION

The goal of these experiments was largely to determine to what extent the previously-performed characterization of human CYB5 and Cygb held true in zebrafish. To that end, many of the experiments performed very closely replicated those already documented in Chapter 3, but with the zebrafish proteins substituted in place of the human proteins. The first experiments performed showed that reduction of Cygb by the CYB5 system at roughly physiologic concentrations results in very rapid, thorough reduction, as was shown for the equivalent human proteins. This suggests strong evolutionary conservation of Cygb and CYB5 reaction; as had already been speculated in chapter 3 based on human CYB5's ability to reduce the zebrafish Cygbs. This provides further evidence for the claim introduced in Chapter 3 that Cygb and CYB5 may have a lengthy evolutionary history of existing as a functional redox pair, and that these two proteins may have co-evolved to function together.

This work also provides novel information regarding the oxygen affinity of the zebrafish Cygbs, which has not been directly measured before. Cygb1 shows very high oxygen affinity, and combined with its slow autoxidation, seems well-suited to function as a respiratory globin

intended to store or transport oxygen. Previous work has speculated that Cygb1, which is expressed in red blood cells, may function as an oxygen transport protein specialized to function at low oxygen partial pressures, and these data seem to support that conclusion.

The ramifications of *DreCygb2*'s affinity for oxygen are less clear. The oxygen affinity of the protein, while not as high as *DreCygb1* or Mb, still suggests it should be in the ferrous-oxy form most of the time under normal conditions. Like other hexacoordinate globins, however, the protein's rapid autoxidation suggests that the protein is poorly suited for a respiratory function. Like its human homolog *HsaCygb*, *DreCygb2* seems more likely to participate in some sort of electron transfer function. Control of NO signaling via rapid dioxygenation reactions, which has been suggested as a putative function of *HsaCygb*, seems to also be a likely function of *DreCygb2*. In this context, the protein's oxygen affinity would ensure that the ferrous-oxy protein, which is necessary for NO dioxygenation, is present, but would presumably be consumed by NO dioxygenation rather than by autoxidation. Combined with the very rapid reduction of this protein by both CYB5 proteins from zebrafish following NO dioxygenation, it seems possible or even likely that *DreCygb2*, with the support of the CYB5 reducing system, could function as a catalytic pathway for NO consumption, as has been theorized for *HsaCygb*.

4.4 CONCLUSIONS

The results obtained in this section demonstrate that the efficient reduction of Cygb by CYB5, documented for the human forms of these proteins in Chapter 3, appears well-conserved, with the corresponding zebrafish proteins showing similarly rapid and efficient reduction. The oxygen affinity of the zebrafish Cygbs was measured for the first time and provides important insight

into the potential physiologic roles of these proteins *in vivo*. The high oxygen affinity of *DreCygb1*, combined with the protein's slow autoxidation rate and localization in red blood cells [4], provides further support for the previously published conclusion that this protein might function as an oxygen transporter specialized to function at low oxygen partial pressures. The rapid autoxidation of *DreCygb2* makes a respiratory role very unlikely, despite the fairly high oxygen affinity of this protein, but much like its homolog *HsaCygb*, a role for *DreCygb2* and the zebrafish CYB5 system in catalytic NO consumption via dioxygenation seems to be a distinct possibility.

5.0 CHARACTERIZING NOVEL GLOBIN MUTANTS

Rationale and aims

While previously existing data on Mb and Ngb mutants provides some insight into the function of specific amino acid residues and guided the selection of which mutants to generate, each mutant must be extensively characterized after it has been expressed to determine the exact characteristics resulting from the chosen mutations.

The primary characteristics that can be analyzed with the equipment present in our laboratory are nitrite reduction, autoxidation, and cyanide binding. I performed all nitrite reduction and autoxidation testing myself, while cyanide binding analysis of the mutants was performed by another member of the lab.

5.1 MATERIALS AND METHODS

5.1.1 Nitrite reduction

Nitrite reduction experiments were conducted anaerobically in 1.7 mL optical glass cuvettes, at 37°C in 100 mM sodium phosphate pH 7.4. These experiments were all conducted under 2.5 mM sodium dithionite, which consumes any oxygen present and reduces the globins far faster

than the rates of nitrite reduction, preventing accumulation of any oxidized globin. The reaction is followed by UV-Vis spectroscopy, as any NO generated via nitrite reduction will be rapidly bound by ferrous Cygb, resulting in a spectral shift to the Fe^{II}-NO iron nitrosyl spectrum.

Reactions were initiated by addition of sodium nitrite from an anaerobic stock solution (prepared at 1 to 100 mM) to the desired final concentration (0.1-10 mM). The time period over which the reaction was followed depended on the reaction rate, but reactions were typically followed for 1000 seconds. Kinetic analysis is performed by fitting the absorbance data (typically at the deoxy peak, around 560nm) to an exponential, typically a double exponential for these data. This yielded observed rate constants for each concentration of nitrite. Fitting a line to a plot of observed rate constants vs. nitrite concentration yielded a slope equal to the second-order rate constant for the reaction.

5.1.2 Autoxidation

The first step in measuring autoxidation of globin is the generation of the ferrous oxy (Fe^{II}-O₂) form of the globin. This is accomplished by complete reduction to the ferrous deoxy form via addition of excess sodium dithionite. These reduced samples were then passed through a Sephadex G25 desalting column to remove the dithionite. This column was equilibrated with 100 mM sodium phosphate, pH 7.4. The buffer used to equilibrate the column was not anaerobic, allowing oxygen binding as the protein passed through the column. The end result is elution from the column of ferrous-oxy globin, which is immediately transferred to a Cary 50 UV-Vis spectrophotometer to begin spectral measurements. This spectrophotometer was fitted with a thermostated cell holder, which rapidly heated the sample to 37°C and maintained it there throughout the reaction.

The mutants characterized by this method were all relatively slow autoxidizers, allowing measurement of spectra between 450-700 nm, and not requiring dithionite removal to be performed in anaerobic conditions. The only rapid autoxidizer characterized was L46H Cygb (more detail in chapter 3), and this was seen to visibly autoxidize within a matter of seconds. At these rates, anaerobic dithionite removal and faster spectral measurements would still not allow for the reaction to be measured; stopped-flow spectroscopy is the only way to observe such fast autoxidation. Because a mutant that oxidizes this rapidly could not be used for any clinical purpose that requires the ferrous form, the exact quantification of the autoxidation rate was deemed a low priority and has not yet been performed.

The absorbance data was analyzed by fitting the decay of the oxy peak (around 578nm) to an exponential equation to calculate the autoxidation rate constant (or constants).

5.1.3 Cyanide Binding

All cyanide binding studies were carried out by Dr. Anthony DeMartino, PhD, a postdoctoral researcher in the Gladwin lab group.

Cytoglobin (wild type or mutants) was mixed with dissolved excess potassium ferricyanide ($K_3[Fe(CN)_6]$, Sigma Aldrich) in 100 mM phosphate buffer, pH 7.1 to oxidize any remaining ferrous protein, as the ferric form of these proteins is the only one to preferentially bind cyanide. The oxidized globin is then passed through a G-25 desalting column equilibrated with pH 7.1, 100 mM phosphate buffer to remove excess ferricyanide. The concentration is then determined ($\epsilon = 11 \text{ mM}^{-1}\text{cm}^{-1}$ at 530 nm for hexacoordinate metglobins or 500 nm for pentacoordinate metglobins) using UV-Vis spectroscopy and diluted to 10 μM in the pH 7.1 buffer. Pseudo first order kinetic analysis was performed using a thermostatted ($37.0^\circ\text{C} \pm 0.2$)

SX-20 stopped-flow instrument fitted with a direct mount photodiode array (Applied Photophysics, Ltd.). A 100 mM stock solution of potassium cyanide (KCN, Sigma Aldrich) was prepared in a sealed container on the day of the experiment in 100 mM phosphate buffer, pH 11.5. The basic pH is chosen to avoid loss of cyanide as gaseous HCN ($pK_a = 9.2$). The KCN stock was diluted to 250 μ M–5mM (25x–500x) in 4 mL samples of 1 mM, pH 11.5 phosphate buffer. 50/50 mixing of this buffer in the stopped-flow with the 100 mM, pH 7.1 phosphate buffer containing cytoglobin results in a pH of 7.4 as confirmed after experiments. Note that the stopped-flow performs equal mixing of the two samples being mixed, and so all concentrations during the reaction are half of those in the prepared solutions. Kinetic analysis was performed using Prism GraphPad 7.0. The best fit was chosen (*i.e.*, single, double, or triple exponentials) according to the best residuals of each fit at three wavelengths: the Soret decrease (407-416 nm) the Soret increase (425 nm) and the Q-band increase (548 nm). Each calculated k_{obs} value represents the average of 3–4 experiments at each cyanide concentration. All pseudo first order plots (k_{obs} vs concentration KCN) exhibited near 0 intercepts, indicating very limited back reaction. The slope of these plots represents the rate constant for the reaction.

5.1.4 Reduction by CYB5 and Ascorbate

Prior to mouse trials using the V85I Cygb mutant, it was important to measure the effect (if any) of the V85I mutation on the reduction of the protein by both the CYB5 system and ascorbate. Reactions were followed in anaerobic conditions in 100 mM sodium phosphate, pH 7.4, at 37°C. 20 μ M V85I Cygb was mixed with either 1 mM ascorbate or 2 μ M CYB5, 0.2 μ M CYB5R, and 100 μ M NADH. Ascorbate-mediated reduction was followed for 900 seconds, while CYB5-

mediated reduction was followed for 300 seconds (as this was sufficient to reach 100% reduction).

5.2 RESULTS

In section 2.3.1, all *Cygb* mutants identified as promising were listed. This list included the high-priority mutants L46F, L46F + H81Q, V85F, and V85I, as well as the lower-priority mutants L46H, L46H + H81Q, V85A, and V85H. After obtaining primers to generate all of these mutants, successful mutagenesis reactions were performed, resulting in the generation of plasmid for each of these eight mutants. All plasmids were confirmed to have the proper sequences by the genomics research core and were successfully transformed into SoluBL-21 *E. coli* cells for protein expression.

Upon attempted expression of these mutants in *E. coli*, problems became apparent with half the mutants previously identified. While the equivalents of many of these mutants were expressed in *Ngb* apparently without issue, the results of bacterial protein expression suggested that many of these *Cygb* mutants suffered from little or no heme insertion, possibly resulting from misfolding of the protein or simply alterations to the heme pocket that prevented the heme prosthetic group from being properly inserted into the protein. Despite multiple expression attempts for these proteins, including expression alongside other proteins that were successfully expressed (to ensure the problem was not with the growth conditions), the V85F, L46H + H81Q, V85A, and V85H mutants were not successfully recovered from bacteria at any point. Of these four, L46H + H81Q would yield a red supernatant after lysis, suggesting the presence of heme proteins, but during purification this product showed no affinity for the Ni-NTA resin and was

washed off the column almost immediately. This suggests heme incorporation to an incomplete or malformed protein, one that retained its heme binding sites but not the poly-histidine tag necessary for purification.

This left four successfully expressed mutants: the L46F single mutant, the L46F + H81Q double mutant, and the L46H and V85I single mutants. Luckily, three of these were among the four mutants identified as the highest priority. All four were then subjected to extensive characterization.

5.2.1 Nitrite reduction

The first reaction characterized for all newly-generated mutants was nitrite reduction, as this determines the protein's capability to produce NO and is thus an important characteristic for a potential oxygen carrier. In broader terms, the nitrite reductase activity also provides some insight into the overall reactivity of the protein and the distal histidine binding state, as mutating away the distal histidine or promoting its dissociation has been reported to greatly increase the rate of nitrite reduction [5, 13, 102].

A recent publication, which has been mentioned previously, showed data suggesting that the nitrite reductase activity of Cygb can be greatly modulated by the redox state of the thiols on the protein's surface cysteine residues [15]. In that report, the authors claim to have isolated specific forms of the protein and characterized them separately, namely the monomer with an intramolecular disulfide (S-S monomer), monomer with reduced thiols (S-H monomer), and dimer arising from the formation of intermolecular disulfides. The S-S monomer is reported to reduce nitrite very quickly, while the S-H monomer and dimer exhibited similar and much slower rates of nitrite reduction. The specific values were previously shown in table 3.

Rather than attempt to isolate specific thiol states, this analysis instead looks for multiple reaction phases in the proteins characterized. In nearly all cases, barring a few exceptions that will be discussed shortly, clear two-phase kinetics were observed. Nearly all mutants exhibit a fast phase, likely corresponding to the portion of the protein with an intramolecular disulfide, and a slow phase, which could be the dimer, the reduced thiol form, or a mixture of both, as these two forms have been reported to have very similar rate constants for nitrite reduction. These data were fit to double exponential models, which typically provided markedly more accurate fits than single exponentials.

The results obtained from fitting double exponentials to the measured absorbance data for four mutants, as well as the calculated overall rate constants, can be seen in figure 29.

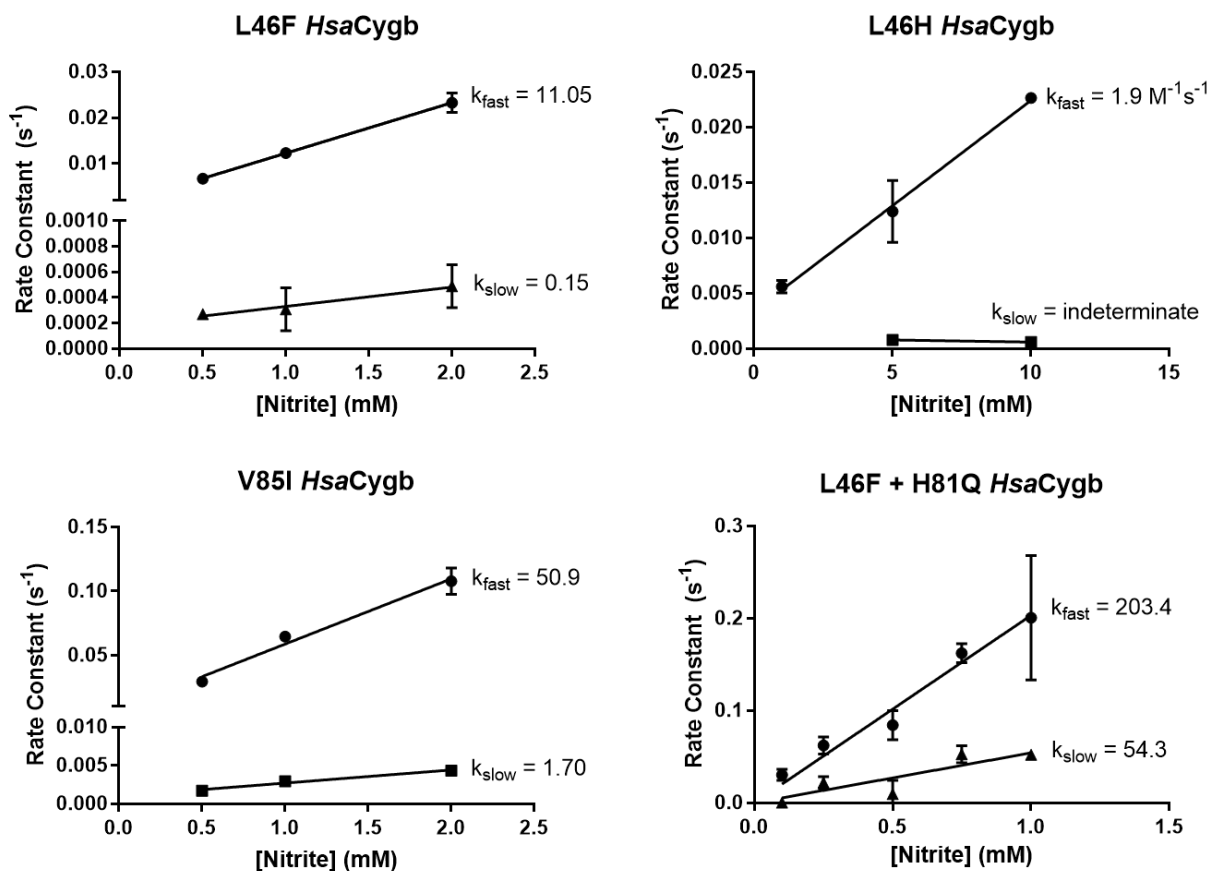


Figure 29: Two-phase kinetics of nitrite reduction by *HsaCygb* mutants

These results reveal that initial predictions of the mutation effects on nitrite reduction, based on the corresponding *Ngb* mutants, proved largely accurate. The L46F mutant showed the expected effect of the phenylalanine at position B10, with nitrite reduction slowing significantly (roughly by a factor of 3 vs. published values for the wild-type protein). This is, within a reasonable margin, essentially the reverse of the change seen in *Ngb* when the phenylalanine native to position B10 in that protein was replaced with leucine (the F28L *Ngb* mutant) [5].

The L46F + H81Q mutant showed very fast nitrite reduction, as was expected for a mutant without the distal histidine. Previous work in our lab had estimated a single-phase nitrite

reduction rate constant for H81Q Cygb of $210 \text{ M}^{-1}\text{s}^{-1}$. While H81Q is likely to exhibit two-phase nitrite reduction (and appears to do so, at least in some conditions, as will be explained shortly), it seems that the L46F mutation reduces nitrite reduction rates in both the hexacoordinate (wild-type) and pentacoordinate (H81Q) forms of the protein.

The V85I mutant also had roughly the expected effect, with a notable increase in nitrite reduction (nearly 2-fold increase for the fast phase, 3 to 7-fold increase for the slow phase). The mechanism of this change is unclear

One interesting fact to observe is the ratio of the rate constants for the fast phase and the slow phase for each mutant: about 100:1 for L46F, 50:1 for V85I, and 4:1 for L46F + H81Q. This variation likely arises from the putative mechanism for these multiple phases of nitrite reduction by Cygb; the primary effect of intramolecular disulfide formation is to slightly alter the geometry of the heme pocket, promoting distal histidine dissociation and leading to the fast phase. When the distal histidine is removed, the effect of opening the pocket is greatly blunted, resulting in only a four-fold increase in the rate, rather than a much larger increase when the distal histidine is still present and affected by the molecular rearrangement.

The L46H mutant shows unique and potentially interesting behavior. The reaction is relatively slow, and at 1 mM nitrite exhibits only a single phase, requiring higher concentrations of nitrite for a second, slower phase to be observed. The mechanism of this is unclear, but may relate to the effect of the additional histidine in the distal pocket on the electronic environment of the distal heme pocket. Figure 30 depicts the distal heme pocket of an L46H mutant of *HsaCygb*, with the distal histidine (and heme iron) shown in red, and the histidine inserted at position 46 (B10) shown in green/blue.

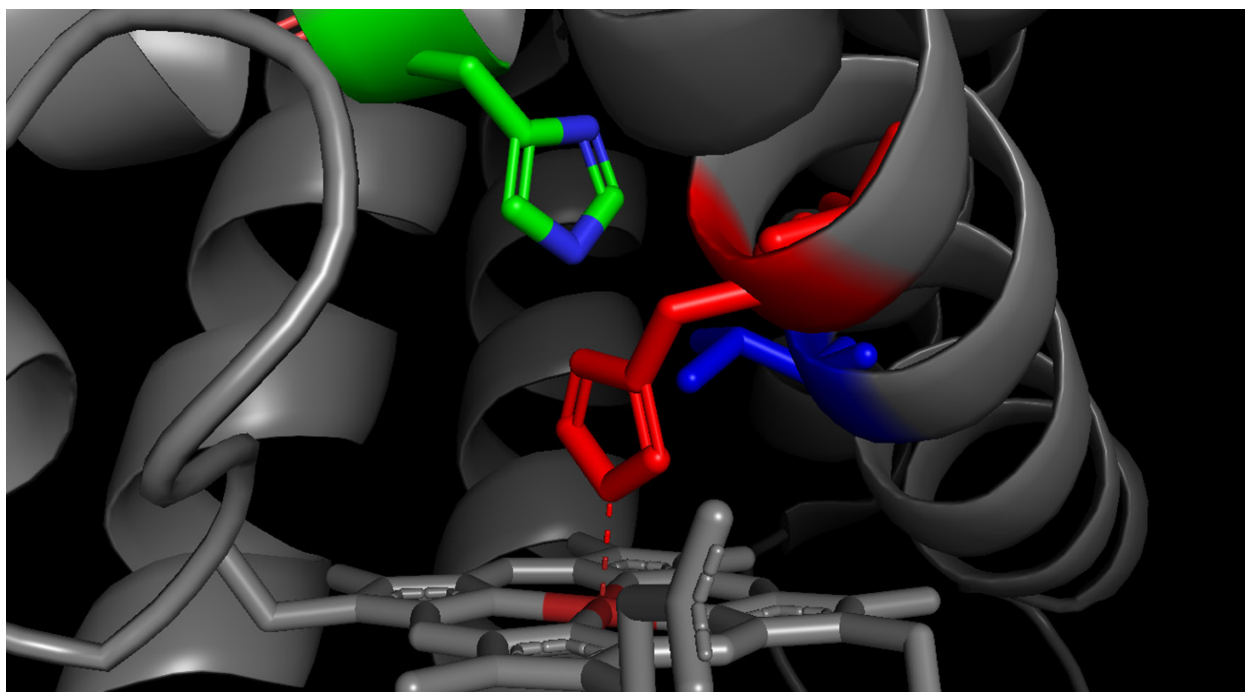


Figure 30: distal heme pocket of L46H *HsaCygb*

The close proximity of the added histidine to the distal histidine may allow this new histidine to abstract a proton from the distal histidine. This would make the distal histidine decidedly more electronegative, resulting in a far stronger bond between the distal histidine and the electropositive heme iron. The end result of this change is likely to be a sharp reduction in the rate of distal histidine dissociation, resulting in nearly permanent hexacoordination. Indeed, the corresponding mutant in Ngb has been shown to exhibit slow nitrite reduction as well as a redox potential roughly 70 mV more negative than the wild-type protein [5]. In the case of the Cygb mutant, however, intramolecular disulfide formation may shift the distal heme pocket enough to allow some distal histidine dissociation despite this electronic change, accounting for the faster phase observed for this mutant. A second slow phase of nitrite reduction does appear, but it is only seen at high nitrite concentrations. The low observed rate of this phase may

correlate to a very infrequent dissociation of the distal histidine in the absence of the intramolecular disulfide. In this case, a high concentration of nitrite may be required to successfully react during the brief window of distal histidine dissociation. This phase was only observed at two nitrite concentrations, preventing any calculation of a rate constant. Furthermore, the observed rate constant did not increase as the concentration of nitrite doubled; while this may be just be a random variation in a small sample, it may also suggest that above some threshold nitrite level, the reaction rate is limited by some other concentration-independent process like distal histidine dissociation.

Because all of the mutants examined showed double exponentials for at least some concentrations of nitrite, it seemed appropriate to revisit the H81Q distal histidine Cygb mutant, which had been previously characterized by members of our lab group. The initial characterization, which was documented in unpublished data from Dr. Jesús Tejero, reported a single-phase reaction with a rate constant of $210 \text{ M}^{-1}\text{s}^{-1}$. The reported speed of this reaction led me to use stopped-flow spectroscopy to follow nitrite reduction by this mutant, and the rapid measurement capacity of this device allowed for the use of fairly high nitrite concentrations (1, 5 and 10 mM). The results of this analysis can be seen in figure 31.

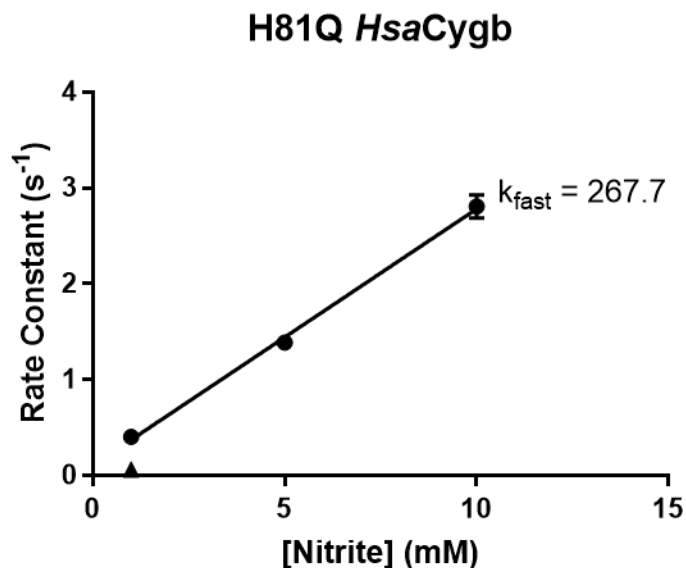


Figure 31: Kinetics of nitrite reduction by the H81Q *Cygb* mutant

Interestingly, this mutant showed double exponential behavior only at 1 mM nitrite, with the slower phase disappearing as the nitrite concentration was increased. This suggests that sufficiently high concentrations of nitrite may be able to induce thiol oxidation and subsequent disulfide bridge formation via an unknown mechanism. Of note, this interaction is unlikely to be physiologically relevant, as 5 mM represents a distinctly supraphysiologic concentration of nitrite which is very unlikely to ever occur *in vivo*. These results yielded a single rate constant of $268 \text{ M}^{-1}\text{s}^{-1}$ for this mutant, but it appears a second phase may also be present at nitrite concentrations at or below 1 mM. This further suggests that previous or ongoing work that has found or reported a single rate constant for nitrite reduction by *HsaCygb*, or mutants derived from *HsaCygb*, may need to be revisited in order to determine if double exponentials provide a better fit.

The calculated rate constants for nitrite reduction of the novel mutants and the H81Q mutant are summarized in table 10, along with previously reported values for the wild-type protein for comparison. Asterisks denote that, while the phase marked with an asterisk does appear to exist under at least some conditions, the data are insufficient to allow calculation of a rate constant for that phase.

Table 10: Calculated nitrite reduction rate constants for *HsaCygb* mutants

Protein	Fast rate constant ($M^{-1}s^{-1}$)	Slow rate constant ($M^{-1}s^{-1}$)	Source
<i>HsaCygb</i> , wt	1.1 ± 0.1 at 37°C		[4]
<i>HsaCygb</i> , wt (at 25°C)	32.3	0.26-0.63	Ref [15]
<i>HsaCygb</i> , H81Q	210		Unpublished data
<i>HsaCygb</i> , H81Q	268 ± 11	*	This work
<i>HsaCygb</i> , L46F	11.05 ± 0.04	0.15 ± 0.03	This work
<i>HsaCygb</i> , L46H	1.9 ± 0.1	*	This work
<i>HsaCygb</i> , V85I	50.9 ± 6.7	1.7 ± 0.3	This work
<i>HsaCygb</i> , L46F + H81Q	203 ± 12	54.3 ± 5.5	This work

5.2.2 Autoxidation

The second characteristic examined for all of the *HsaCygb* mutants that were generated was autoxidation, as slow autoxidation is important for development of an oxygen carrier and a CO scavenger.

While the nitrite reduction results suggested that L46H *HsaCygb* exhibited some atypical function, possibly related to near permanent hexacoordination, this mutant's performance in autoxidation testing was equally atypical. After reduction with dithionite, the protein was loaded into a G25 desalting column. As soon as the protein entered the resin of the column and achieved some separation from the dithionite, it could be seen to visibly and almost immediately change color; by the time it eluted from the end of the column, the protein was 100% oxidized. Consulting previously published work, the F28H *Ngb* mutant exhibited very similar behavior, with an autoxidation rate constant of roughly 11 min^{-1} , nearly two orders of magnitude faster than the wild-type [5]. As mentioned previously, the L46H mutant is likely to have a very negative redox potential and a near-permanent bond between the distal histidine and the heme iron. The autoxidation reaction thus likely occurs exclusively via a bimolecular outer-sphere reaction, with direct electron transfer from the heme to oxygen without any formation of a ferrous-oxy intermediate in between [103]. While completely anaerobic prep of this protein and stopped-flow spectroscopy could be used to determine its autoxidation rate constant, this rate of autoxidation makes this protein completely ineligible for use as an oxygen carrier or CO scavenger, and so further characterization was considered a low priority and has not been completed.

The other three mutants (L46F, V85I, and L46F + H81Q) were tested as described in the methods chapter. All three mutants showed decreased autoxidation rates compared to wild-type

HsaCygb. Figure 32 shows the progression of each mutant's spectra from the two peaks of the ferrous-oxy form to the flatter ferric form (main plot), as well as a trace of the ferrous-oxy peak's absorbance value throughout the course of the reaction (insets). Interestingly, all three of these proteins showed biphasic autoxidation, with an initial fast phase and a second slower phase; the red line in each inset plot is double exponential fit to the measured data.

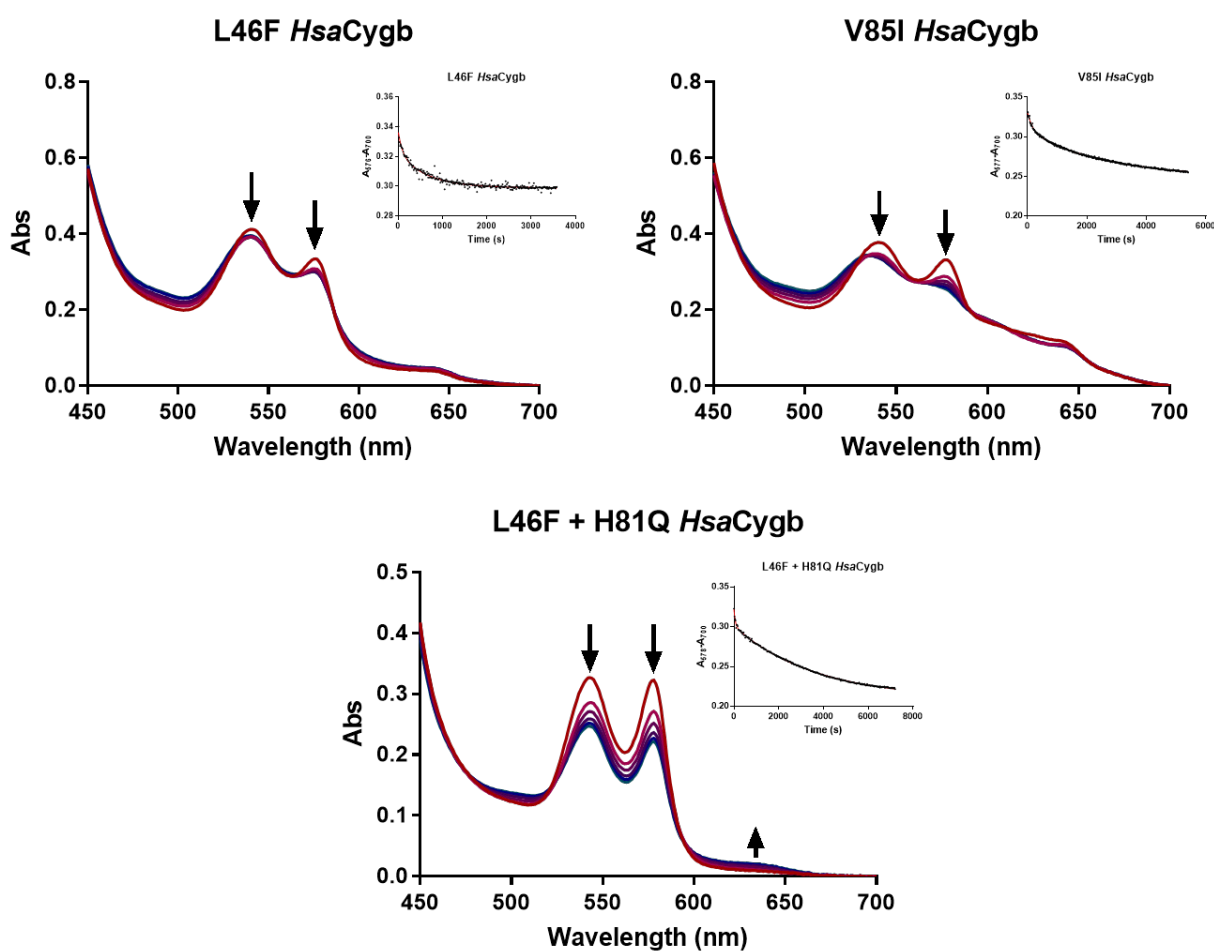


Figure 32: Autoxidation of *HsaCygb* mutants

The observed biphasic nature of these autoxidation reactions may be related to the effect of disulfide bridge formation, although to my knowledge a disulfide influence on autoxidation has not previously been reported for Cygb or any other heme globin. In general, the first fast phase exhibited a very small amplitude compared to the slower phase. There are several potential explanations for this small amplitude: first, it may not be related to an intrinsic protein process, but might instead be an artifact arising from the heating of the globin (which is collected from a room temperature column and heated to 37°C upon placement in the spectrophotometer). Second, it may be the case that, by the time the globin has eluted from the desalting column, the fast phase is largely complete, leaving mostly the slow phase left to be observed. This seems unlikely, however, as the initial spectra measured for both the V85I and L46F + H81Q mutants look to be very nearly 100% ferrous-oxy globin, suggesting that no appreciable autoxidation reaction occurs prior to measurement.

This question could likely be addressed by diluting the globin into pre-heated buffer after dithionite removal to eliminate any potential heating artifacts, and/or by using a mutant of *HsaCygb* that does not form disulfides (typically achieved by mutating away the two surface cysteines). If the biphasic reaction arises from disulfide formation, a double cysteine mutant with no surface thiols should show a simple one-phase autoxidation reaction.

The slower and larger of the two phases seems to be more representative of the autoxidation behavior of the protein; indeed, a single exponential fit to the autoxidation data seems to completely disregard the small fast phase, and returns a rate constant very similar (if not identical) to that of the second phase in a double exponential fit. These rate constants are summarized in table 11.

Table 11: Autoxidation rate constants for wild-type *HsaCygb* and mutants

Protein	Fast rate constant (s⁻¹)	Slow rate constant (s⁻¹)	Source
<i>HsaCygb</i> , wild type	N/A	0.270 ± 0.02	Ref [4]
<i>HsaCygb</i> , L46F	0.44 ± 0.18	0.09 ± 0.01	This work
<i>HsaCygb</i> , L46H	Too rapid to measure; near-instant		This work
<i>HsaCygb</i> , V85I	0.32 ± 0.66	0.03 ± 0.01	This work
<i>HsaCygb</i> , L46F + H81Q	0.75 ± 0.23	0.017 ± 0.001	This work

These mutations can all be seen to reduce autoxidation at least threefold vs. the wild-type protein, with the V85I and L46F + H81Q mutants both autoxidizing a full order of magnitude slower than the wild-type. Once again, this is consistent with the observed effect of similar mutations in *Ngb*, and suggests that all three proteins may be candidates for development as therapeutic molecules if their other characteristics are found to be optimal; combined with the rapid reduction of *Cygb* by *CYB5* and *Asc*, these three mutants should be fairly easy to maintain in the ferrous state under most conditions.

5.2.3 Cyanide Binding

As mentioned in the methods section, characterization of cyanide binding by my *Cygb* mutants was performed by Dr. Anthony DeMartino, PhD. In addition to the four mutants developed in this section of this dissertation, this analysis was also performed for wild-type *HsaCygb*, H81Q *HsaCygb*, and H81A *HsaCygb* (alanine possesses an even smaller side chain than glutamine, and

H81A mutants are generally expected to react even more rapidly than H81Q mutants). The calculated rate constants are summarized in table 12.

Table 12: Rate constants for cyanide binding by wild type and mutant *HsaCygb*

hCygb	k_1 ($M^{-1}s^{-1}$)	k_2 ($M^{-1}s^{-1}$)	k_3 ($M^{-1}s^{-1}$)	A_1	A_2	A_3
wt	4180 ± 120	540 ± 40	--	0.53	0.47	--
H81Q	28410 ± 850	3690 ± 110	590 ± 25	0.37	0.26	0.37
H81Q (NEM treated)	--	930	294	--	0.37	0.63
H81Q/L46F	38600 ± 1700	3900 ± 200	805 ± 35	0.32	0.4	0.28
H81A	34800 ± 2460	9200 ± 650	--	0.65	0.35	--
L46F	1090 ± 30	230 ± 20	--	0.71	0.29	--
L46H	no reaction (30 min, 1000x [KCN])					
V85I	4810 ± 110	298 ± 20	--	0.79	0.21	--

These results include two or three rate constants, denoted by k , with the number of constants reflecting how many exponentials provided the best fit, and thus corresponding to the number of distinct phases of the reaction. Also shown is the relative amplitude of each phase, denoted by A .

As is the case for reactions of the ferrous form, the distal histidine mutants exhibit dramatic increases in the kinetics of cyanide binding. H81Q binds cyanide roughly 7-fold faster than wild-type *HsaCygb*, while the L46F + H81Q and H81A mutants react even more rapidly than H81Q. This is not surprising, as removal of the distal histidine should greatly facilitate

ligand binding in the ferric form as well as the ferrous, but does suggest that one molecule may be able to scavenge both CO and cyanide.

The L46F and V85I mutants also show effects similar to those seen in these mutants for nitrite reduction. The L46F mutant appears 2 to 4-fold slower than the wild-type, while the V85I mutant is comparable to or perhaps slightly faster than the wild-type protein.

Perhaps the most interesting result, however, is the behavior of the L46H mutant. When mixed with a 1000-fold excess of cyanide, the protein shows absolutely no reaction over 30 minutes. As discussed above, there is some evidence that the distal histidine binding in this mutant is nearly irreversible in the ferrous state, but this assay suggests that in the ferric state the distal histidine is quite literally irreversibly bound to the heme iron. Once again, the presence of an extra histidine in the distal heme pocket seems to have a very large influence on the protein function, and while this mutant has no potential clinical utility, it provides some very interesting insight into structure-function relationships of hexacoordinate globins.

At this point, the factors that influence the relative amplitude of each phase, as well as those that lead to the appearance of a third phase for some mutants, are not known. The redox state of the protein thiols was expected to play a significant role, and it does appear to do so. Treatment of the H81Q mutant with *n*-ethyl maleimide, a compound that binds thiols and prevents disulfide bridge formation, completely abolished the fast phase for this mutant, suggesting that the disulfide exerts a major effect on cyanide binding by Cygb. For all other reactions, however, variation in the thiol redox state has resulted in formation of a double exponential, but never a triple, and even after NEM treatment, H81Q Cygb appears to exhibit two-phase binding. This suggests that some other factor can modulate the kinetics cyanide binding by ferric Cygb, but what this might be has not been identified.

5.2.4 Reduction of V85I Cygb by CYB5 and ascorbate

When the V85I mutant emerged as the leading candidate as a potential Cygb-based oxygen carrier, a brief set of experiments was performed to assess whether or not this mutation affected the reduction of the protein by the CYB5 system or by 1 mM ascorbate. The results of these tests are shown in figure 33.

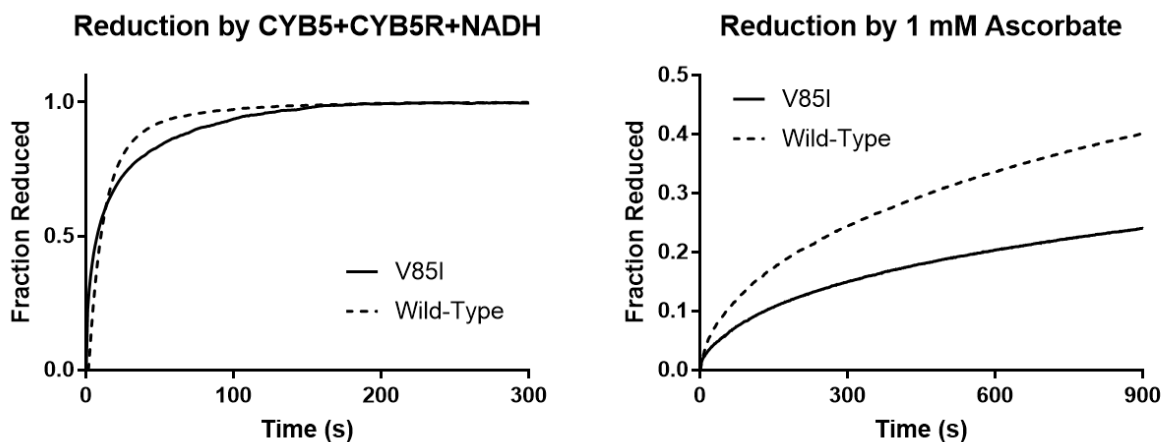


Figure 33: Reduction of V85I and wild-type *HsaCygb* by the CYB5 system and Asc

Reduction by the CYB5 system appears largely unaffected by the presence of the V85I mutation; while the reduction traces for the mutant and wild-type proteins are not identical, they show very similar behavior, and both are completely reduced within roughly 3 minutes. Reduction by ascorbate, on the other hand, does seem to slow somewhat, with roughly 25% reduction of the V85I mutant after 15 minutes vs. just over 40% reduction of the wild-type at the same time. The reduction of the V85I mutant by Asc is still fairly rapid compared to most other globins: Hb, for example, is approximately 25% reduced after 15 minutes when reduced by 5

mM ascorbate. Nevertheless, this may result in less efficient redox cycling *in vivo* if Asc is used to keep V85I reduced, as the rate of protein turnover would almost certainly be lower for this mutant.

5.3 DISCUSSION

The functional characteristics of the mutant Cygb's produced and characterized in this section provide valuable insight into efforts to develop Cygb-based therapeutics, but also more broadly into the effect of certain structural changes in the Cygb molecule on protein function.

The first insight gained is that Cygb seems more sensitive to perturbations of the heme pocket than closely related proteins such as Ngb, as several mutants that were expressed in Ngb without incident did not successfully incorporate heme when created in *HsaCygb*. In the case of V85I mutants showing poor heme integration, this may be related to the relatively close proximity of the V85I to the plane of the heme prosthetic group. Consulting figure 9, it appears that the side chain of V85 in Cygb may sit slightly lower in the heme pocket than the side chain on Ngb's V68. Furthermore, both V85A (smaller side chain) and V85F (larger side chain) Cygb mutants showed poor heme integration. This suggests that the side chain of this residue may in some way be necessary for proper heme insertion, and that a very small side chain is unable to perform some necessary role, while a large aromatic side chain could simply block heme access to the insertion site. The only mutant at this site that showed successful heme insertion was V85I, in which the side chain is just one methyl group larger, which may be a small enough change to preserve whatever role is filled by this side chain.

The characterization of these mutants also underscores the importance of the redox state of Cygb's surface thiols for protein function, as all mutants were shown to exhibit two-phase kinetics for nitrite reduction and seemingly autoxidation as well. Perhaps the most surprising result here is that even mutants without the distal histidine show two distinct phases in most of their reactions, suggesting that the geometric rearrangement of the protein following disulfide formation modulates protein function through mechanisms beyond just alteration of the distal histidine binding and dissociation constants. These other effects do seem far less influential than alterations of distal histidine binding kinetics, however, as the two rate constants for the L46F + H81Q mutant differed only by a factor of four, while those for the L46F single mutant with the distal histidine intact differed by nearly two orders of magnitude.

On a related note, the L46F + H81Q double mutant provides some insight into the importance of the distal histidine in determining the functional characteristics of hexacoordinate globins. While the addition of the second mutation at L46 lowered autoxidation and nitrite reduction compared to the H81Q single mutant (as the same mutation does for the wild-type protein), the double mutant far more closely resembles the H81Q single mutant than the L46F single mutant. This suggests, perhaps unsurprisingly, that the relatively contributions of other residues in the heme pocket of Cygb (and presumably Ngb and other hexacoordinate globins) to the overall function of the protein pale in comparison to the influence of the distal histidine. For future protein engineering efforts, this suggests that distal histidine mutations represent a path to dramatically alter protein function, while mutations elsewhere in the heme pocket may represent a way to "fine tune" protein function, with or without the distal histidine, but are unlikely to dramatically affect the protein's behavior.

The analysis of those mutants that were successfully expressed confirmed that the effects of single amino-acid mutations in Cygb appear to relatively closely mimic those seen in Ngb. In all cases, the effect of the single mutations lined up well with those predicted from previously-published Ngb data. As mentioned above, the results for the L46F + H81Q double mutant also show that removal of the distal histidine does not seem to substantially alter the effects of mutations elsewhere in the distal heme pocket. This suggests that the combination of several different single amino acid mutations should have relatively predictable effects based on characterization of each individual mutation in single mutants.

The cyanide binding data reveals significant variation in the rates of cyanide binding by different *HsaCygb* mutants, with certain mutants reacting very quickly and others reacting slowly or (in the case of L46H) not at all. Most mutagenesis work performed on heme globins has focused on mutations' effect on the activity of the ferrous form. Because cyanide binding is one of the few reactions to require the ferric form of the globin, previous literature provided little insight into how to alter the kinetics of this reaction. Fortunately, the results obtained were largely in accordance with the effects seen in the ferrous form, with distal histidine mutations greatly increasing binding rates and the redox state of the protein's thiols greatly affecting activity. This suggests that mutants with high CO affinity in the ferrous form may also exhibit rapid cyanide binding in the ferric form, and thus it may be possible to develop a single molecule that can be used to treat both.

Finally, this characterization suggests that two of the mutants generated in this work may merit further exploration as possible therapeutic molecules. The V85I mutant shows increased nitrite reduction and greatly decreased autoxidation compared to the wild-type protein, both desirable characteristics for an oxygen carrier that can produce sufficient NO to offset

vasoconstriction. The mutation also appears to have left the reduction of the protein by Asc and CYB5 similar to that of the wild-type protein, which would further facilitate oxygen delivery and nitrite reduction *in vivo*. The L46F + H81Q mutant shows slow autoxidation and very rapid cyanide binding, and while its affinity for carbon monoxide has not been measured directly, its similarity to H64Q Ngb suggests it should have sufficient CO affinity to function as an antidote for CO and/or cyanide poisoning.

5.4 CONCLUSIONS

In this section, plasmids were generated for eight novel Cygb mutants, and all of these plasmids were successfully transformed into *E. coli* for expression. Unfortunately, four of these mutants were not successfully expressed by *E. coli*, suggesting sensitivity of Cygb to perturbations of the structure in and around the distal heme pocket, with some changes resulting in non-functional protein and no heme insertion. The four mutants that were expressed were characterized for nitrite reduction, autoxidation, and (in the ferric form) cyanide binding.

Of these mutants, V85I exhibited faster nitrite reduction and slower autoxidation than the wild-type protein but retained the distal histidine, suggesting this mutant may be able to function as an oxygen carrier. The L46F + H81Q mutant behaved similarly to H81Q Cygb and H64Q Ngb, but also bound cyanide very rapidly, suggesting potential value for this mutant as a CO and cyanide antidote.

6.0 ASSESSING PROTEIN VASOACTIVITY IN A MOUSE MODEL

Rationale and aims

The primary goal of the animal work completed here is to assess the potential of a novel Cygb mutant to function as an NO donor and oxygen carrier. Because NO consumption has been a recurrent problem in HBOC development and clinical trials, a globin that can deliver oxygen and produce NO via rapid nitrite reduction has the potential to mitigate the adverse effects of earlier generation HBOCs.

After characterizing several different globin mutants, V85I Cygb mutant was chosen as a potential candidate HBOC. This work aims to compare this molecule to cell-free Hb in terms of the blood pressure increase resulting from infusion of the protein, as well as the effect of subsequent infusions of nitrite and a reducing agent (ascorbate or the CYB5 reducing system) on mean arterial pressure. Cell-free Hb was chosen as a control because it is the canonical mediator of cell-free globin-associated toxicity and vasoactivity. As the purpose of developing novel Cygb mutants was to reduce the vasoactivity of a globin-based oxygen carrier compared to cell-free Hb, a direct comparison of the V85I Cygb mutant and cell-free Hb was chosen as an appropriate model. Ideally, the novel mutant will show greater vasodilation in response to nitrite, with a reducing agent further increasing this effect by allowing more nitrite reduction.

6.1 MATERIALS AND METHODS

6.1.1 Experimental Groups

This experiment was initially conceived with two separate experimental groups: a Hb group and a Cygb mutant group. Each group would receive an infusion of the protein of choice, followed by an infusion of nitrite, and finally an infusion of ascorbate. Ascorbate was initially chosen over the CYB5 system for a number of reasons. It's a simpler system, consisting of only a single small molecule. As a vitamin, very high plasma levels of ascorbate are known to be well-tolerated, suggesting that co-infusion of ascorbate alongside an HBOC would not pose any safety concerns. Finally, looking ahead to potential translation, a well-known vitamin would face far fewer regulatory hurdles as an adjuvant to HBOC therapy than a system consisting of two separate proteins, which would be subject to extensive regulation as biologics.

Following initial experiments with these two groups, a number of additional groups were created to explore more aspects of the response to globin infusion. These groups were primarily intended to observe the effects of the CYB5 reducing system on protein vasoactivity, and in one case to observe the effects of nitrite and NADH on mean arterial pressure. These groups are summarized in table 13.

Table 13: Experimental groups for study of globin vasoactivity in mice

<i>Group Number</i>	<i>First infusion</i>	<i>Second infusion</i>	<i>Third infusion</i>
1	Hb	Nitrite	Ascorbate
2	V85I Cygb	Nitrite	Ascorbate
3	V85I Cygb + CYB5 + CYB5R	Nitrite	NADH
4	N/A	Nitrite	NADH
5	Hb + CYB5 + CYB5R	Nitrite	NADH

6.1.2 Protein Preparation

For both Hb and V85I Cygb, the protein should be infused in the reduced, oxygen bound form. Unfortunately, like all heme globins, these proteins tend to oxidize slowly in storage. As such, the first step in preparing these proteins for infusion is to reduce them. Complete reduction is achieved by adding a small (3 to 5-fold) excess of sodium dithionite to the protein, mixing well, and loading the protein onto a G25 desalting column (PD10, GE Healthcare) to remove the dithionite.

Hb autoxidizes extremely slowly (roughly 2% per day), and so once Hb has been reduced with dithionite and passed through a G25 column, it is essentially ready for use. It is concentrated down to a concentration of at least 4 mM (required for infusion) in centrifugal concentrators, and can then be frozen until it is needed. This allows for the preparation of a large amount of ferrous-oxy Hb, which can be left in storage until it is needed, at which a small portion can be used.

V85I Cygb, on the other hand, autoxidizes far faster than Hb (k_{autox} is roughly $.03 \text{ min}^{-1}$). Even though this rate is far slower than that of the wild-type Cygb, or most other hexacoordinate globins, it is rapid enough to complicate preparation of the protein. As soon as the protein separates from the dithionite in the G25 column, it begins to autoxidize. As a result, all protein preparation is performed at 4°C in the cold room, to limit the rate of the autoxidation reaction. The protein is also prepared in small amounts, with just enough for one mouse being prepared at a time. After the reduced protein comes off the column, it is concentrated as soon as possible down to a concentration of at least 4 mM.

Once the time has come to infuse the protein into a mouse, the concentrated solution of protein is diluted down to 4 mM. If this protein is being used with the CYB5 reducing system, this is also the point at which CYB5 and CYB5R are added to the protein solution to final concentrations of about $10 \mu\text{M}$ and $5 \mu\text{M}$, respectively. For V85I Cygb, NADH is also added at this stage to a final concentration of $150 \mu\text{M}$; spectral measurements taken after this NADH addition suggest that this NADH is rapidly consumed, but is able to keep the protein 80% reduced (or more).

6.1.3 Experimental Protocol

All animal experiments were performed with Dr. Qinzi Xu, a member of the Gladwin lab who has spent years developing models of globin infusion in small animals. The first step of these experiments is surgical preparation of the mouse, usually performed by Dr. Xu. Male C57BL/6 mice are anesthetized with 1-3% isoflurane, followed by tracheal intubation and cannulation with both jugular and carotid catheters. Blood pressure and heart rate are monitored through the arterial catheter. Once the surgery is complete, the mouse is mechanically ventilated with 10%

oxygen and 1.5% isoflurane for continuous anesthesia. The initiation of 10% oxygen marks the official start of the experiment, and is defined as $t = 0$ minutes. The switch to 10% oxygen results in changes to blood pressure and other parameters; no further work is performed for 15 minutes to allow the mice time to stabilize at 10% oxygen.

After 15 minutes have elapsed, at $t = 15$ min, the mouse receives 5 $\mu\text{L/g}$ of body weight of either 4 mM hemoglobin or 4 mM V85I Cygb (500 nmol of protein for a 25g mouse). This infusion is performed over a 2 minute duration using a Hamilton syringe mounted on a standard Harvard syringe pump. This infusion should result in plasma heme concentrations of approximately 300-400 μM . Direct measurement of the plasma heme concentration will be performed by taking a 15 μL blood sample through the arterial catheter five minutes after globin infusion ($t = 20$ minutes). If CYB5 and CYB5R are being used, they are also present in this infusion, and should reach final plasma concentrations of just under 1 μM (CYB5) or just under 500 nM (CYB5R).

At the same time, $t = 20$ minutes, the mice receive a second infusion (over 2 minutes) of 1 $\mu\text{L/g}$ of body weight sodium nitrite at a concentration of 10 mM (250 nmol for a 25g mouse), resulting in a plasma concentration of nitrite around 150 μM before nitrite consumption. A similar dosage has been previously reported to decrease the vasoactive effects of HBOCs in animal models [3, 104]. Ten minutes after the globin infusion, at $t = 30$ minutes, the final infusion is given, again over 2 minutes. This infusion is 1 $\mu\text{L/g}$ body weight of the chosen reducing agent for the experiment, either Asc or NADH, at a concentration of 30 mM (750 nmol for a 25g mouse). This dose was chosen to ensure a slight (roughly 1.5-fold) excess of reducing agent vs. globin, to ensure a considerable amount of redox cycling is possible. Figure 34 provides a visual depiction of this experimental protocol.

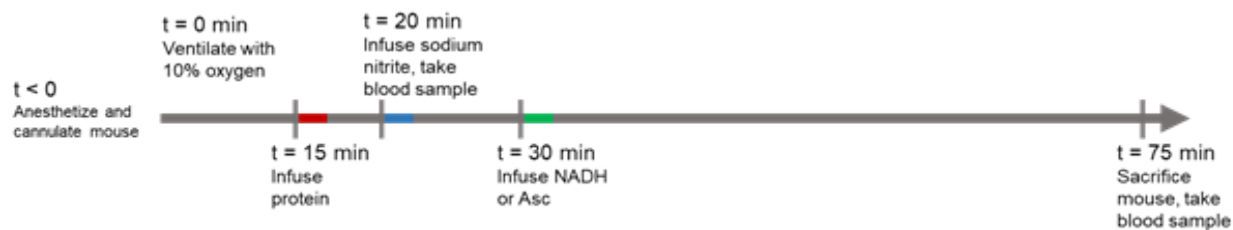


Figure 34: Timeline of mouse vasoactivity experiments documenting all infusions performed

When these experiments were mostly completed, Dr. Xu explained that the nature of the pump used to perform the infusions was such that an additional 20 μL was added onto each infusion (this is dead space volume in the tubing that has to be flushed following the infusion). This increases the dose of globin by 15-20%, and of nitrite and the reducing agent by nearly 70% vs. what was initially intended. This represents a significant alteration, but if anything, the increased doses should amplify the effects of the infusions, and so it was not deemed necessary to start the experiments over. Instead, the experiments continued with the larger than initially planned doses, as changing the protocol at that point would have likely invalidated all of the data that had been gathered.

6.1.4 Data Analysis

All data analysis was performed using LabChartReader 8 for Windows. The uncorrected pressure measured from the mouse was first increased at all time points by 32.5 mmHg in order to correct for the vertical displacement of the transducer above the mouse. These data were then converted into the mean arterial pressure (MAP), defined as $1/3 \times \text{systolic pressure} + 2/3 \times \text{diastolic pressure}$. Finally, these data were smoothed with a 5-second smoothing window.

6.2 RESULTS

For all mouse experiments detailed in this section, results are presented as the change in the mean arterial pressure (MAP) compared to a baseline value. This baseline is defined as the MAP in the two minutes prior to globin infusion, at which point the mouse had been mechanically ventilated with 10% oxygen for 13 to 15 minutes, which was observed to be enough for MAP to stabilize.

In addition to monitoring the effect of numerous combinations of globins, nitrite, and reducing agents on blood pressure, each mouse treated with globins also had two blood samples taken, one shortly after globin infusion and the other at the end of the experiment. These samples were separated into RBCs and plasma, and the plasma concentrations of heme are used to estimate the plasma residence time of the proteins.

6.2.1 Hb + nitrite + ascorbate

Before using recombinant protein, which is relatively labor-intensive to produce, several mice were infused with “stripped” Hb (isolated Hb with no 2,3-DPG, obtained in large quantities from expired human red blood cells by Dr. Qinzi Xu), followed by nitrite and finally ascorbate. This provided an opportunity to ensure the animal model worked properly, and to establish a baseline level of blood pressure changes after each infusion against which V85I Cygb could be compared. Figure 34 depicts the averaged blood pressure readings from three mice treated with this series of infusions.

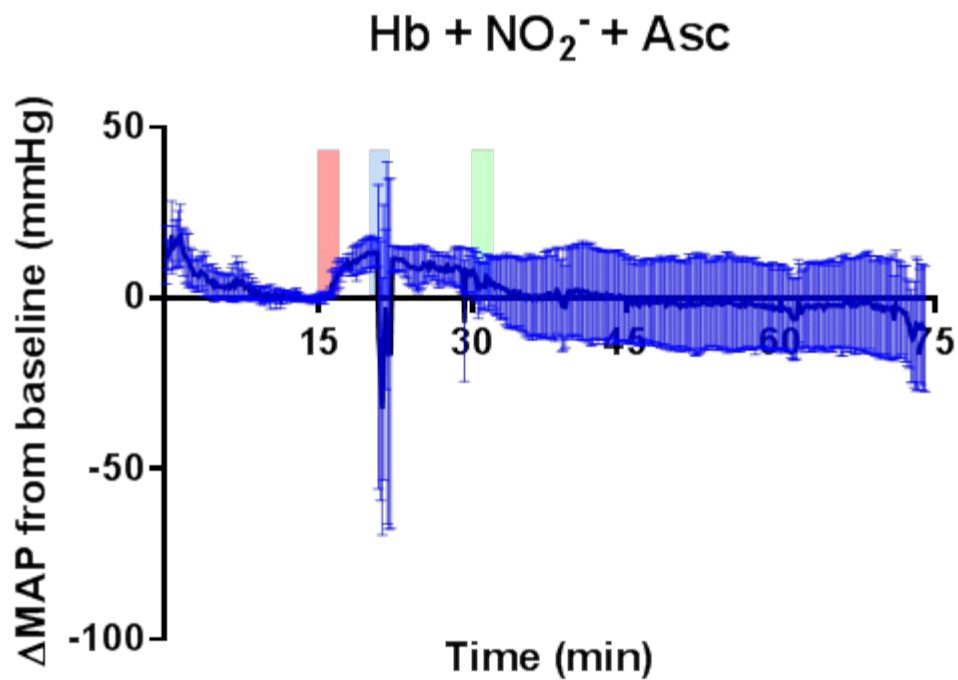


Figure 35: MAP change in mice (n = 3) infused with Hb, nitrite, and ascorbate

These data suggest a repeatable model of globin-induced hypertension, with a repeatable increase in MAP of roughly 12 mmHg following Hb infusion. Nitrite infusion appears to lead to a small decrease in MAP (3-5 mmHg), and after infusion of ascorbate the MAP returns more or less to its baseline level. It is difficult to determine if the blood pressure decrease after ascorbate infusion occurs as a result of the ascorbate infusion, or whether it is merely a continuation of a decline in MAP that begins after nitrite infusion.

6.2.2 V85I Cygb + nitrite + ascorbate

Once Hb + nitrite + ascorbate infusion had been found to provide fairly repeatable results, three mice were infused using the same protocol, but with V85I Cygb in place of Hb. The resultant changes in the blood pressure of three mice are shown in figure 35.

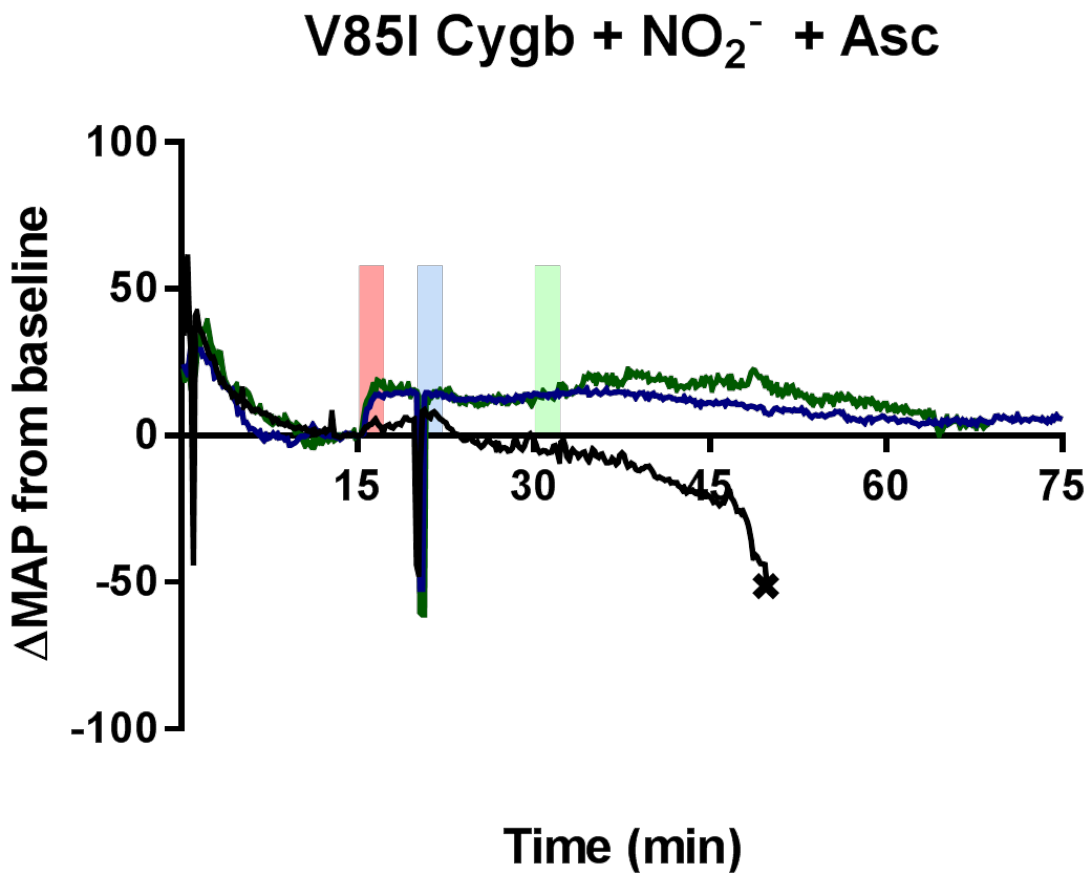


Figure 36: MAP change in mice (n = 3) infused with V85I Cygb, nitrite, and ascorbate

The most immediately obvious result in this figure is the premature death of one mouse for reasons that are not immediately apparent. In this and all subsequent figures, the death of a mouse is indicated with an X superimposed on (and color-coordinated with) the relevant MAP trace. This was observed in a small but not insignificant portion of all the mice studied in this portion of the study and may in some way be related to the effects of anesthesia and surgery (even with minimal blood loss) followed immediately by mechanical ventilation with oxygen-poor air. This is a series of several not-insignificant insults in a short period of time, and it is not unreasonable that it may carry some mortality. The other two mice, however, remained stable for the whole duration of the experiment, and showed a clear increase in blood pressure of about 15 mmHg following infusion of V85I Cygb, followed by a small and apparently transient decrease in MAP several minutes after nitrite infusion.

Perhaps the most noteworthy result here, however, is the increase in MAP after ascorbate infusion for the surviving mice. This is the opposite of the effect that had been expected, as Asc was predicted to facilitate more nitrite reduction, leading to NO production and a decrease in MAP. In the presence of oxygen, however, reducing Cygb would instead allow more ferrous-oxy Cygb to form, which can subsequently scavenge NO rather than produce it. The elevation in MAP has a relatively small magnitude and may not arise directly from Cygb reduction by Asc, but nonetheless stands in contrast to Hb, where ascorbate infusion was followed by a decrease in blood pressure. While one mouse does see a drop in blood pressure after ascorbate infusion, this mouse's MAP had begun to drop prior to Asc infusion and rapidly progresses to the point of death, suggesting it may be more related to some fatal process beginning in the mouse than to any NO production by Cygb in the plasma.

Overall, these data suggest that V85I Cygb is not an effective NO donor in the plasma when ascorbate is present as the only reducing agent. This may stem from certain intrinsic characteristics of the protein itself. For example, the oxygen affinity of this protein may be sufficiently high (wild-type *HsaCygb* has an oxygen P_{50} of roughly 1-2 mmHg [14], and the slow autoxidation of this mutant suggests its affinity may be even higher) that unbound ferrous Cygb is not present in sufficient amounts to generate a meaningful amount of NO. Furthermore, if oxygen is bound to the protein, it would retain the ability to scavenge NO produced by red cell Hb, potentially leading to vasoconstriction.

Even if binding sites are available for nitrite reduction, the relatively high concentration of the protein (especially prior to infusion, when it is concentrated to 4 mM) is likely to promote formation of dimers, which arise from intermolecular disulfide formation. This prevents the formation of intramolecular disulfides, which enable the previously shown fast phase of nitrite reduction ($k = 50.9 \text{ M}^{-1} \text{ s}^{-1}$). It may be the case that V85I Cygb is present, reduced, and unbound, but is simply not a fast nitrite reductase under these conditions, and thus does not generate meaningful amounts of NO. Some combination of dimer formation and high oxygen affinity seems to be the most likely cause of the lack of vasodilation observed after nitrite and ascorbate infusion.

It may also be the case that the amount of ascorbate infused is simply insufficient to efficiently reduce the Cygb present. The reduction of V85I Cygb by ascorbate does appear slightly slower than the reduction of wild-type Cygb (see section 5.1.4), and the final concentration of ascorbate in the plasma for the given dose ($< 1 \text{ mM}$) does not appear to reduce Cygb very rapidly even at much lower Cygb concentrations [105]. This may compound the autoxidation rate of V85I Cygb which, despite being slow by the standards of hexacoordinate

globins (roughly $.03 \text{ min}^{-1}$), is very rapid compared to Hb ($.001 \text{ min}^{-1}$ or lower). If insufficient reduction is the primary reason no vasodilation is observed with V85I Cygb, addition of more ascorbate or a more efficient reducing system may lead to a decrease in blood pressure that is not observed here.

6.2.3 Coinfusion of the CYB5 reducing system

The first few mice infused with V85I Cygb, nitrite, and ascorbate did not show any result that suggested significant NO production by vasodilation. While it seems likely that some intrinsic characteristics of the V85I Cygb mutant may be at least partially to blame for this effect, the next experimental group was nonetheless chosen to explore the effect of more efficient reduction of the Cygb on blood pressure. To speed the reduction of the Cygb, Asc was replaced with the CYB5/CYB5R/NADH system. Just before protein infusion, CYB5 to a final concentration of roughly $10 \mu\text{M}$ and CYB5R to a final concentration of roughly $5 \mu\text{M}$ were added to the 4 mM protein stock. The infusions of protein (with CYB5 and CYB5R this time) and nitrite proceeded as detailed above, but in place of Asc, an equivalent amount of NADH was infused. The results of this infusion protocol in three mice (group 3 from table 13) are shown in figure 36.

V85I Cygb + NO₂⁻ + CYB5 System

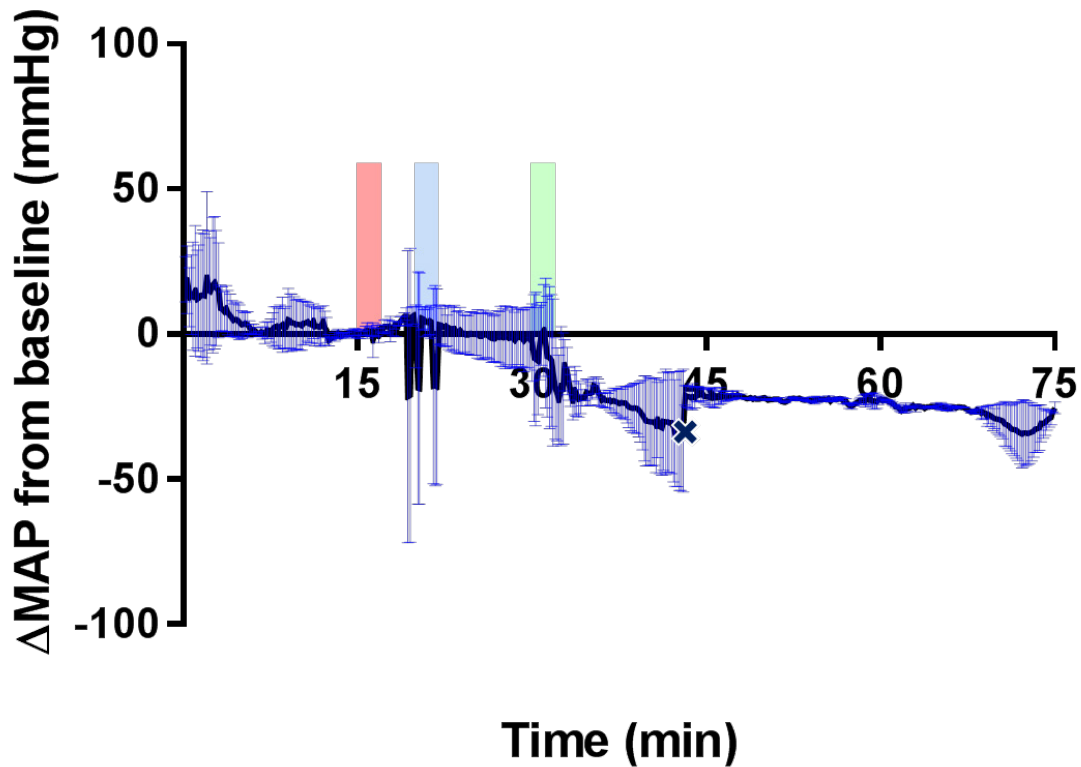


Figure 37: MAP change in mice (n = 3) infused with V85I Cygb+CYB5+CYB5R, nitrite, and NADH

These mice showed a slightly smaller but still appreciable increase in MAP following globin infusion than the mice documented above (6-8 mmHg here vs. 12-15 in previous experiments). Following nitrite infusion, a decrease in the MAP can be seen that appears to be greater than that observed after nitrite infusion in the V85I + ascorbate group.

By far the most impressive effect, however, is that seen after infusion of NADH. The MAP sharply declines to a much lower level, dropping well in excess of 20 mmHg within just a few minutes. After NADH infusion, one mouse rapidly became severely hypotensive and expired, perhaps as a result of excessive vasodilation leading to hypotension and hypoperfusion.

The other two showed a remarkably consistent decrease in blood pressure, with a MAP roughly 20-25 mmHg lower than their baseline levels that was sustained for more than 30 minutes, and was still present at the end of the experiment. This is a dramatic departure from the results when ascorbate was used as the reducing agent, and suggested that more efficient reduction of V85I Cygb may indeed allow for increased NO production and subsequent vasodilation.

6.2.4 The apparent effect of NADH on hypoxic vasodilation

In order to determine if the vasodilation seen after NADH infusion in the prior experiment was indeed a result of NO production by V85I Cygb, the same experiment documented in figure 37 was repeated in two mice, but without any infusion of globin (group 4 from table 13). The infusions of nitrite and NADH were performed as in the prior experiment. The only variation was in the rate of NADH delivery; in one trial, the dose was delivered over a 2-minute period, as before, but for the second mouse, the infusion rate was slowed to deliver the same dose over a 20-minute time period. The effect of the infusions on the MAP of these two mice can be seen in figure 37.

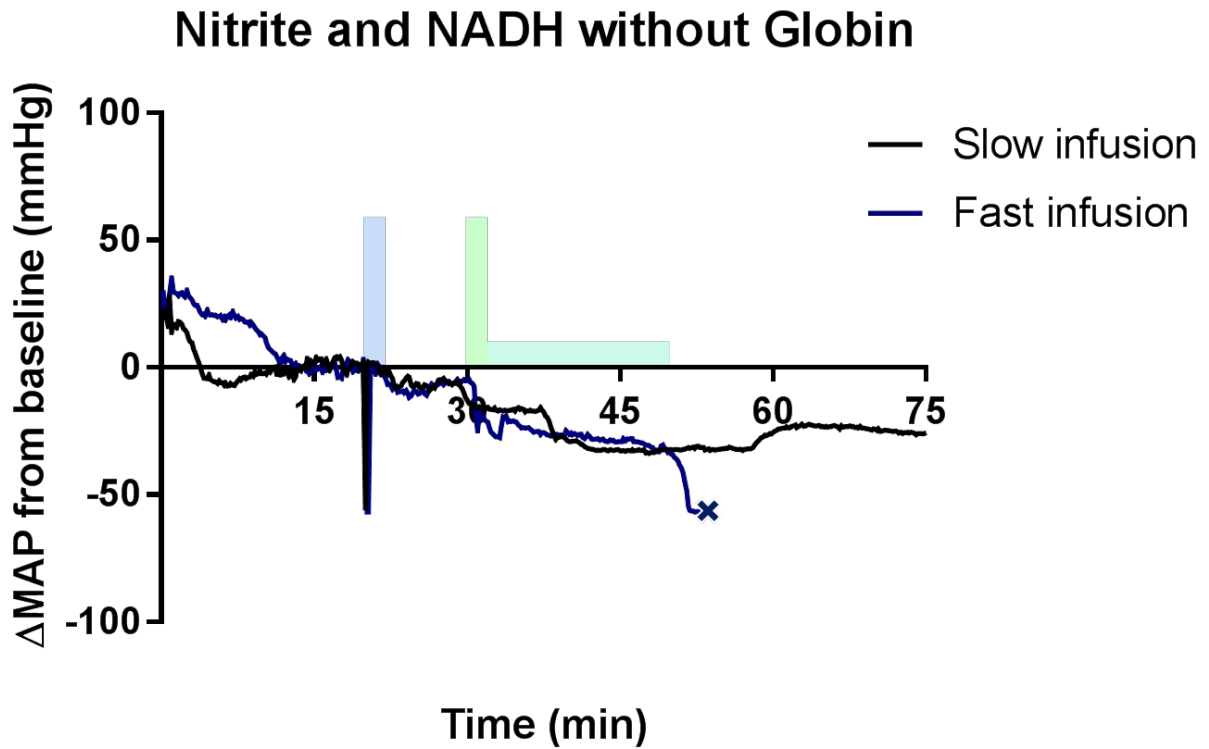


Figure 38: Effect of nitrite and NADH infusions on MAP of mice (n = 2)

These results came as quite a surprise, as the effect of NADH in the absence of any globin appears comparable to, if not greater than, the effect seen in the presence of several hundred micromolar concentrations of globin! Once again, one mouse saw its blood pressure drop sharply leading to death sometime after the final infusion. While the changes in MAP for the two mice are very similar, the baseline MAP for the mouse that expired was notably lower, meaning this mouse reached a notably lower MAP level than the surviving mouse before ultimately dying.

Finally, to determine if this NADH effect is completely globin-independent, one mouse (group 5 from table 13) received sequential infusions of Hb + CYB5 + CYB5R, nitrite, and

NADH. The results for this mouse are shown in figure 38 alongside the results for the mice treated with both V85I Cygb (from figure 36) and no globin (from figure 37).

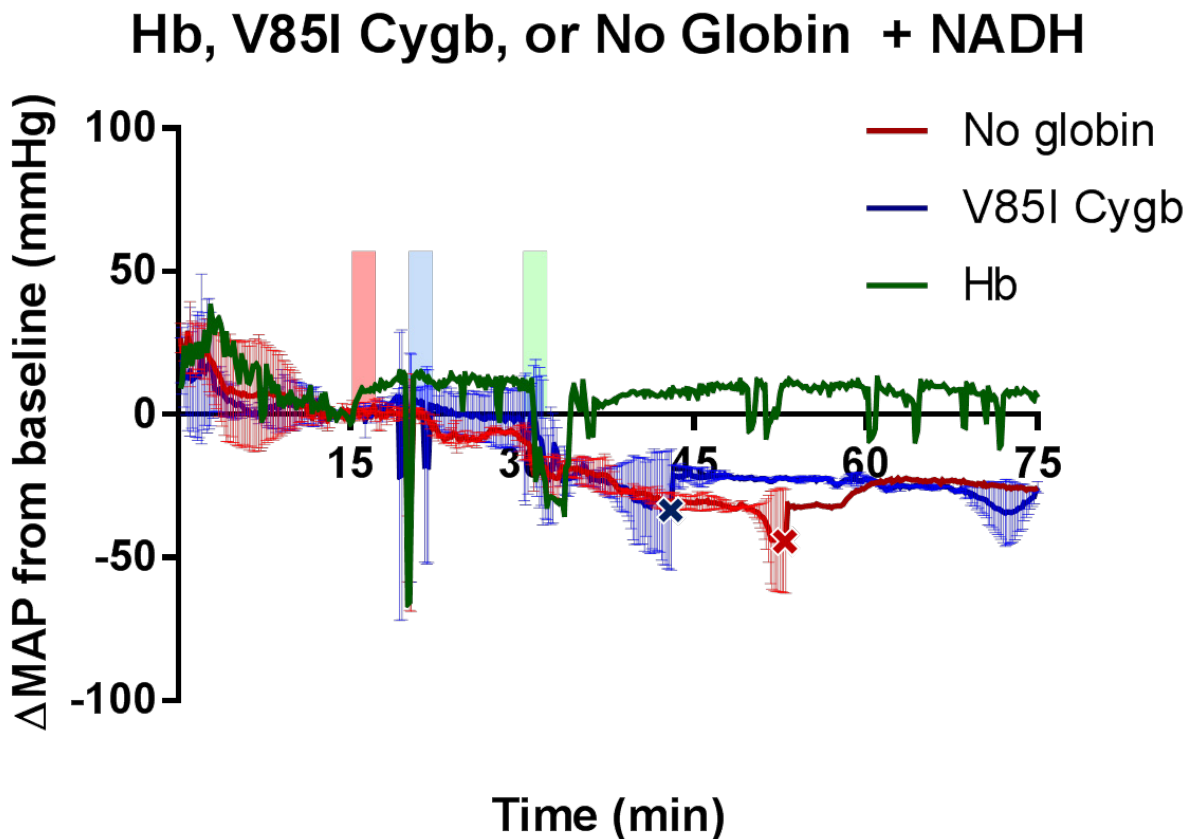


Figure 39: Effect on MAP of NADH administration with V85I Cygb, Hb, or no globin

As had been previously alluded to, direct comparison reveals that the presence or absence of V85I Cygb appears to have little effect on the vasodilation that occurs after NADH infusion. Hb, on the other hand, appears to significantly blunt the vasodilation caused by NADH administration. This is not immediately true, as the infusion of NADH causes a sharp drop in the Hb-treated mouse just as it does in the other groups. The difference comes 3-5 minutes after the

NADH infusion, where the Hb-treated mouse sees its MAP recover back to nearly the pre-NADH level, while the other two groups do not. The cause of this discrepancy is not obvious, but it may be related to slower clearance of Hb from the vasculature due to its increased molecular weight, resulting in comparatively higher levels of Hb in the plasma and thus increased NO scavenging by Hb vs. V85I Cygb. This effect is apparent as little as 20 minutes after globin infusion, however, at which point clearance of even a monomeric globin from the plasma should be relatively minimal. Arguably the most interesting conclusion, however, is that NADH itself is sufficient to cause substantial vasodilation in the presence of nitrite and hypoxia, and that substantial concentrations of heme globins in the plasma may in fact reduce the vasodilatory effect of nitrite and NADH administration under hypoxia.

6.2.5 Clearance of V85I Cygb from plasma

While plasma samples were taken from all mice treated with V85I *HsaCygb*, in some cases the samples were of sufficiently low volume that accurate measurements could not be taken, while in other the mice died before the final timepoint to assess clearance. While samples were still taken from these mice after the time of death (via left ventricular puncture), these samples uniformly showed higher plasma heme concentrations at death than they had five minutes after globin infusion. This indicates a significant degree of hemolysis.

Three of the mice treated with V85I Cygb survived long enough for the second plasma sample, and yielded samples that gave clear results. These three mice had a mean plasma V85I concentration of $187 \pm 25 \mu\text{M}$ at five minutes after globin infusion. One hour after globin infusion, this concentration had decline to $108 \pm 25 \mu\text{M}$. This is a decrease of about 42% in the plasma heme concentration over the course of 55 minutes, suggesting a plasma half-life for the

protein just over one hour. This is a much greater plasma half-life than was anticipated, as previous experience in with Ngb-based therapeutics for treatment of CO poisoning showed more rapid clearance.

The Hb treated mice tested, in contrast, typically saw an approximately 30% decrease in their plasma heme concentration over the same time period. The relatively slow clearance of the V85I Cygb, and the similarity in the clearance rates of V85I *HsaCygb* and Hb, suggest that the relatively small monomeric Cygb has formed larger complexes in the plasma, most likely via disulfide formation. While the most obvious target for intermolecular disulfide formation is another molecule of Cygb, resulting in formation of a homodimer, many plasma proteins express surface thiols. This includes albumin, the most abundant protein in plasma, which possesses one reactive surface thiol [106]. Based on this clearance data, it seems likely that V85I Cygb is not present in the plasma as free monomers, but rather as part of larger protein-protein complexes composed of not just additional Cygb molecules, but likely native plasma proteins as well.

6.3 DISCUSSION

The primary purpose of these experiments was to evaluate the V85I mutant of *HsaCygb* as a potential oxygen carrier. More specifically, this work sought to assess whether or not this mutant's high rate of nitrite reduction, combined with rapid reduction by ascorbate or the CYB5 system, could reverse the vasoactivity seen following infusion of cell-free globins. These results unfortunately provide little (if any) evidence for potential clinical utility of this mutant, with the mutant performing no better (and perhaps worse) than Hb when ascorbate is used as the reducing agent. When CYB5 + CYB5R + NADH is used instead, a notable drop in blood pressure is

observed with V85I Cygb but not with Hb, but this drop does not exceed that caused by NADH infusion in the absence of any globin.

These data nonetheless offer a variety of interesting conclusions that may merit further investigation. Before discussing those, however, it is worth considering if any other proteins exist that may be able to fill the dual roles of oxygen transporter and NO donor, since V85I Cygb does not appear promising following these experiments. One protein worth examining is *DreCygb1* from zebrafish. This protein has been shown (partially in this work, and partially elsewhere) to exhibit slow autoxidation, very fast nitrite reduction independent of disulfide formation (as it lacks surface thiols), and an oxygen P_{50} of roughly 2 mmHg at 37°C, all ideal characteristics for a potential HBOC. It is also reduced very quickly by CYB5 and ascorbate. However, because it is a zebrafish protein there is some concern that it may provoke an immune response if given to human patients. These risks are far lower for purified protein than for cells or tissues, but cannot be entirely discounted. Genetic modification of this protein may still be desirable, but rather than aiming to optimize the function of the protein, it could be geared toward “humanizing” the protein. This process has been used to develop FDA-approved therapies from murine antibodies, and relies on modifying regions of the protein to more closely resemble its human equivalent, hopefully making it less immunogenic.

These results introduce an interesting possibility that, in certain conditions, NADH might be a potent vasodilator. A literature review does not readily reveal any prior references to this effect, even with the availability of NADH as an over-the-counter dietary supplement, suggesting that NADH alone is not sufficient to cause a significant change in blood pressure. The specific combination of hypoxia and nitrite present in these animals may be required for a vasodilatory effect of NADH infusion. A potential mechanism for this effect may relate to the interaction of

exogenous NADH with the CYB5 reducing system present in red blood cells. Conditions like hypoxia and oxidative stress can lead to rapid depletion of red blood cell NADH [107]; repleting this NADH pool might greatly enhance redox cycling of, and NO production by, native Hb within the erythrocytes.

The reason for the differential effect of Hb vs. V85I with the CYB5 reducing system and NADH isn't clear. It may relate to rates of nitrite reduction, NO scavenging, or even potentially the amount of metHb that may accumulate; nitrite has been used to oxidize Hb, which will be reduced more slowly. Hb + b5 reducing system only has $n=1$, due to time and animal constraints, but replication in more animals should be a high priority.

Previous studies have found that infusion of sodium nitrite can attenuate the vasoactivity arising from infusion of HBOCs [3]. These results suggest that NADH may be able to further modulate these effects. These data also suggest at least a possibility that even in the presence of significant amounts of extracellular heme globins, the vasodilatory effect of nitrite is mediated primarily by RBC Hb. This is not inconsistent with the previously-documented role of RBC Hb in mediating vasodilation in response to hypoxia and nitrite[108]. RBCs have been shown to increase their uptake and consumption of nitrite as the Hb oxygen saturation decreases [109]. This increase in nitrite consumption, presumably via nitrite reduction by deoxyHb, may be further increased by exogenous NADH, which would support redox cycling of Hb in the red cell and thus support NO generation from nitrite.

6.4 CONCLUSIONS

The animal studies conducted in this section suggest that, unfortunately, V85I Cygb may not exhibit the characteristics desired for a globin-based oxygen carrier. Specifically, this mutant does not appear to generate NO in quantities that are sufficient to notably effect blood pressure. While a large drop in MAP was observed when this mutant was combined with nitrite and the CYB5/CYB5R/NADH reducing system, the decrease is not any greater than that observed after the addition of only nitrite and NADH. This effect was not preserved following Hb infusion, however, suggesting that under certain very specific conditions this mutant may reduce the vasoconstriction seen with Hb infusion. Interestingly, exogenous NADH may potentiate the mouse's native nitrite-induced hypoxic vasodilation, possibly through repletion of depleted erythrocyte NADH and facilitation of nitrite reduction by erythrocyte Hb. In future clinical trials of globin-based therapeutics, the addition of exogenous NADH to nitrite may represent a possible strategy to further modulate blood pressure and prevent undesired hypertension. The effects of NADH administration on hypoxic vasodilation in the presence and absence of exogenous nitrite merit further examination.

7.0 OVERALL CONCLUSIONS AND NEXT STEPS

7.1 OVERALL CONCLUSIONS

Looking back over the entirety of the work detailed within this dissertation, a few broad conclusions emerge with potential significance for the future work with hexacoordinate globins, especially cytoglobin. These conclusions are summarized here.

Cytoglobin is reduced very rapidly by CYB5

In studying both human and zebrafish proteins, there is a clear and well-conserved interaction by which the CYB5 reducing system reduces Cygb extremely rapidly, typically multiple orders of magnitude faster than such canonical redox partners as Hb and Mb. This suggests possible coevolution of these two proteins, and also strengthens existing theories that Cygb's *in vivo* function may include catalytic NO consumption, a function that is very well supported by the CYB5 reducing system.

Mutagenesis can be used to effectively tailor the function of cytoglobin

Compared to other heme globins, there is relatively little published work summarizing the effect of specific amino acid mutations in Cygb. Generation of novel Cygb mutants was able to

demonstrate that mutation effects in Cygb generally closely resemble the effects of corresponding mutations in Ngb. Furthermore, these mutations can substantially alter such protein functions as nitrite reduction, autoxidation, and cyanide binding. These mutations can also interact with the surface thiols on the protein to further modulate protein function. This work provides a strong foundation for ongoing efforts to develop therapeutics based on Cygb mutants.

The therapeutic potential of Cygb mutants remains unclear

Unfortunately, the V85I *HsaCygb* mutant evaluated as a possible oxygen carrier and NO donor did not show very promising results in a small animal study of vasoactivity. Other Cygb mutants may still show potential for clinical applications, however; the L46F + H81Q double mutant merits further evaluation as a CO and cyanide antidote, and a humanized mutant of *DreCygb1* may represent a significant improvement over V85I Cygb as a potential oxygen carrier.

7.2 ONGOING AND SUGGESTED WORK

7.2.1 Cytoglobin-based oxygen carrier

With V85I not showing promise as a potential oxygen carrier, the search for other mutants that can fill this role should be continued. The V85F mutant that was initially identified as a high priority was not successfully expressed, but so far this has only been attempted via soluble prep expression. Inclusion body expression and purification may be able to produce a functional version of this protein.

As previously mentioned, it seems that Cygb1 from zebrafish possesses relatively ideal characteristics to function as an oxygen carrier and NO donor. Further evaluation of this protein should focus not only on vasoactivity studies such as the one completed for V85I *HsaCygb* in this work, but also an assessment of possible immunogenicity of this protein in mammalian recipients. If immunogenicity does emerge as a concern, it may be possible to humanize the protein and reduce this threat.

7.2.2 CO and cyanide antidotes

The L46F + H81Q double mutant shows promise as an antidote for both CO and cyanide poisoning. Its rapid binding of cyanide has been documented, but thus far this mutant's ability to bind CO has not been extensively explored. Preliminary data suggests very rapid binding of CO, and further exploration of this function of the mutant remains a priority and an ongoing area of work. This mutant is expected to show very high CO affinity, similar to the H64Q *Ngb* mutant that has been published as a possible CO antidote.

7.2.3 Vascular physiology during globin/nitrite infusion

Finally, this work at least hints at a possible role for NADH in potentiating nitrite-induced vasodilation under hypoxia. This is an interesting interaction, and if it can be reproduced, study of this effect could provide new insights into nitrite's effect on blood pressure. Further, as nitrite continues to be explored as a potential therapy for a variety of conditions, including some that are marked by high blood pressure, NADH may even have potential as a well-tolerated adjuvant therapy that could increase the effect of nitrite treatment. This effect should be studied further,

with specific attention paid to the effect of NADH dose and whether or not the effect is also seen in normoxia.

APPENDIX A

SPECTRAL DECONVOLUTION: MATLAB CODE AND REFERENCE SPECTRA

A number of the experiments performed within this document required mathematical deconvolution of complex, multi-species absorbance spectra. This technique was used most heavily in analyzing globin reduction following nitric oxide dioxygenation. In these reactions, four different globin spectra (oxidized, reduced with no ligand bound, reduced and bound to oxygen, and reduced and bound to nitric oxide) coexist with two different CYB5 spectra (reduced and oxidized).

While the general theory of deconvolution is discussed earlier in the document, this section provides the MATLAB code used to actually perform these deconvolutions, as well as the reference spectra for various globin and CYB5 species.

A.1 MATLAB CODE FOR DECONVOLUTION

Included below is a function, `formatserialdeconv.m` written and used in MATLAB (Mathworks, Inc.) for spectral deconvolution. I designed, coded, and used this function to perform deconvolution of numerous back-to-back spectra, allowing for tracking of changes in globin

oxidation state and ligand binding during various experiments. The inputs, outputs, and function of each section of the code are addressed in comments (green text) within the code itself; note that these green lines are not executed by the program, and exist simply to provide explanation of the working segments of the code.

This code includes a second function, `deconv3.m`, which I also wrote within MATLAB. This function performs the actual deconvolution process, loading a series of reference spectra (which vary depending on the specific proteins being studied) that correspond to different protein species, and calculating the concentration of each species that yields a spectrum most similar to what was measured.

A few small variations in the use of this code existed. Namely, the specific spectra that are loaded at the beginning of `deconv3.m` would vary based on both the specific globin and, when present, the specific CYB5 protein that was used. I primarily performed these analyses on human cytoglobin, as well as the two zebrafish cytoglobins cytoglobin 1 and cytoglobin 2. Reference spectra for all of these proteins can be found in the next section of this appendix. Finally, in the event that I needed to deconvolute only a single spectrum, I would use `deconv3.m` on its own, as that function is sufficient for deconvolution of a single spectrum.

```
function [ species ] = formateserialdeconv( data, reductant, tstep )
%formateserialdeconv.m: performs deconvolution of multiple consecutive
%UV-Vis spectra
% Perform deconvolution of numerous UV-Vis spectra, measured
% continuously, to track the relative concentration of different globin
% and CYB5 species throughout various experimental manipulation.
% OUTPUTS
% species: the absolute concentration of each of the four Cygb species
% and, when present, the two CYB5 species, at each time point. This
% output is an nx6 matrix, where n is the number of spectra deconvoluted,
% and the columns are the concentrations at each point for:
%     Column 1: Fe(III) oxidized globin
%     Column 2: Fe(II), reduced, oxygen-bound globin
%     Column 3: Fe(II), reduced globin with no bound ligand
%     Column 4: Fe(II), reduced, nitric oxide-bound globin
%     Column 5: Fe(II), reduced CYB5
%     Column 6: Fe(III), oxidized CYB5
% INPUTS
```

```

% data: all measured spectra, with each spectrum measured between 450 and
% 700 nm, and represented as a 251-element row of an nx251 matrix, where
% n is the number of individual spectra
% reductant: a 2-character string indicating the reducing agent used
%   -accepted values: 'b5' (CYB5) or 'aa' (ascorbic acid)
% tstep: the number of seconds between measured spectra in the data file:
% this value is typically 1, as the instrument measures one spectrum per
% second, but faster analysis can be obtained by taking every 5th or
% 10th spectra and changing this value accordingly.

% Determine the size of the data matrix, use the size and user-provided
% tstep value to create the time vector (used later for plotting), and
% initialize empty matrices for the species concentrations and total
% protein concentration.
[dim1 dim2] = size(data);
time = [1:dim1]*tstep;
species = [];
total = [];

% Using a for loop, the code analyzes all uploaded spectra, starting with
% the first; for each spectrum, the first step is to subtract the
% absorbance measured at 700nm from all points in that spectrum; this
% absorbance value should be the same for all proteine species, and this
% subtraction is done to counteract drift or noise in the measured data.
for n = 1:dim1
    spectrum = data(n,:);
    spectrum = spectrum - spectrum(251);
% Following subtraction of the 700nm absorbance, the spectrum is also
% stored as a row in a matrix, named 'sub700', which is used to plot a
% few individual spectra below. This allows for storage of previous
% spectra, which would otherwise be lost when 'spectrum' is rewritten on
% the following pass through the loop.
    sub700(n,:) = spectrum;
% Deconvolution itself is performed using deconv3.m (included below) and
% the user-specified reductant. The results of this are added as the last
% row of the previously-initialized 'species' matrix. They concentrations
% of the four globin species are also summed together to calculate the
% total globin concentration.
    concs = deconv3(spectrum,reductant);
    species = [species; concs];
    total = [total; sum(concs(1:4))];
end
% Following these operations, the code loops around, takes the next
% spectrum, and repeats the analysis until the calculation has been
% performed for every spectrum in the original data.

% First, plot the spectra (following subtraction of the 700nm absorbance
% value) every 10 seconds between 20 and 80 seconds. As my typical
% experimental protocol includes NADH or ascorbate addition around
% 30-40s, these time points are chosen to observe the initial spectrum
% and to confirm that reduction occurs following addition of the reducing
% agent.
hold on;
load('wavelengths.mat')
plot(wavelengths,sub700(20,:));
plot(wavelengths,sub700(30,:));
plot(wavelengths,sub700(40,:));

```

```

plot(wavelengths,sub700(50,:));
plot(wavelengths,sub700(60,:));
plot(wavelengths,sub700(70,:));
plot(wavelengths,sub700(80,:));

legend('20s','30s','40s','50s','60s','70s','80s')

% Generate a new figure, and split this figure into two subplots
figure
subplot(2,1,1)
% In the top subplot, plot the calculated concentrations of the different
% globin species, as well as the total globin concentration, as a
% function of time.
plot(time,species(:,1),'b-')
hold on;plot(time,species(:,2),'g-')
hold on;plot(time,species(:,3),'c-')
hold on;plot(time,species(:,4),'r-')
hold on;plot(time,total,'black-')
legend('met','oxy','deoxy','nitrosyl','total')
xlabel('Time (s)')
ylabel('Concentration (mM)')
title('Globin Species')

% In the bottom subplot, plot the calculated concentrations of the two
% species of CYB5. If CYB5 was not used, this plot will simply show
% constant values of zero, and can be disregarded.
subplot(2,1,2)
plot(time,species(:,5),'b-')
hold on;plot(time,species(:,6),'g-')
legend('reduced b5','oxidized b5')
xlabel('Time (s)')
ylabel('Concentration (mM)')
title('CYB5 Redox State')

end

function [ concs,percents ] = deconv3(spectrum,reductant)
%deconv3.m: performs deconvolution of a single UV-vis spectrum
% Perform deconvolution of measured Cygb spectrum, taken on Agilent spec
% in glovebox, into the deoxy, oxy, met, and iron-nitrosyl components.
% Can be used for experiments with either 2 uM CYB5 or any concentration
% of ascorbate as a reducing agent (specified in inputs).
% OUTPUTS
% concs: the absolute concentration of each of the four Cygb species
% percents: the relative percentages of each of the Cygb species present
% INPUTS
% spectrum: the spectrum to be deconvoluted, taken from the Gladwin lab's
% Agilent spectrophotometer: wavelength range is 450-700nm
% reductant: a 2-character string indicating the reducing agent used
% -accepted values: 'b5' (CYB5) or 'aa' (ascorbic acid)

% First, load the pre-measured reference spectra for all 4 species of
% Cygb, and for 2 species of CYB5:
load('wavelengths.mat')
load('metcoeffsold.mat')
load('oxycoeffs.mat')
load('deoxycoeffs.mat')

```

```

load('nitrosylcoeffsold.mat')
load('FeIIb5.mat')
load('FeIIIb5.mat')
% Note that the exact titles of the reference spectra may vary slightly
% between versions of this function, as different proteins and different
% batches require the use of different reference spectra.

% Next, define the error function, and provide initial guesses for the
% concentrations of the protein species present. The initial guesses are
% set as the 100% oxidized forms of both the globin and CYB5, as
% measurement begins before NADH addition, a point at which no reduced
% protein should be present.
fun = @(x) sum((x(1)*metcoeffsold + x(2)*oxycoeffs + x(3)*deoxycoeffs +
x(4)*nitrosylcoeffsold + x(5)*FeIIb5 + x(6)*FeIIIb5)-spectrum).^2);
x0 = [.02,0,0,0,0,.002];
A = []; b = [];

% The function requires the user to specify the reductant. Because only 2
% concentrations of CYB5 are ever used (2 uM for samples with CYB5, 0 uM
% for samples without), the 2-character string used to denote the
% reductant influences the fitting. If CYB5 is present (reductant =
% 'b5'), then the solver is told to ensure that the concentrations of the
% 2 CYB5 species add to 2 uM. Otherwise, they are set to a total value of
% 0.
if reductant == 'b5'
    Aeq = [0 0 0 0 1 1]; beq = [.002];
else Aeq = [0 0 0 0 1 1]; beq = [0];
end

% Define boundaries for species concentrations: all lower bounds are set
% to zero (as negative concentrations cannot exist), and all upper bounds
% are left unconstrained.
lb = [0,0,0,0,0,0];
ub = [inf,inf,inf,inf,inf,inf];
nonlcon = [];
options = optimset('Display','off');
x = fmincon(fun,x0,A,b,Aeq,beq,lb,ub,nonlcon,options);

fitcurve = x(1)*metcoeffsold + x(2)*oxycoeffs + x(3)*deoxycoeffs +
x(4)*nitrosylcoeffsold + x(5)*FeIIb5 + x(6)*FeIIIb5;
concs = x;

% The following sections were used when deconvoluting single spectra, but
% for longer time-based data (1000 seconds or more), were commented out
% to ensure the amount of information provided at the end was more
% manageable.

% Plot calculated fits vs. measured spectrum
%subplot(2,1,1)
%hold on;plot(wavelengths,spectrum,'b-')
%hold on;plot(wavelengths,fitcurve,'r-')

% Plot residuals for each calculated fit
%subplot(2,1,2)
%hold on;plot(wavelengths,fitcurve-spectrum,'r-')
%hold on;plot(wavelengths,zeros(251),'black-')

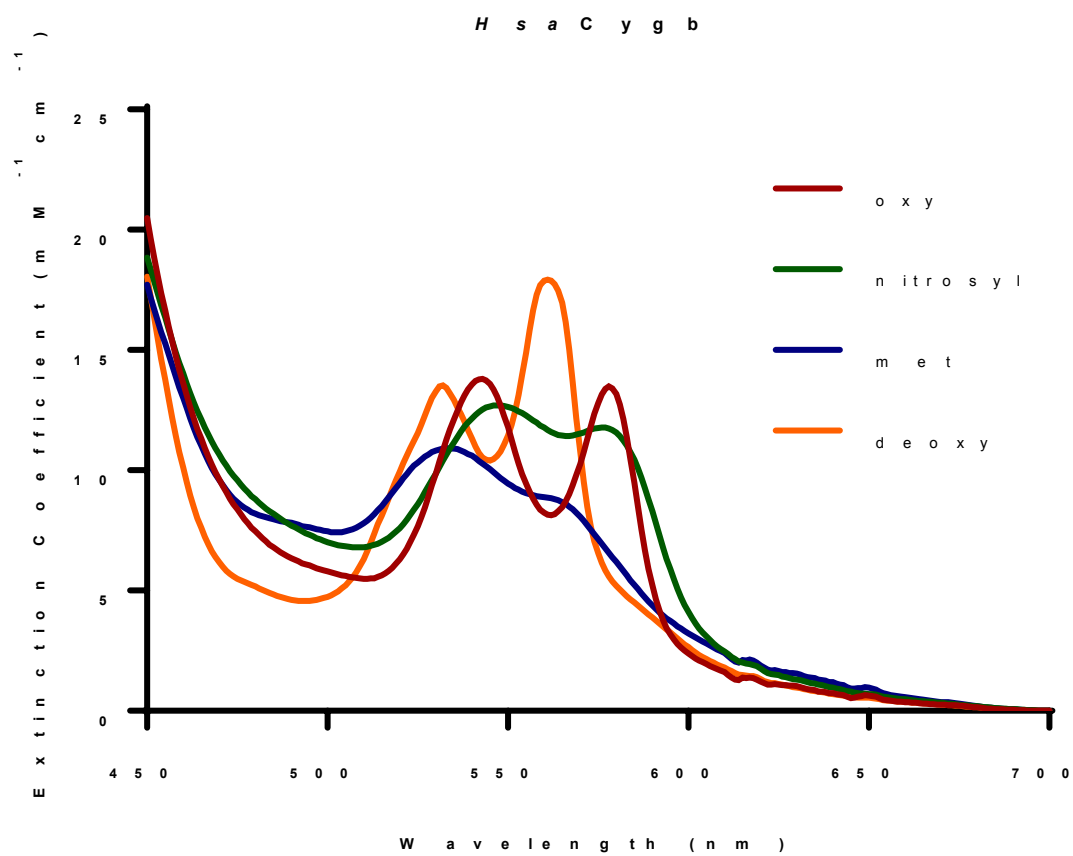
```

end

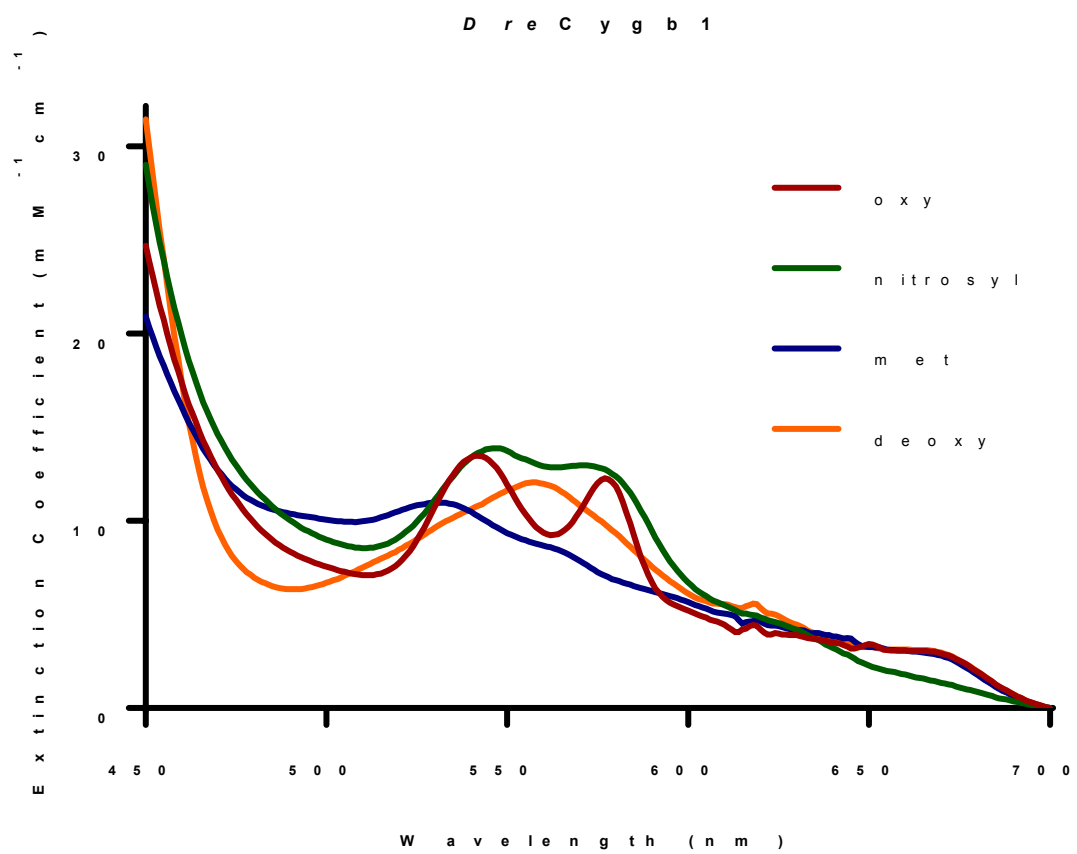
A.2 REFERENCE SPECTRA FOR DECONVOLUTION

This section displays the reference spectra used for spectral deconvolution. All spectra were measured on an Agilent Hp8453 UV-Vis spectrophotometer, and raw spectra were converted to extinction coefficients using published extinction coefficients, or in the case of species without published extinction coefficients, extrapolating from known extinction coefficients.

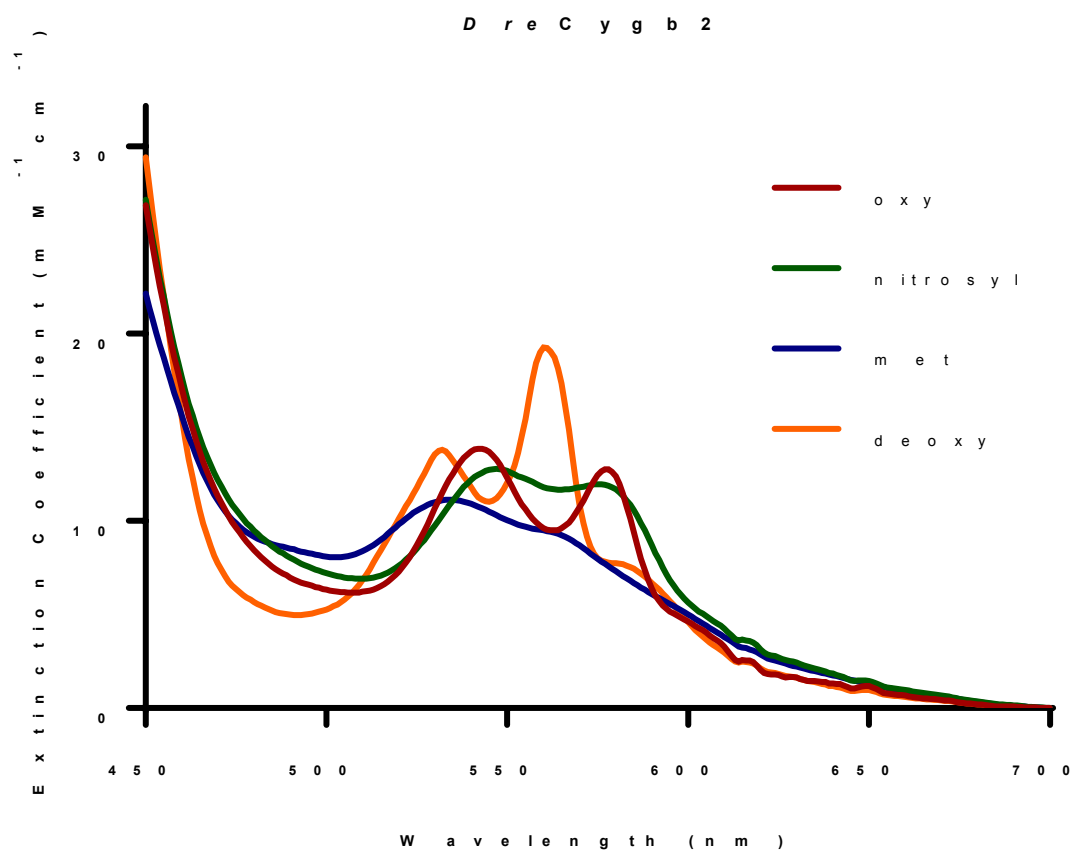
A.2.1 Human Cygb reference spectra



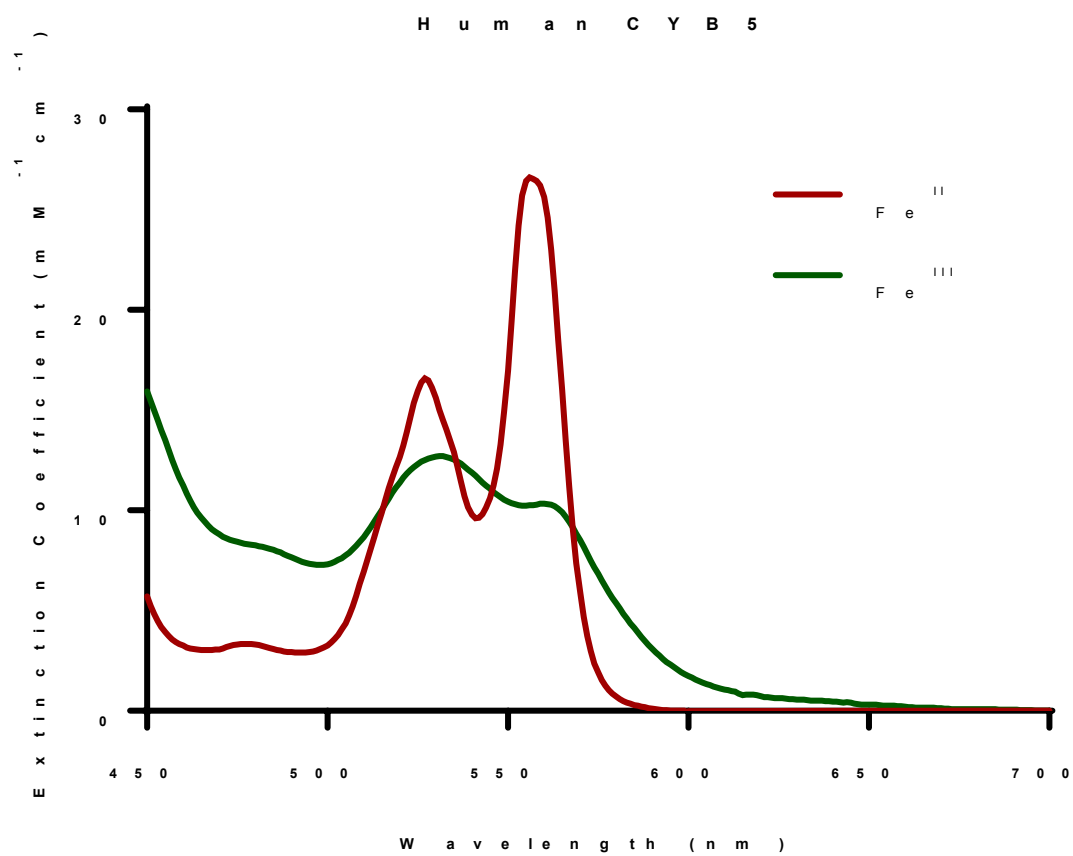
A.2.2 Zebrafish Cygb1 reference spectra



A.2.3 Zebrafish Cygb2 reference spectra



A.2.4 CYB5 reference spectra



BIBLIOGRAPHY

1. Wang, X., et al., *Biological activity of nitric oxide in the plasmatic compartment*. Proc Natl Acad Sci U S A, 2004. **101**(31): p. 11477-82.
2. Rubio-Navarro, A., et al., *Hemoglobin induces monocyte recruitment and CD163-macrophage polarization in abdominal aortic aneurysm*. Int J Cardiol, 2015. **201**: p. 66-78.
3. Rodriguez, C., et al., *Sodium nitrite therapy attenuates the hypertensive effects of HBOC-201 via nitrite reduction*. Biochem J, 2009. **422**(3): p. 423-32.
4. Corti, P., M. Ieraci, and J. Tejero, *Characterization of zebrafish neuroglobin and cytoglobins 1 and 2: Zebrafish cytoglobins provide insights into the transition from six-coordinate to five-coordinate globins*. Nitric Oxide, 2016. **53**: p. 22-34.
5. Tejero, J., et al., *Exploring the mechanisms of the reductase activity of neuroglobin by site-directed mutagenesis of the heme distal pocket*. Biochemistry, 2015. **54**(3): p. 722-33.
6. Corti, P., et al., *Globin X is a six-coordinate globin that reduces nitrite to nitric oxide in fish red blood cells*. Proc Natl Acad Sci U S A, 2016. **113**(30): p. 8538-43.
7. Varadarajan, R., et al., *Effects of buried ionizable amino acids on the reduction potential of recombinant myoglobin*. Science, 1989. **243**(4887): p. 69-72.
8. Bonaventura, C., et al., *Heme redox properties of S-nitrosated hemoglobin A0 and hemoglobin S: implications for interactions of nitric oxide with normal and sickle red blood cells*. J Biol Chem, 2002. **277**(17): p. 14557-63.
9. Altuve, A., et al., *Mammalian mitochondrial and microsomal cytochromes b(5) exhibit divergent structural and biophysical characteristics*. Biochem Biophys Res Commun, 2004. **314**(2): p. 602-9.
10. Henderson, C.J., L.A. McLaughlin, and C.R. Wolf, *Evidence that cytochrome b5 and cytochrome b5 reductase can act as sole electron donors to the hepatic cytochrome P450 system*. Mol Pharmacol, 2013. **83**(6): p. 1209-17.
11. Tejero, J., et al., *Low NO concentration dependence of reductive nitrosylation reaction of hemoglobin*. J Biol Chem, 2012. **287**(22): p. 18262-74.

12. Culbertson, D.S. and J.S. Olson, *Role of heme in the unfolding and assembly of myoglobin*. *Biochemistry*, 2010. **49**(29): p. 6052-63.
13. Tiso, M., et al., *Human neuroglobin functions as a redox-regulated nitrite reductase*. *J Biol Chem*, 2011. **286**(20): p. 18277-89.
14. Hamdane, D., et al., *The redox state of the cell regulates the ligand binding affinity of human neuroglobin and cytoglobin*. *J Biol Chem*, 2003. **278**(51): p. 51713-21.
15. Reeder, B.J. and J. Ukeri, *Strong modulation of nitrite reductase activity of cytoglobin by disulfide bond oxidation: Implications for nitric oxide homeostasis*. *Nitric Oxide*, 2018. **72**: p. 16-23.
16. Guimaraes, B.G., et al., *The crystal structure of wild-type human brain neuroglobin reveals flexibility of the disulfide bond that regulates oxygen affinity*. *Acta Crystallogr D Biol Crystallogr*, 2014. **70**(Pt 4): p. 1005-14.
17. Vinck, E., et al., *Structural change of the heme pocket due to disulfide bridge formation is significantly larger for neuroglobin than for cytoglobin*. *J Am Chem Soc*, 2004. **126**(14): p. 4516-7.
18. Broniowska, K.A. and N. Hogg, *The chemical biology of S-nitrosothiols*. *Antioxid Redox Signal*, 2012. **17**(7): p. 969-80.
19. Di Giulio, A. and A. Bonamore, *Globin interactions with lipids and membranes*. *Methods Enzymol*, 2008. **436**: p. 239-53.
20. Reeder, B.J., D.A. Svistunenko, and M.T. Wilson, *Lipid binding to cytoglobin leads to a change in haem co-ordination: a role for cytoglobin in lipid signalling of oxidative stress*. *Biochem J*, 2011. **434**(3): p. 483-92.
21. Kawada, N., et al., *Characterization of a stellate cell activation-associated protein (STAP) with peroxidase activity found in rat hepatic stellate cells*. *J Biol Chem*, 2001. **276**(27): p. 25318-23.
22. Huang, Z., et al., *Enzymatic function of hemoglobin as a nitrite reductase that produces NO under allosteric control*. *J Clin Invest*, 2005. **115**(8): p. 2099-107.
23. Tejero, J., et al., *Peroxidase activation of cytoglobin by anionic phospholipids: Mechanisms and consequences*. *Biochim Biophys Acta*, 2016. **1861**(5): p. 391-401.
24. Burmester, T., et al., *Cytoglobin: a novel globin type ubiquitously expressed in vertebrate tissues*. *Mol Biol Evol*, 2002. **19**(4): p. 416-21.
25. Geuens, E., et al., *A globin in the nucleus!* *J Biol Chem*, 2003. **278**(33): p. 30417-20.
26. Hankeln, T., et al., *The cellular and subcellular localization of neuroglobin and cytoglobin -- a clue to their function?* *IUBMB Life*, 2004. **56**(11-12): p. 671-9.

27. Xi, Y., et al., *Gene expression and tissue distribution of cytoglobin and myoglobin in the Amphibia and Reptilia: possible compensation of myoglobin with cytoglobin in skeletal muscle cells of anurans that lack the myoglobin gene*. *Gene*, 2007. **398**(1-2): p. 94-102.
28. Halligan, K.E., F.L. Jourd'heuil, and D. Jourd'heuil, *Cytoglobin is expressed in the vasculature and regulates cell respiration and proliferation via nitric oxide dioxygenation*. *J Biol Chem*, 2009. **284**(13): p. 8539-47.
29. Singh, S., et al., *Calcineurin activates cytoglobin transcription in hypoxic myocytes*. *J Biol Chem*, 2009. **284**(16): p. 10409-21.
30. Xu, R., et al., *Cytoglobin overexpression protects against damage-induced fibrosis*. *Mol Ther*, 2006. **13**(6): p. 1093-100.
31. Mimura, I., et al., *Cytoglobin, a novel globin, plays an antifibrotic role in the kidney*. *Am J Physiol Renal Physiol*, 2010. **299**(5): p. F1120-33.
32. Thuy le, T.T., et al., *Absence of cytoglobin promotes multiple organ abnormalities in aged mice*. *Sci Rep*, 2016. **6**: p. 24990.
33. Li, D., et al., *Cytoglobin up-regulated by hydrogen peroxide plays a protective role in oxidative stress*. *Neurochem Res*, 2007. **32**(8): p. 1375-80.
34. Fang, J., I. Ma, and J. Allalunis-Turner, *Knockdown of cytoglobin expression sensitizes human glioma cells to radiation and oxidative stress*. *Radiat Res*, 2011. **176**(2): p. 198-207.
35. Shivapurkar, N., et al., *Cytoglobin, the newest member of the globin family, functions as a tumor suppressor gene*. *Cancer Res*, 2008. **68**(18): p. 7448-56.
36. Fordel, E., et al., *Hypoxia/ischemia and the regulation of neuroglobin and cytoglobin expression*. *IUBMB Life*, 2004. **56**(11-12): p. 681-7.
37. Fordel, E., et al., *Anoxia or oxygen and glucose deprivation in SH-SY5Y cells: a step closer to the unraveling of neuroglobin and cytoglobin functions*. *Gene*, 2007. **398**(1-2): p. 114-22.
38. Shaw, R.J., et al., *Cytoglobin is upregulated by tumour hypoxia and silenced by promoter hypermethylation in head and neck cancer*. *Br J Cancer*, 2009. **101**(1): p. 139-44.
39. Emara, M., A.R. Turner, and J. Allalunis-Turner, *Hypoxic regulation of cytoglobin and neuroglobin expression in human normal and tumor tissues*. *Cancer Cell Int*, 2010. **10**: p. 33.
40. Tanaka, F., et al., *Cytoglobin may be involved in the healing process of gastric mucosal injuries in the late phase without angiogenesis*. *Dig Dis Sci*, 2013. **58**(5): p. 1198-206.

41. Liu, X., et al., *Cytoglobin regulates blood pressure and vascular tone through nitric oxide metabolism in the vascular wall*. Nat Commun, 2017. **8**: p. 14807.
42. Jourd'heuil, F.L., et al., *The Hemoglobin Homolog Cytoglobin in Smooth Muscle Inhibits Apoptosis and Regulates Vascular Remodeling*. Arterioscler Thromb Vasc Biol, 2017. **37**(10): p. 1944-1955.
43. Wawrowski, A., et al., *Changes of globin expression in the Japanese medaka (Oryzias latipes) in response to acute and chronic hypoxia*. J Comp Physiol B, 2011. **181**(2): p. 199-208.
44. Tiedke, J., et al., *Ontogeny of globin expression in zebrafish (Danio rerio)*. J Comp Physiol B, 2011. **181**(8): p. 1011-21.
45. Amberson, W.R., et al., *Mammalian Life without Red Blood Corpuscles*. Science, 1933. **78**(2014): p. 106-7.
46. Amberson, W.R., J.J. Jennings, and C.M. Rhode, *Clinical experience with hemoglobin-saline solutions*. J Appl Physiol, 1949. **1**(7): p. 469-89.
47. Amberson, W.R., et al., *On the use of Ringer-Locke solutions containing hemoglobin as a substitute for normal blood in mammals*. Journal of Cellular and Comparative Physiology, 1934. **5**(3): p. 359-381.
48. Brandt, J.L., N.R. Frank, and H.C. Lichtman, *The effects of hemoglobin solutions on renal functions in man*. Blood, 1951. **6**(11): p. 1152-8.
49. Savitsky, J.P., et al., *A clinical safety trial of stroma-free hemoglobin*. Clin Pharmacol Ther, 1978. **23**(1): p. 73-80.
50. Przybelski, R.J., et al., *Phase I study of the safety and pharmacologic effects of diaspirin cross-linked hemoglobin solution*. Crit Care Med, 1996. **24**(12): p. 1993-2000.
51. Vandegriff, K.D., et al., *MP4, a new nonvasoactive PEG-Hb conjugate*. Transfusion, 2003. **43**(4): p. 509-16.
52. Przybelski, R.J., et al., *A safety assessment of diaspirin cross-linked hemoglobin (DCLHb) in the treatment of hemorrhagic, hypovolemic shock*. Prehosp Disaster Med, 1999. **14**(4): p. 251-64.
53. Sloan, E.P., et al., *Diaspirin cross-linked hemoglobin (DCLHb) in the treatment of severe traumatic hemorrhagic shock: a randomized controlled efficacy trial*. JAMA, 1999. **282**(19): p. 1857-64.
54. Schubert, A., et al., *Diaspirin-crosslinked hemoglobin reduces blood transfusion in noncardiac surgery: a multicenter, randomized, controlled, double-blinded trial*. Anesth Analg, 2003. **97**(2): p. 323-32, table of contents.

55. Kerner, T., et al., *DCL-Hb for trauma patients with severe hemorrhagic shock: the European "On-Scene" multicenter study*. Intensive Care Med, 2003. **29**(3): p. 378-85.
56. Jahr, J.S., et al., *HBOC-201 as an alternative to blood transfusion: efficacy and safety evaluation in a multicenter phase III trial in elective orthopedic surgery*. J Trauma, 2008. **64**(6): p. 1484-97.
57. Jahr, J.S., et al., *Does HBOC-201 (Hemopure) affect platelet function in orthopedic surgery: a single-site analysis from a multicenter study*. Am J Ther, 2010. **17**(2): p. 140-7.
58. Levien, L.J., *South Africa: clinical experience with Hemopure*. ISBT Science Series, 2006. **1**(1): p. 167-173.
59. Lundy, J.B., et al., *Experience with the use of Hemopure in the care of a massively burned adult*. Int J Burns Trauma, 2014. **4**(1): p. 45-8.
60. Gould, S.A., et al., *The first randomized trial of human polymerized hemoglobin as a blood substitute in acute trauma and emergent surgery*. J Am Coll Surg, 1998. **187**(2): p. 113-20; discussion 120-2.
61. Gould, S.A., et al., *The life-sustaining capacity of human polymerized hemoglobin when red cells might be unavailable*. J Am Coll Surg, 2002. **195**(4): p. 445-52; discussion 452-5.
62. Moore, E.E., et al., *Human polymerized hemoglobin for the treatment of hemorrhagic shock when blood is unavailable: the USA multicenter trial*. J Am Coll Surg, 2009. **208**(1): p. 1-13.
63. Chen, J.Y., M. Scerbo, and G. Kramer, *A review of blood substitutes: examining the history, clinical trial results, and ethics of hemoglobin-based oxygen carriers*. Clinics (Sao Paulo), 2009. **64**(8): p. 803-13.
64. Kipnis, K., N.M. King, and R.M. Nelson, *Trials and errors: barriers to oversight of research conducted under the emergency research consent waiver*. IRB, 2006. **28**(2): p. 16-9.
65. Kipnis, K., N.M. King, and R.M. Nelson, *An open letter to institutional review boards considering Northfield Laboratories' PolyHeme trial*. Am J Bioeth, 2006. **6**(3): p. 18-21.
66. Apte, S.S., *Blood substitutes--the polyheme trials*. McGill J Med, 2008. **11**(1): p. 59-65.
67. Olofsson, C., et al., *A multicenter clinical study of the safety and activity of maleimide-polyethylene glycol-modified Hemoglobin (Hemospan) in patients undergoing major orthopedic surgery*. Anesthesiology, 2006. **105**(6): p. 1153-63.

68. Olofsson, C., et al., *A randomized, single-blind, increasing dose safety trial of an oxygen-carrying plasma expander (Hemospan) administered to orthopaedic surgery patients with spinal anaesthesia*. *Transfus Med*, 2008. **18**(1): p. 28-39.
69. Olofsson, C.I., et al., *Evaluation of MP4OX for prevention of perioperative hypotension in patients undergoing primary hip arthroplasty with spinal anesthesia: a randomized, double-blind, multicenter study*. *Anesthesiology*, 2011. **114**(5): p. 1048-63.
70. Gladwin, M.T. and S.F. Ofori-Acquah, *Erythroid DAMPs drive inflammation in SCD*. *Blood*, 2014. **123**(24): p. 3689-90.
71. Harrington, J.P. and H. Wollocko, *Molecular Design Properties of OxyVita Hemoglobin, a New Generation Therapeutic Oxygen Carrier: A Review*. *J Funct Biomater*, 2011. **2**(4): p. 414-24.
72. Harrington, J.P. and H. Wollocko, *Pre-clinical studies using OxyVita hemoglobin, a zero-linked polymeric hemoglobin: a review*. *J Artif Organs*, 2010. **13**(4): p. 183-8.
73. Song, B.K., et al., *Effects of top-loading a zero-link bovine hemoglobin, OxyVita, on systemic and microcirculatory variables*. *Mil Med*, 2013. **178**(5): p. 570-7.
74. Harrington, J.P., et al., *Physicochemical characteristics of OxyVita hemoglobin, a zero-linked polymer: liquid and powder preparations*. *Artif Cells Blood Substit Immobil Biotechnol*, 2011. **39**(1): p. 12-8.
75. Wollocko, H., et al., *Zero-link polymerized hemoglobin (OxyVita(R)Hb) stabilizes the heme environment: potential for lowering vascular oxidative stress*. *Artif Cells Nanomed Biotechnol*, 2017. **45**(4): p. 701-709.
76. Rameez, S. and A.F. Palmer, *Simple method for preparing poly(ethylene glycol)-surface-conjugated liposome-encapsulated hemoglobins: physicochemical properties, long-term storage stability, and their reactions with O₂, CO, and NO*. *Langmuir*, 2011. **27**(14): p. 8829-40.
77. Cabrales, P., S. Rameez, and A.F. Palmer, *Hemoglobin encapsulated poly(ethylene glycol) surface conjugated vesicles attenuate vasoactivity of cell-free hemoglobin*. *Curr Drug Discov Technol*, 2012. **9**(3): p. 224-34.
78. Azarov, I., et al., *Five-coordinate H64Q neuroglobin as a ligand-trap antidote for carbon monoxide poisoning*. *Sci Transl Med*, 2016. **8**(368): p. 368ra173.
79. Eggenreich, B., et al., *Production strategies for active heme-containing peroxidases from E. coli inclusion bodies - a review*. *Biotechnol Rep (Amst)*, 2016. **10**: p. 75-83.
80. Yamaguchi, H. and M. Miyazaki, *Refolding techniques for recovering biologically active recombinant proteins from inclusion bodies*. *Biomolecules*, 2014. **4**(1): p. 235-51.

81. Egeberg, K.D., et al., *The role of Val68(E11) in ligand binding to sperm whale myoglobin. Site-directed mutagenesis of a synthetic gene.* J Biol Chem, 1990. **265**(20): p. 11788-95.
82. Carver, T.E., et al., *A novel site-directed mutant of myoglobin with an unusually high O₂ affinity and low autooxidation rate.* J Biol Chem, 1992. **267**(20): p. 14443-50.
83. Gibson, Q.H., et al., *Distal pocket residues affect picosecond ligand recombination in myoglobin. An experimental and molecular dynamics study of position 29 mutants.* J Biol Chem, 1992. **267**(31): p. 22022-34.
84. Kurian, J.R., et al., *Reductive detoxification of arylhydroxylamine carcinogens by human NADH cytochrome b5 reductase and cytochrome b5.* Chem Res Toxicol, 2006. **19**(10): p. 1366-73.
85. Gardner, A.M., M.R. Cook, and P.R. Gardner, *Nitric-oxide dioxygenase function of human cytoglobin with cellular reductants and in rat hepatocytes.* J Biol Chem, 2010. **285**(31): p. 23850-7.
86. Liu, X., et al., *Differences in oxygen-dependent nitric oxide metabolism by cytoglobin and myoglobin account for their differing functional roles.* FEBS J, 2013. **280**(15): p. 3621-31.
87. Ascenzi, P., S. Gustincich, and M. Marino, *Mammalian nerve globins in search of functions.* IUBMB Life, 2014. **66**(4): p. 268-76.
88. Kuma, F., *Properties of methemoglobin reductase and kinetic study of methemoglobin reduction.* J Biol Chem, 1981. **256**(11): p. 5518-23.
89. Bekedam, M.A., et al., *Myoglobin concentration in skeletal muscle fibers of chronic heart failure patients.* J Appl Physiol (1985), 2009. **107**(4): p. 1138-43.
90. Liu, X., et al., *Characterization of the function of cytoglobin as an oxygen-dependent regulator of nitric oxide concentration.* Biochemistry, 2012. **51**(25): p. 5072-82.
91. Tong, J., et al., *Effect of temperature, pH and heme ligands on the reduction of Cygb(Fe(3+)) by ascorbate.* Arch Biochem Biophys, 2014. **554**: p. 1-5.
92. Beckerson, P., et al., *Cytoglobin ligand binding regulated by changing haem-coordination in response to intramolecular disulfide bond formation and lipid interaction.* Biochem J, 2015. **465**(1): p. 127-37.
93. Fago, A., et al., *The reaction of neuroglobin with potential redox protein partners cytochrome b5 and cytochrome c.* FEBS Lett, 2006. **580**(20): p. 4884-8.
94. Trent, J.T., 3rd and M.S. Hargrove, *A ubiquitously expressed human hexacoordinate hemoglobin.* J Biol Chem, 2002. **277**(22): p. 19538-45.

95. Livingston, D.J., et al., *Myoglobin: cytochrome b5 interactions and the kinetic mechanism of metmyoglobin reductase*. J Biol Chem, 1985. **260**(29): p. 15699-707.
96. Harrison, F.E. and J.M. May, *Vitamin C function in the brain: vital role of the ascorbate transporter SVCT2*. Free Radic Biol Med, 2009. **46**(6): p. 719-30.
97. Du, J., J.J. Cullen, and G.R. Buettner, *Ascorbic acid: chemistry, biology and the treatment of cancer*. Biochim Biophys Acta, 2012. **1826**(2): p. 443-57.
98. Qiao, H., et al., *Ascorbic acid uptake and regulation of type I collagen synthesis in cultured vascular smooth muscle cells*. J Vasc Res, 2009. **46**(1): p. 15-24.
99. Davidson, J.M., et al., *Ascorbate differentially regulates elastin and collagen biosynthesis in vascular smooth muscle cells and skin fibroblasts by pretranslational mechanisms*. J Biol Chem, 1997. **272**(1): p. 345-52.
100. Evans, R.M., L. Currie, and A. Campbell, *The distribution of ascorbic acid between various cellular components of blood, in normal individuals, and its relation to the plasma concentration*. Br J Nutr, 1982. **47**(3): p. 473-82.
101. Gotting, M. and M. Nikinmaa, *More than hemoglobin - the unexpected diversity of globins in vertebrate red blood cells*. Physiol Rep, 2015. **3**(2).
102. Beckerson, P., B.J. Reeder, and M.T. Wilson, *Coupling of disulfide bond and distal histidine dissociation in human ferrous cytoglobin regulates ligand binding*. FEBS Lett, 2015. **589**(4): p. 507-12.
103. Brantley, R.E., Jr., et al., *The mechanism of autooxidation of myoglobin*. J Biol Chem, 1993. **268**(10): p. 6995-7010.
104. Arnaud, F., et al., *Dose response of sodium nitrite on vasoactivity associated with HBOC-201 in a swine model of controlled hemorrhage*. Artif Cells Blood Substit Immobil Biotechnol, 2011. **39**(4): p. 195-205.
105. Amdahl, M.B., et al., *Efficient Reduction of Vertebrate Cytoglobins by the Cytochrome b5/Cytochrome b5 Reductase/NADH System*. Biochemistry, 2017. **56**(30): p. 3993-4004.
106. Torres, M.J., et al., *Modulation of the reactivity of the thiol of human serum albumin and its sulfenic derivative by fatty acids*. Arch Biochem Biophys, 2012. **521**(1-2): p. 102-10.
107. Rogers, S.C., et al., *Hypoxia limits antioxidant capacity in red blood cells by altering glycolytic pathway dominance*. FASEB J, 2009. **23**(9): p. 3159-70.
108. Gladwin, M.T., et al., *Relative role of heme nitrosylation and beta-cysteine 93 nitrosation in the transport and metabolism of nitric oxide by hemoglobin in the human circulation*. Proc Natl Acad Sci U S A, 2000. **97**(18): p. 9943-8.

109. Vitturi, D.A., et al., *Regulation of nitrite transport in red blood cells by hemoglobin oxygen fractional saturation*. Am J Physiol Heart Circ Physiol, 2009. **296**(5): p. H1398-407.